



Jagiellonian University

Chemistry Faculty

Department of Inorganic Chemistry

Heterogeneous Reactions Kinetics Group

[k]* zespół kinetyki
reakcji heterogenicznych



**DEGRADATION OF NATURAL FIBERS
IN ARTEFACTS:
MECHANISM AND INHIBITION**

by
Monika Adelajda Koperska

under supervision of Joanna Łojewska, PhD

Thesis for the degree of Doctor of Philosophy

Kraków 2015

To my beloved grandmother Krysia for her love and support.

Contents

Acknowledgements	4
1. INTRODUCTION	5
2. SILK	6
2.1 Short history of silk and silk banners.....	6
2.2 Silk's biological origin [5]	8
2.3 Structure of silk	9
2.4 Silk's processing [11]	12
3. Paths of silk's degradation	14
3.1 Natural ageing	14
3.2 Provoking artificial ageing	16
4. Assessment of thermo-degradation of model silk samples	17
4.1 Instrumental analyses strategy	17
4.2 Historic samples choice and sampling.....	18
4.3 Initial characterization of initial model silk samples	19
4.3.1 Recognizing texture by microscope.....	19
4.3.2 Inorganic additives recognition studied by XRF	19
4.4 Optimization of aging protocol.....	20
4.4.1 Choosing ageing agent: thermo- and photo- aging assessed by colour and pH change	21
4.4.2 Choosing aging temperature: changes in model samples assessed by Tg and FT IR	22
4.5 Macroscopic estimators of fibroin degradation evaluation.....	25
4.6 Microscopic degradation markers of fibroin in silk through infrared spectroscopy.....	26
5. Evaluating degradation of fibroin by ATR-FTIR: case study of historic textiles from Polish collections.....	28
6. Conclusions and guidelines for conservators.....	29
Bibliography.....	31
List of figures	33
List of tables	33
Abbreviations	33

Acknowledgements

I would like to thank the Wawel Castle Museum, especially Magdalena Ozga and Jerzy Holc for their help in gathering historic samples and historical advise.

I would also like to appreciate Maria Cybulska, PhD from Politechnika Łodzka for providing historic samples and information on techniques of designing, processing and documenting historic textiles.

The authors thank to Anna Klisińska-Kopacz from Laboratory of Analysis and Non-destructive Investigation of Heritage Objects (LANBOZ), National Museum in Krakow, Poland for her help and support.

Project funded from the funds of NCN 2011/01/N/ST4/03604, FNP EX/04/2012 and 11/III/2009/ FWK.

1. INTRODUCTION

The motivation for this thesis is to prepare a firm scientific foundations for the understanding of silk degradation phenomena with particular reference to cultural heritage applications. Therefore on one side this work gives the explanations to silk ageing effects and on the other draws from museum backbone problems in textile conservation. Finding an immediate cure for problems connected to preservation and restoration of historically important artefacts is very often impossible. However, we believe that thorough comprehension of the structure and degradation mechanism we can give rational basis for the conservator's decisions. This hoped to be achieved by the structural and chemical spectroscopic analyses of model and historic samples artificially aged at various conditions. The problem although the first set of analysed ageing procedures is broad as well as the techniques used to evaluate both historic and artificially aged model samples, it still an attempted at answering basic conservation questions. These concerns natural fibroin degradation mechanism, atmosphere storage designed for preservation guidelines, risk assessment for more efficient restoration planning.

For these reasons the thesis is woven with threads of conservator and historian based information and scientific analysis. In this way the basic information about silk (chapter 2) collaborated two types of fields: historical (section 2.1) and scientific (section 2.2-2.4). In chapter three you will find descriptions of degradation that silk can adopt under natural and artificially induced conditions. Assessment of artificial degradation is described in chapter 4. First experiments were planned in terms of approaching the degradation mechanism (4.1) historic samples had to be gathered (4.2) and model samples chosen (4.3). Optimization of the aging protocol did involve some estimators of degradation had to be pre-chosen (4.4). These can be divided into two groups: macroscopic such as colour and mechanical strength and microscopic based on spectroscopic analyses of silk structure and composition further discussed in section 4.5 and 4.6, respectively. The estimators were then taken to evaluate historic samples described in chapter 5 That lead to final interpretation of structural change which gave understanding to how silk degrades naturally and artificially. That to some extent gave us chance to formulate guidelines for art textile conservators described in chapter 6.

2. SILK

2.1 Short history of silk and silk banners

The history of silk is so old that it is told in legends. Especially the Chinese ancient tales go into the details of silk origin. They explain that in 27 century BC the wife of the mythological Yellow Emperor, Huangdi (黃帝), taught the Chinese the art of silk production. The record states that Leizu (嫫祖) was having a cup of tea under a mulberry tree while a cocoon fell into the hot liquid. The temperature and the moist caused the follicle to unwrap and the empress found that she could unwind this soft and fine thread around her finger. Soon she began her own cocoonery [1].

There are some archaeological findings indicating that sericulture was known even earlier. Drawings on ivory from 5000 BC give rise to this thesis. Moreover in 1980 scientists found some pieces of silk textile dating back to neolith period [1].

Nevertheless, today we can be certain that the silk discovery took place in China. There it became the object of almost religious value with several festivities around the year ensuring the growth and quality of larva. With flow of history the silk soon grew to be the most tradable item. The Silk Road, a route across central Asia, enabled the transport of Chinese product to the west and ensured country stayed the biggest exporter of silk until the XVIIth century [2].

Meantime, in about 140 BC sericulture had spread overland from China to India. By the second century AD India was shipping their manufactured goods to Persia and Japan. That made Persia a centre of silk trade between East and West. From there it was shipped to Syria, Egypt, Greece, and Rome where silk dyeing and weaving developed as crafts [1].

The growing demand for raw silk created a need to manufacture some in Europe. In the 4th century BC Aristotle mentioned that sericulture was practiced on the island of Kos. This art must have been lost as in 6th emperor Justinian I ordered to steal eggs of silkworm and smuggle them to Constantinople. Seven silkworms were to travel hidden under monks' robes to Europe safely. And legendary that single event has started the entire sericulture in Europe [2].

Silk culture flourished on the European continent for many centuries, especially in the Italian city-states and (from 1480) in France. Unfortunately, a silkworm plague started in 1854 and continued until 1865 when Louis Pasteur discovered the cause of the disaster and developed a cure. Unlike Italian industry, French never did return to its splendour and size. After World War II the demand for silk diminished with the discovery of synthetic fibres, such as nylon and polyester. Nevertheless silk is still a luxury material and remains an important product of Japan, South Korea, and Thailand [2].



Fig. 1. Court Banner
XVIth century, Poland



Stanisław Barzi's Funeral Banner
XVIth century, Poland



The Inscription Banner
XVIth century, Turkey

Silk is also widely present in museums not only in the world but also in Poland. Silk banners, cloths of religious and casual purpose, tapestries, parts of furniture, these are all under watchful eye of polish conservators. Some found in the Wawel Castle Museum date back to as far as even XVIth and include: Court Banner, Stanisław Barzi's Funeral Banner and Turkish Inscription Banner.

The first one was painted in Cracow for the occasion of the wedding and coronation of Sigismund Augustus. Since then it was used during state ceremonies, coronations and important funerals [3]. After 1848 was relocated from Wawel, stolen by the Russians, and returned to Cracow in 1928 [4]. It is one of the few objects once stored in the king's treasury, which survived to our times [3].

Barzi's Funeral Banner is the oldest tombstone banner (1530-1571), one of several surviving fabric of this kind [3]. These type of banners were suspended initially over tombstones of knights who died in the fight against pagans, but soon they became part of the funeral ceremony [3]. Similarly to the Court Banner it spend the First World War in Russia and was returned to Poland in 1928 [4]. For the Second World War it was hidden in Quebec and finally came back to Cracow in 1961 [3].

Turkish Inscription Banner was woven and painted in Turkey. It was captured on September the 12th, 1683 in the Battle of Vienna, by the army of Martin Zamoyski, a friend of King Jan III Sobieski.

2.2 Silk's biological origin [5]

The simplest definition of silk is that it is an animal fibre produced by certain insects (described in table 1) as building material for its cocoons and webs.

Depending on an animal, specialists distinguish several types of silks. The most common type is obtained from cocoons made by glands in the head of the larvae of the mulberry silkworm. The less exploited silks are waved during nests construction by the insects form Hymenoptera order (bees, wasps, and ants). Also types of arachnids, such as spiders, generate silk in their abdomen.

The types of silks, mainly produced by spiders, may differ on the basis of its purpose. Specialized silks have evolved with material properties optimized for their intended use. For example, *Argiope argentata* has five different types of silk, each serve a different purpose:

- dragline silk (very strong; used for the web's outer rim and spokes, as well as for the lifeline);
- capture-spiral silk (sticky and stretchy; used as the capturing lines of the web);
- tubiliform silk (very stiff; used for protecting egg);
- aciniform silk (two or three times stronger than other silks; used to wrap and secure freshly captured prey);
- minor-ampullate silk (used during web construction for temporary scaffolding).

But from all of the types of silk two have gathered special attention: the *Bombyx mori*

Table 1. Silk producing animal's scientific classification:

Domain:	Eukarya
Kingdom:	Animalia
Phylum:	Arthropoda

Class:	Insecta
Subclass:	Pterygota
Infraclass:	Neoptera
Superorder:	Endopterygota

Class:	Insecta
Order:	Lepidoptera
Family:	Bombycidae
Genus:	Bombyx
Species:	B. Mori

Class:	Arachnida
Order:	Araneae
Family:	Araneidae
Genus:	Argiope

silkworm and *Nephila clavipes* spider type. The first one because of its commercial use, the second, more for the scientific reasons. Gradually all of the silk types are being characterized so the understanding of silk sequences, structures and properties is becoming clearer.

2.3 Structure of silk

Silk is built up of two main proteins: **fibroin** and **sericine**. The first one constructs the inside of a fibre whereas the second forms the outside layer. The structure of silk is arranged hierarchically from chains through nanofibrils to fibres organizations. It is important to highlight, that depending on the origin of silk, we distinguish different proportions of the two proteins (see table 2 [6]). The proteins have been distinguished there by the animal origin. Additionally, low levels of sugars and minerals that can be found in some silk systems were noted as “other” in the table.

Table 2. Composition of silk proteins depending on the origin.

	Silkworm			
protein	<i>Bombyx mori</i> (Mulberry worm silk)	<i>Antherarea permi</i> (Tussah or wild silk)	<i>Andracea assamensis</i> (Muga silk)	<i>Samia Cynthia ricini</i> (Eri silk)
fibroin	70-80%	80-90%	80-90%	80-90%
sericine	20-30%	8-10%	8-10%	4-5%
others	2-3%	3-5%	3-5%	3-5%

9

Fibroin is made up of series of aminoacids to form a polypeptide structure. There are two types of these classified in the literature: the light chain of molecular weights of about 25 000 Da; the heavy chain of 375 000 Da [6]. The two are linked by a single disulfide bond to form a larger protein. That structure is retained during processing into fiber and probably plays a role in the regulation of chain folding. The most important aminoacids in the fibroin are **glycine (44.6%), alanine (29.4%), serine (12.1%), tyrosine (5.1%), leucine (1.2%), threonine (0.9%), aspartic acid (1.3%), glutamic acid (1.0%), cysteine (0.2%) proline (0.4%), valine (2.2%), phenylalanine (0.4%), histidine (0.1%), lysine (0.3%), tryptophan (0.1%), arginine (0.5%)** [6].

Segments of proteins with or without side groups (such as iso-propyl side group in valine) are attracted together by several forces:

- van der Waals bonds - between segments of peptides;
- hydrogen bonds - at distance of 0.5 nm between C=O and N-H atoms of neighbouring peptides;
- salt bonds – at distance 0.1 nm between COO⁻ and NH₄⁺ groups of peptides around their isoelectric point at pH 2.8;

- disulphide cross-links - covalent bonds between two cysteine aminoacids of neighboring chains or within one chain;
- peptide cross-links – covalent bonds between two chains of aminoacids to provide considerable strength to the material [7].

It is worth pointing out that the crystalline structure of silk is due to only 4 types of aminoacids (small molecules). For example the 59-aminoacid mer: **GAGAGSGAAG[SGAGAG]₈Y¹** (of course variations of the sequence and sub domains representing aspects of the sequence are common) is responsible for β -sheet formation in the fibres in *Bombyx mori* silk. It is surrounded by less regular parts of the aminoacidic chain composed of the rest of the aminoacids. Unlike in *Bombyx mori* originated silk, in the net silk fibre from a spider *Nephila clavipes*, the repetitive mer contains 6 to 12 amino acids. Nevertheless, this repetitively distinguishes fibrous proteins as those included in silk from the globular ones like enzymes and antibodies [9].

The β -sheet ordering calls for more careful explanation as it is responsible for the crystallinity of the material. Silks are considered semi crystals with 30-50% crystallinity in spider silks, **62-65%** in the cocoon silks of *Bombyx mori* and 50-63% of wild-type silkworm. Within the crystalline arrangements the polymer chain axis and the fibre axis are parallel. The 3 crystalline forms of *Bombyx mori* fibroin are distinguished in the literature: **silk I – prespun; silk II – spun; silk III – interfacial** [8].

As regards the structural parameters of silk crystal, the orthogonal unit cell parameters in the silk II structure are 0.94 nm (a, interchain), 0.697 nm (b, fibre axis), 0.92 nm (c, intersheet). The forces playing an important role at this level of magnitude are: the hydrogen bonds between carbonyl and amine groups (perpendicular to the chain axis) and the Van der Waals interactions. The β -sheets consisting of the glycine-alanine crystalline regions in the *Bombyx mori* fiber are asymmetric; with one surface primarily projecting alanyl methyl groups and the other surface of the same sheet containing hydrogen atoms from the glycine residues [8]. There are two theories that explain the arrangement of the sheets in silk II structure. First one assumes that these sheets are arranged back-to-back so that for every other sheet, the sheet-to-sheet interacting faces are the glycy side-chains (3.70 Å of distance) and the alternating interacting faces are the alanyl methyl groups (5.27 Å of spacing) [8]. The other one by Takahasi et al. [8] assumes that the two surfaces of a sheet have both alanyl and glycy side-groups (the spacing in-between the sheets must be a half of c-axis).

¹ Where G = glycine, A = alanine, S = serine, Y = tyrosine [8].

The silk I is soluble in water but very unstable and easily converts to silk II. This change can be triggered by shearing, drawing, heating, spinning, exposure to the electric field or polar solvents (methanol or acetone). Based on the modelling predictions, this change results in the 18.3% decrease in distance between the overlaying sheets. Thermodynamically silk II is more stable than silk I and the energy of the transition from silk I to II is high and considered essentially irreversible [8].

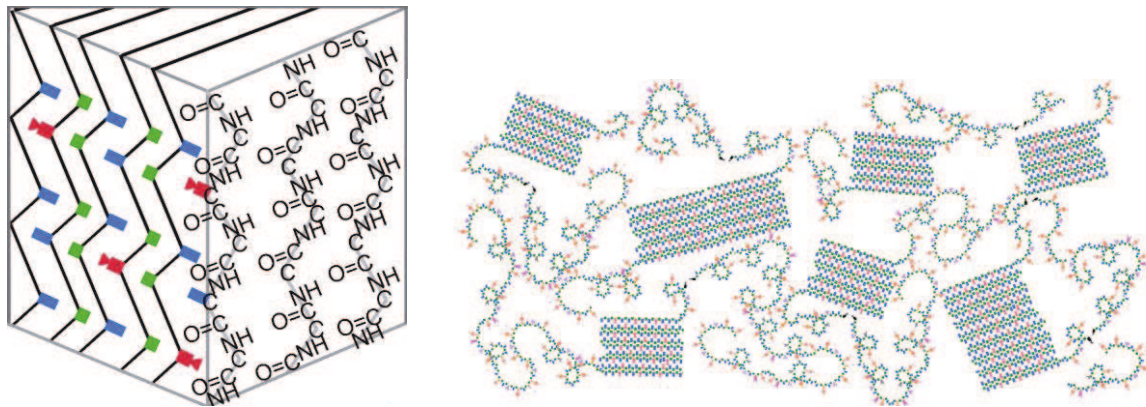


Figure 2. Left - unit cell of fibroin *Bombyx mori* and right – structure of long-chain polymers exhibiting crystalline and amorphous regions “fringed micelle” structure.

The sequence of amino acids explained above is arranged in a “fringed micelle” structure, where the micelles should be understood as the β -sheet crystalline regions, and the fringes as amorphous regions. The fringed regions deserve their name as they are, unlike crystalline ones, easily penetrable for all small molecules, are more dynamic and easier undergo changes while exposed to light. According to the “fringed micelle” theory, each polymer chain within the structure of the fibre passes through both crystalline and amorphous stages [6].

Sericine, ranges in the molecular weight between 20 000 and 310 000 Da. It is completely dissolvable in acid of 2.5 pH and alkali of 9.5 pH solutions. Certainly, not all silk types have its shell made of sericine. Spider *Nephila clavipes*, due to retaining more durability of a self-produced thread, has no sericine-shell proteins [6].

The structure of the spider produced silk is less crystalline. The data collected in the literature prove that all crystalline fractions of dragline silk is composed of the alanine-rich sequences and these consist of two orientations: one, 40% of all, highly organized along the fibre axis, second, remaining 60 %, less ordered and less dense. This fact is understandable as this silk is designated to dissipate the energy of the impact of an insect flying on the web. Therefore the mechanical properties: the stiffness and strength against extensibility of the fibre must be balanced by the size of the crystal region of the β -sheets [10].

Due to its structure, but mainly the extensive hydrogen bonding and van der Waals forces, silk fibroin is very difficult to solubilize. It does not dilute in water, acids and alkali nor in most organic solvents. On the other hand, sericine shell-like cover is easy to get rid of in the process called degumming (meaning boiling in soap water or sodium bicarbonate solution). Aggressive solvents like high concentration lithium bromide, lithium thiocyanate or calcium nitrate are needed to solubilize fibroin. They can be then removed by dialysis into water or buffer [8].

2.4 Silk's processing [11]

The full picture of the silk structure and composition cannot be grasped without knowing the chemical process of fibres treatment and fabrication. Silk's processing can be divided into several stages: degumming; bleaching; weighting; dyeing.

The first step - degumming – is simply removing the outside layer of sericine. It serves to make the fabric soft and increase its lustre. It is performed by extraction with water with alkali or acids and digestion with enzymes. However, the treatment that is less destructive to the fibre is carried out in water acidic or alkaline solution. Usually, also detergents are added. To extract sericine the solution is boiled from 30 minutes to 4 hours. For rapid elimination of sericine the alkali baths (at over 8.5 pH for up to 2 hours) are recommended. Chemicals used for those are sodium carbonate, sodium bicarbonate, trisodium phosphate. Degumming with enzymes is more expensive and therefore scarcely used. Trypsin (pH at 8.0 and 40-50 °C) and papain (pH of 5.2 and 70 °C) are the most common enzymes used for degumming.

The second step – bleaching - is needed due to the fact that silk is naturally coloured (ranges from white to brown through shades of yellow). Bleaching can be performed by reduction or oxidation of the fibre, although the first leads in the end to fibre yellowing (reoxidation). Oxidation is carried out by soaking bulks of threads in solutions of hydrogen peroxide, sodium perborate or persulfate whereas reduction is triggered by sodium hydrosulphite or sodium sulfoxylates. In historic silks bleaching would be achieved by smoking with sulphur which can be recognized by the increased content of sulphur in comparison with contemporary silk fabrics.

The third step of silk processing – weighting – is based on soaking silk threads in a solution of metallic salts for the purpose of increasing the weight of the finished product. The commonly used mass additives to ancient silks are black, tannin, sugar, mineral, tin, tin-tannin, tin-phosphate-silicate. The historically oldest is black weighting applied in the very beginning of 17th century and performed with ferrous sulphate, iron acetate or ferrocyanide.

Its addition to silk influenced the textile lustre, handle and drape as it made the fibres more swollen and also the colour making the textile brown. The black weighting was often combined with tannin weighting (obtained from sumach, gambier, chestnut, alder bark, gallnuts, catechu, myrabolams, valonia, acacias, and divi divi). In the search for colourless weighting agents for white or light colour silks, sugar was explored as a possible option. It, however, never got popular as it resulted in sticky, lustre-less, water staining fabric. The most recent weighting technique is the one using tin invented in about 1870s. At that time stannous chloride (tin(II) chloride) was used as a mordant in fashion, but when accidentally used as a silk weighting agent turned out to be a revelation. Tin weighted black silk possessed greater colour-fastness, was thicker and heavier. Soon after the tin-tannin method was discovered to work very well with medium to dark shades of dyes. In 1892 the tin-phosphate-silicate method of weighting was developed for white and lighter coloured silks. All of the parameters of silk: volume, handle, lustre, drape, scoop; improved after this last technique implementation.

Dilute organic acids have been used as a silk yarns finishing agent. Tartaric and citric acids are known for producing a rustling effect to a finished goods. Additionally, citric acid or epoxides are responsible for improving launder-ability of silk (due to the formation of cross links) [6]. Silk weighting can alter some properties of silk. It can improve the drape and handle of the textile, increase the fibre volume and impart scoop. It can be done using variety of inorganic and organic compounds. After weighting the silk is ready to dye with all, including mordant, dyes.

There are a few methods used by conservators to identify the agent that was utilized to make the silk heavier, unfortunately all of them destroy the sample. They include weighting the residual after incineration and diluting it with hydrochloric acid followed by precipitation with hydrogen sulphide (yellow colour indicates tin). Black silk identification is performed as first by making water or ether extractions of silk and then soaking the extracted sample in hydrochloric acid (iron tannin weighting turns silk red and acid brown colour). Yet another is Kjeldahl method. It is based on measuring the nitrogen content of silk sample and calculating the excess weight of the sample given the fact that pure silk should have 17,6% of nitrogen by weight. In Lemiski test the colour of burning silk is observed for tin and spot test with potassium ferrocyanide performed for iron.

Silk, as a fabric and commercial product, from a chemical point of view, should be considered as material of basic to neutral pH composed of oxidized protein with anchored or adsorbed ions (weighting agents) or other molecules. Both degumming and weighting cause irreversible changes into the fibre. Although degumming improves many of the qualities of

silk, its consequence, of losing up to 25% of silk's mass, is very undesirable. While silk is a strong and durable fibre, the weighting process is highly damaging to it. If the garment is worn, it wears out quickly and is highly susceptible to perspiration, salt, and tears; if stored away it becomes brittle and breaks.

3. Paths of silk's degradation

3.1 Natural ageing

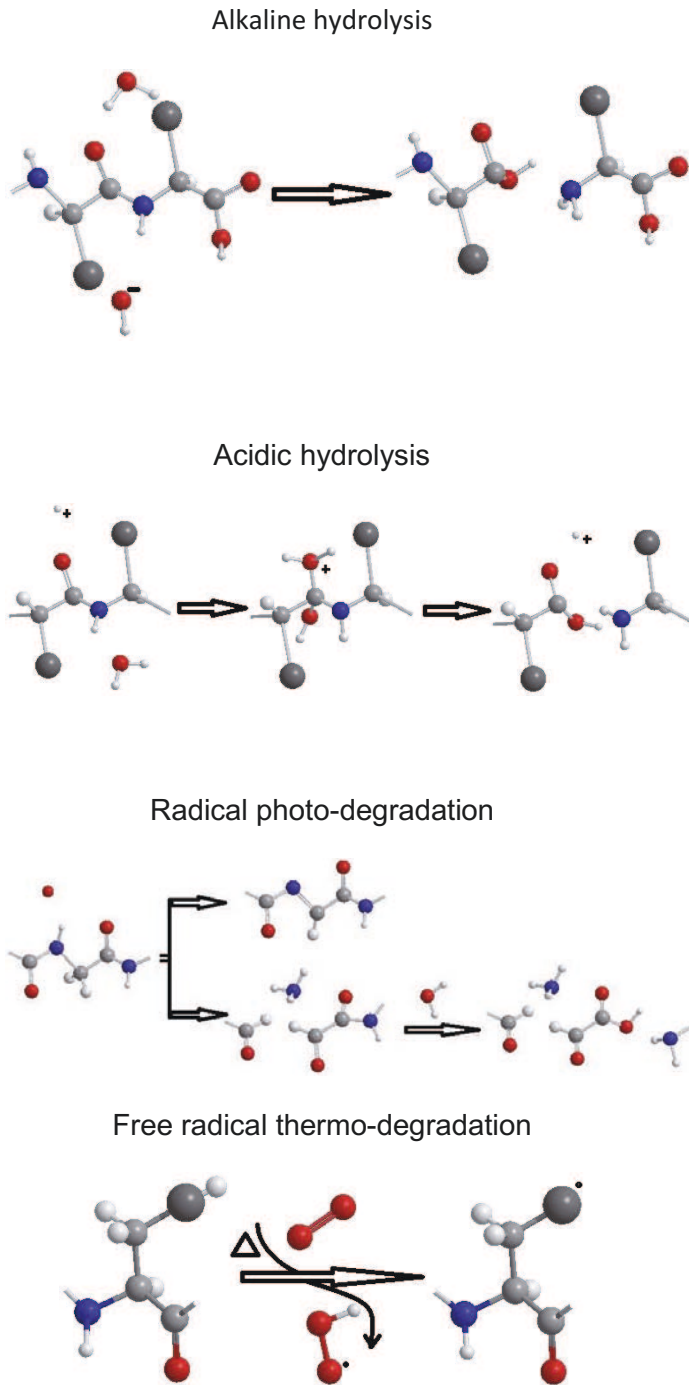
There are five general ways of ageing, each of which affects textiles in different ways [12]. Scientists distinguish physical, photochemical, thermal, chemical and mechanical degradation (see figure 3).

The physical age of the material is calculated since the last time the glass transition temperature was last exceeded. It results from the ordering of non-crystalline polymer chains and includes decreases in free volume, enthalpy and molecular mobility. Since T_g temperatures of most fibre-forming polymers are above the room conditions and all of them contain some non-crystalline areas, therefore most will suffer from physical ageing just by storage in room temperature. That can be overcome by the wetting the sample as the absorption of water lowers the T_g temperature to around standard conditions. It is important to highlight that for every material's physical age can be erased by heating a material above the cloth's T_g.

As suggested in the name, the photochemical degradation is caused by exposure to light. Unlike the previous case it occurs both in the non and in crystalline fragments of fibre as electromagnetic wave penetrates both. As one could expect, the chemical changes caused by the absorption of light, start from the sheath and penetrates to the core. The most noticeable change of photochemical degradation of textiles is the polymer molecular weight drop and cross-linking. As some bonds between monomers are being broken new ones are being formed. That greatly changes the polymers both chemical and physical properties. For silk results in making the material more brittle and less tough as the polymer network becomes rigid.

Thermal degradation effects can be classified into two groups, one involves purely physical structural changes in a fibre, whereas the other involves chemical changes. First mainly cover melting, crystallization and glass transition. Since heat can easily penetrate the fibre they are expected to occur in crystalline and in non-crystalline areas. Fortunately, melting point of protein fibres exists in the temperature above which polymer undergoes thermal decomposition – chemically irreversible changes.

Figure 3. Typical degradation paths of silk [13]



Fibres are rather stable to chemical attack. The rule of the thumb is that the more complex the fibre and the higher the temperature the more vulnerable the cloth is to chemical reaction (for ex. silk more than cotton). As the chemical species cannot directly attack the crystalline areas therefore susceptibility to chemical attack increases in non-ordered regions. With time and consequent concentration of chemical around the crystal, chemical reaction starts to break the structure from surface inwards.

Mechanical stress can be considered in two time scales. Instantaneous responses are called elastic whereas delayed ones viscous. The most fundamental rule is that the viscous response depends on the rate of the stress and is time dependent. For example a historic textile being folded and stored for a long time will finally cause splits in areas of increased stress.

Much attention has been focused at the photochemical degradation of silk [14]. During the kinetic study of the photo-yellowing process, resulting

from light absorption by silk fibroin, it was possible to establish that the colour change relation to the irradiation time can be described by an exponential law. During that process selective destruction of aminoacids accompanied by peptide bond cleavage takes place. Mainly tyrosine, serine, alanine and glycine from the amorphous regions take part in the decomposition (tyrosine's capability of absorbing energy in the UV-range is attributed to the aromatic core in the aminoacid). They decompose to α -ketoacyl polypeptides, whose level

also increases exponentially during irradiation. The Figure on the left hand side presents a scheme that describes the Meybeck and Meybeck formation of α -ketoacyl groups from glycine and alanine.

Also there has been some research done proving that the decomposition of S-S bond runs during exposure to light [15]. Because sulphur containing aminoacids in silk fibroin content is as low as 0.5% it was difficult to analyse that process. Fortunately equipped with Py-GC/SCD it was proved that first the Cys-Cys bond are broken before the Met-Met are affected.

It is important to highlight that silk processing like weighting and dyeing can significantly change the ways of silk degradation and often make the fabric 'live shorter'. Silk weighting causes strength loss in extensibility and increase in fibre volume. Bizarrely the tin-phosphate-silicate treated cloth loses strength in less time when kept in the dark. Moreover most black weighted silks suffer from spontaneous combustion. Also dyed and weighted silk are more likely to suffer from biodegradation – red fungus spots.

3.2 Provoking artificial ageing

16 Two ageing modes were studied for model silk samples: thermal and photo ageing.

The thermal ageing tests were performed in two kinds of reaction conditions:

- 1) In air in a dryer (BMT Venticell) in which temperature can be regulated from 20 to 250°C. This kind of reaction conditions which can be achieved there can be called an open system or an open reactor. There the variables affecting the condition of samples is temperature and oxygen.
- 2) In air in closed vessels in which a given amount of silk sample was closed firmly not allowing for the mass exchange. The vessels were then put into the dryer in order to achieve a given temperature. Such reaction conditions will be called closed system or closed reactor. There the variables in terms except temperature were oxygen and volatile organic compounds (VOC) evolved from silk upon degradation or oxygen, water vapour (if added) and VOC.

The temperature of ageing experiments was set to 150°C.

The open conditions assume that the amount of the sample is infinitesimally small comparing to the amount of oxygen available to oxidize them entirely and the mass of gases evolving from a sample due to degradation can easily diffuse and dilute in a large chamber volume. Converse, under closed conditions the gaseous products and water included in samples cannot leave the reaction system. In a closed reactor oxygen was used in such an amount in order to be able to fully oxidize all C and N atoms (in principle) included in the silk sample

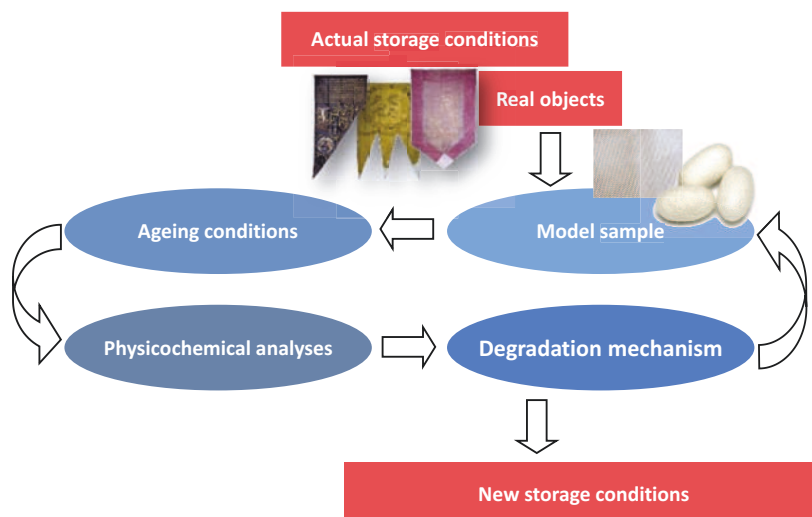
The photo ageing tests were performed using the light ageing chamber (Suntest CPS+) equipped with xenon lamp (ATLAS). Samples were exposed to light in the range 200 - 900 nm and power 765 W/m² in 6 cycles each of duration 720 min. Therefore total light exposure was 3 days. The experiments were repeated with UV filter was placed in between the lamp and the samples in order to mimic the conditions of light in museums. In order to dispose of the temperature effects on the samples the table on which the samples were placed was thermostated. The temperature within the chamber volume varied from about 50 °C near the lamp to 20 °C close to thermostated table.

4. Assessment of thermo-degradation of model silk samples

4.1 Instrumental analyses strategy

Initially a textile is identified by its morphology, chemical properties and dimensions. Next step is to determine the state of the textile, meaning its chemical stability and strength. Below we go into the details of most of the chemical and mechanical

Figure 4. Analytical strategy scheme



methods of testing silk. In Figure 4 you can see the strategy of analysis adopted in this work. First it was crucial to determine the degradation mechanism and for that estimators of degradation had to be chosen. These can be divided into two groups: macroscopic and microscopic and will be further discussed in section 4.5 and 4.6 respectively. These estimators were then taken to evaluate historic samples described in chapter 5. That to some extent gave us chance to formulate guidelines for art textile conservators described in chapter 7.

4.2 Historic samples choice and sampling

Figure 5. Historical silk storage in Wawel Castle Museum magazines:



Thanks to the courtesy of the Museum of Wawel Castle in Cracow, Poland samples from XVIth to XIXth century silks were gathered. These included: Stanisław Barzi's Funeral Banner, Court Banner; 2 different coloured samples from Inscription Banner; samples from 3 different conservation material from XIXth century. Thanks to the courtesy of Lodz University of technology 3 samples from chasuble from XVII/XVIIIth century were added to the group of historic samples. Banners storing conditions are describes in table 3 and in Figure 5.

18

Table 3. Average humidity and temperature in Wawel Castle Museum according to seasons.

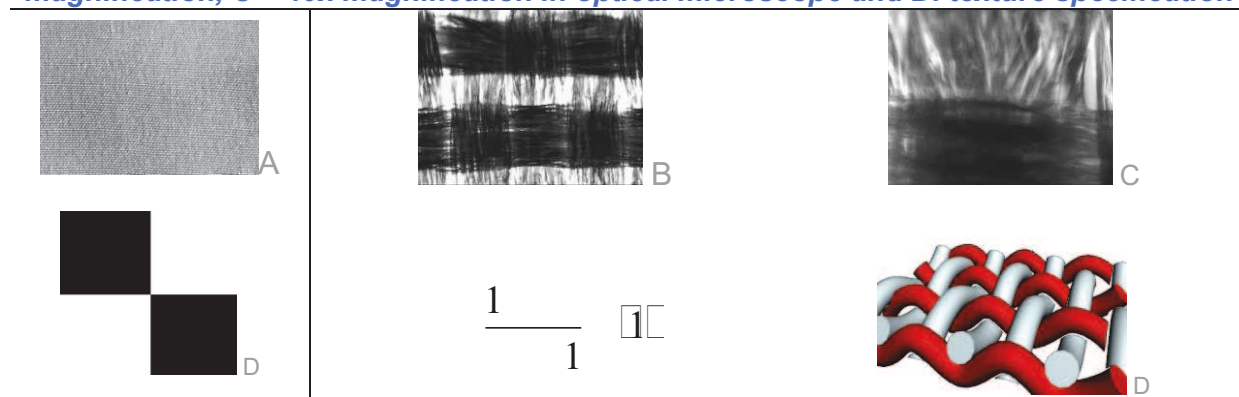
	AUTUMN/WINTER	SPRING/SUMMER
TREASURY	23 - 52% RH, 17-22 °C	34 - 76% RH, 22-28 °C
MAGAZINE 3	33 - 45% RH, 14-18 °C	49 - 55% RH, 18-26 °C

4.3 Initial characterization of initial model silk samples

4.3.1 Recognizing texture by microscope

The images of silk samples were recorded by the optical microscope with 10 to 40 times the magnification and are depicted in table 4. The texture of the fabric and the twist of the thread can be recognized easily from the magnified image. All the samples have linen texture. Threads twist increases for fabrics from right to left in figure 2. Also the textile's covering (the area of textile covered by threads) increases in the same direction.

Table 4. Texture of model samples of silk– A. photographic image, B -10x magnification, C – 40x magnification in optical microscope and D. texture specification



4.3.2 Inorganic additives recognition studied by XRF

There are a few methods used by conservators to identify the agent that was utilized to make the silk heavier in the process of weighting, unfortunately, all of them destroy the samples. Among the traditional methods of analyses several of them can be recognized as most popular ones:

- measuring the mass of the residual after incineration
- diluting with hydrochloric acid followed by precipitation with hydrogen sulfide (turns yellow for tin),
- observing the colour of silk burnt in the flame of a furnace,
- performing the spot test with potassium ferrocyanid (for iron),
- measuring the nitrogen content of silk's sample (and calculating the excess mass of the sample given the fact that pure silk should have 17,6% of nitrogen by weight).

Fortunately modern science delivers non-destructive and fast techniques that can measure the metal content in the samples. For this goal a technique based on X-ray fluorescence was introduced among analytical tools (XRF).

Elemental composition of 5 model silk samples by XRF: elements heavier than $Z > 11$ detected for model silk sample was: S, Ca, Cl, K.

The results give an interesting view on the samples origins and manufacturing handling. The presence of certain elements might be explained by a list of reasons. The signal of sulphur originates from silk's amino acids (cysteine, methionine) and from the sulphur bridges that connect protein chains. The bands of chlorine, potassium and calcium come from their chlorides possibly introduced during manufacturing process – degumming [11]. Additionally, calcium together with increased amount of sulphur produce calcium sulphate that have been used for textile whitening. There are no simple explanations concerning the occurrence of Ca and Ba in cocoons. They may come from the biological residue from larva.

4.4 Optimization of aging protocol

To evidence critical factors influencing changes in silk fibres, within the timeline of project, accelerated ageing experiments were implemented. The aim was to investigate the changes in fibroin that occur while one of the aging variables mentioned above (of potential environmental origin) was acceded. In our study two major ageing factors were considered: temperature and light. Except that the composition of ageing atmosphere was varied to determine the impact of various gases on the degradation progress. The main criterion for the choice of the ageing conditions was to mimic the conditions in museums (open system, visible light range) and in anoxic chambers (closed systems) studied within this project.

20

The temperature of ageing tests should on the one hand be close enough to ambient temperature not to substantially change the sample physical state (glass transition temperature) and not to alter the silk degradation mechanism that occurs spontaneously at ambient conditions. For the silk samples of *Bombyx mori* silk $T_g=175$ °C [8]. According to Kweon et al. first step of slight silk decomposition occurs at 220-300°C, second of abrupt decomposition at 300-370 °C and third at 370-400 °C [16]. On the other side the purpose is to achieve satisfactory results within reasonable time - the time frames of the project.

To assess the temperature and time of aging needed to satisfy the requirements stated above the optical and spectroscopic analyses were performed. To study degradation processes small samples of silks (0.07 g) were aged in closed vessels and in chambers at 50, 150 and 200 °C. Samples were aged from 7-21 days. If after up to 7 days of aging no changes were noticed on spectra and with colour measurements then automatically the temperature was considered too low. On the other hand if the temperature caused to big a change in one day the temperature was considered too high.

4.4.1 Choosing ageing agent: thermo- and photo- aging assessed by colour and pH change

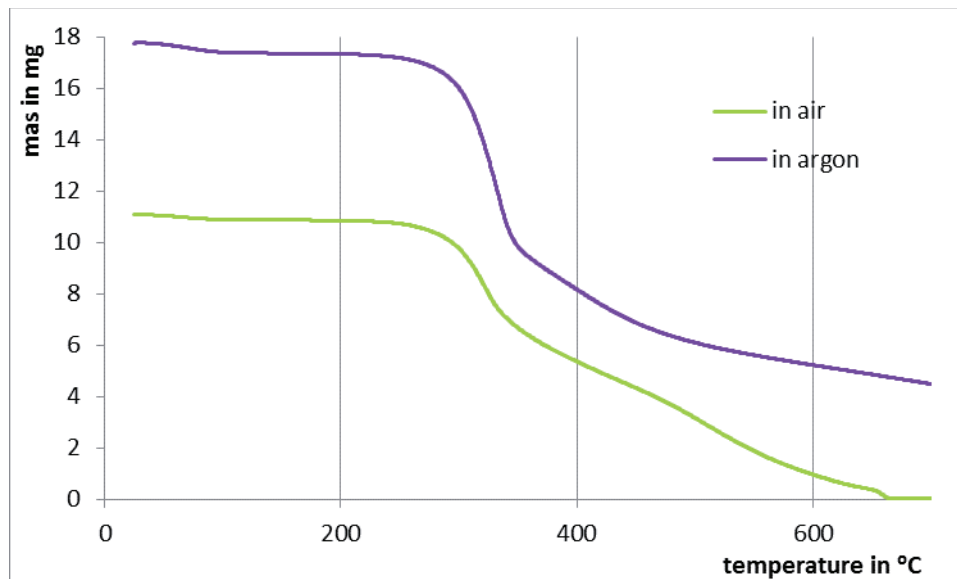
The tendency of the parameter describing overall colour changes of the samples the CIE L*a*b* model was used. The ΔE values grew with the temperature applied to samples during aging as evidenced in Table 5. It is also clear that yellowing is not the only problem which occurs in the samples. The visual assessment of the samples indicates that also the mechanical properties drop significantly under certain ageing conditions. The samples aged at 200 °C were not strong enough for handling. It complies with the largest colour change for those samples for which ΔE was found to be 60. On the other hand ΔE values for the samples aged at 50 °C was below the detection limit. This sets the degradation temperature in the range below 200 °C and above 50 °C.

Aging factor	Model silk sample	Reactor
UV+Vis	8 (+/- 0.1)	OPEN
Vis	9 (+/- 0.1)	
50 °C	3 (+/- 0.1)	
150 °C	44 (+/- 0.3)	CLOSED
200 °C	55 (+/- 0.2)	
50 °C	6 (+/- 0.1)	
150 °C	48 (+/- 0.2)	CLOSED
200 °C	59 (+/- 0.2)	

4.4.2 Choosing aging temperature: changes in model samples assessed by Tg and FT IR

Tg experiments were performed in order to see the nature of thermo-induced fibroin mass loss. The analysis were performed on different size samples in flow of air and argon and are depicted in figure 6. It is clear that silk starts to decompose thermally over 200 °C.

Figure 6. Tg experiments of silk model sample performed in flow of air and argon.



22

The analysis of ATR-FTIR spectra recorded for the samples aged in the open and closed conditions was focused on answering the problem of right temperature for furling project timeline. The evaluation of the degradation progress in the samples was based on the semi-quantitative interpretation of the FTIR spectra. The evaluation utilized the tyrosine marker (E_{TR}) bands to relative tyrosine content in the degraded samples: A_{1621}/A_{1164} and two crystallinity indexes found in the literature $E_{c=01}$, E_{c-n} [18 and see section 4.6]. The indexes are reported to be the most evident degradation gauges possible to obtain from the FTIR spectra according to the literature announcements [19, 20]. Exact calculated values are gathered in table 6.

Upon temperature increase the TR value drop significantly and the slump is higher for the samples aged in the closed reactor especially at the highest temperature used. The latter finding may announce an impact of the volatile products of degradation on degradation progress suggesting possible autocatalytic mechanism. In the literature it is recommended to

measure the E_{TR} from Raman spectra rather than FTIR due to low tyrosine vibration activity in FTIR [20]. Therefore we have decided not to concentrate on this marker.

Comparing the two crystallinity indexes we can infer that the $E_{C_{c=01}}$ is more sensitive to degradation imposed by temperature than the $E_{C_{c=n}}$ whose values do not show any degradation trend. In contrast, the $E_{C_{c=01}}$ values decrease significantly with the temperature of ageing which may signify the growing contribution of amorphous phase in the samples exposed to high temperature and oxygen. However, due to the fact that the bending vibration of water molecules bound to silk material emerge at around 1640 cm^{-1} , the observed tendency can be just an effect of water desorption from the samples. This time the influence of volatile degradation products is more profound as can be judged comparing the samples aged at the same temperature in different reactors. The differences are significant even at temperature as low as $50\text{ }^{\circ}\text{C}$.

To conclude briefly, the results of colour and structure changes show that the temperature $200\text{ }^{\circ}\text{C}$ exerts huge effects on the samples while $50\text{ }^{\circ}\text{C}$ seems too low to observe the measurable changes in short time. Taking into account the T_g temperature for silk the ageing temperature for further tests was set to $150\text{ }^{\circ}\text{C}$ which seems quite high but was a reasonable choice to observe the differences in the material within the reasonable time. Experiments on aging silk in temperature of $150\text{ }^{\circ}\text{C}$ can be found in literature [17, 19].

Figure 7. ATR-FTIR spectra of MS aged at different temperatures in closed and open reactor after 7 days of aging.

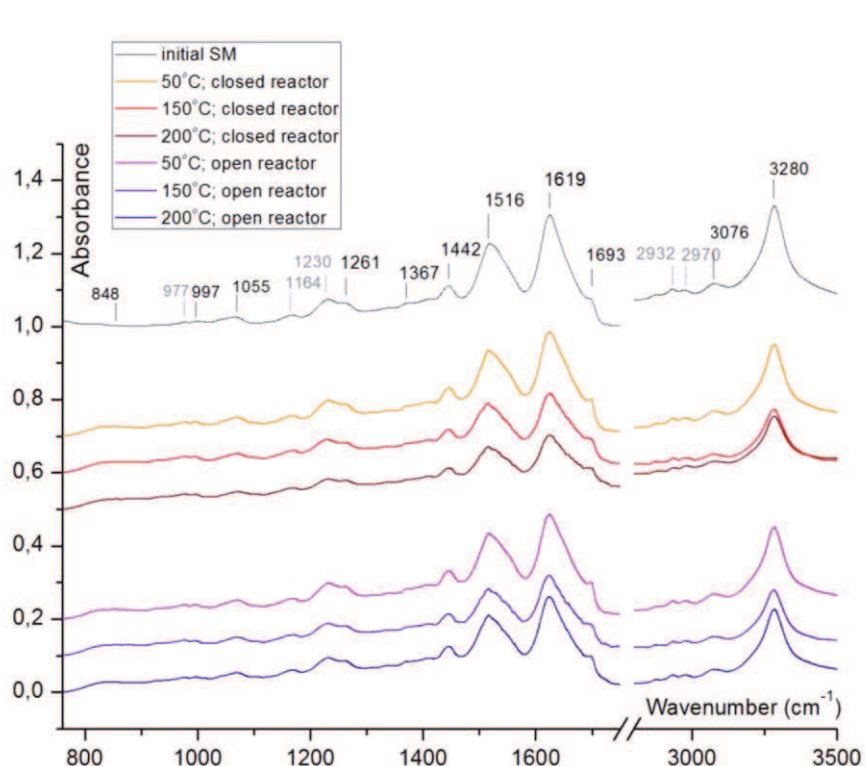


Table 6. Crystallinity indexes E_{C-n} and $E_{C=01}$ and relative tyrosine content E_{TR} calculated from the ATR-FTIR spectra for aged in different temperatures MS samples.

	<i>Aging temperature (°C)</i>	<i>E_{TR}</i>	<i>E_{C-n}</i>	<i>E_{C=01}</i>	<i>Reactor</i>
MS	initial	25	0.42	7.4	OPEN
	50	20	0.41	5.0	
	150	17	0.39	4.7	
	200	17	0.40	4.3	
	initial	25	0.42	7.4	CLOSED
	50	21	0.40	3.8	
	150	14	0.37	3.0	
	200	1.2	0.40	2.7	

4.5 Macroscopic estimators of fibroin degradation evaluation



Fibroin degradation – Critical evaluation of conventional analytical methods



Monika A. Koperska, Dominika Pawcenis, Jakub M. Milczarek, Andrzej Blachecki, Tomasz Łojewski, Joanna Łojewska*

Jagiellonian University, Faculty of Chemistry, Ingardenia 3, 30-060 Kraków, Poland

ARTICLE INFO

Article history:
Received 25 March 2015
Received in revised form 2 July 2015
Accepted 6 July 2015
Available online 15 July 2015

Keywords:
Fibroin
Artificial ageing
Viscosity
Tensile strength
Colour
GC-MS
pH
Degradation

ABSTRACT

Due to their practical importance and widespread application in the studies of polymer degradation, the analytical methods: viscometry, colour and mass change, pH, mechanical strength were selected in this work so as to provide a macroscopic view of silk condition. The aim of the current work is to critically discuss the results obtained by these methods and confront them with the silk structure and degradation mechanism. They were differentiated with several criteria such as chemical (structural) information they bear, sensitivity to the changes induced by environment and their discriminative power. The results show that tensile strength before colour change and viscosity is the most sensitive method to measure silk degradation at various conditions. Significant colour change is typical of oxygen rich degradation atmosphere and was correlated with oxidation products of fibroin. Viscosity was shown to be hard to interpret in terms of mere changes of molecular mass as the most profound effects were observed in oxygen-rich conditions. Detailed research showed that oxygen plays an important role in silk degradation but it is only when combined with closed and humid conditions that results in catastrophic change. © 2015 Elsevier Ltd. All rights reserved.

1. Introduction

Silk fibres have been used for centuries in the textile industry due to their characteristic strength and lustre and thus can be found in many collections in museums and galleries [4]. Nowadays, thanks to its biocompatibility and biodegradability the scientific world is rediscovering silk, using it for new applications in biotechnology and biomedicine (i.e. wound dressing [5], tissue engineering [6], targeted drug delivery [7–11]). But with time silk becomes lighter, yellows and loses its strength making it hard to use and handle. The aim of this paper is to: i) critically evaluate commonly used methods of testing silk properties such as change in viscosity, tensile strength, pH and mass and ii) confront the results with the silk structure and with theory describing the mechanism of silk degradation.

Silk unique properties derive from a semi-crystalline biopolymer structure, with highly organized nanocrystals surrounded by amorphous matrix [12]. The nanocrystals are organised into the secondary structure of β -sheets chains of smaller amino acids

(glycine (44.6%), alanine (29.4%) and serine (12.1%)). They build up to 70% of entire fibroin structure in *Bombyx mori* silk [13]. Packed structure is quite resistant to chemical attack and that is why it is understood that degradation starts in easy to access amorphous regions [14]. Composed of both small and large amino acids (like: tyrosine (5.1%), valine (2.2%), aspartic acid (1.3%), leucine (1.2%), glutamic acid (1.0%), threonine (0.9%), arginine (0.5%), proline (0.4%), phenylalanine (0.4%), lysine (0.3%), cysteine (0.2%), histidine (0.1%), and tryptophan (0.1%) [12]) amorphous regions take on a secondary structure of α -helix and/or random coil arrangements.

The research on silk structure and chemical properties dates back to first half of twentieth century [15]. The study on silk degradation is, however, rather scarce and incomprehensive. Critical evaluation of spectroscopic diffraction and chromatography methods on silk structure determination has been presented in our previous work [1–3]. Amino acid chains of fibroin degrade following the hydrolysis and oxidation pathways simultaneously which results in significant drop of unorganised fibroin domains that leaves silk fibre richer in crystalline regions. Hydrolysis is triggered by water reaching the peptide bond resulting in formation of carbonyl and amine groups [16]. Slower alkali hydrolysis progresses mostly from the ends of the polypeptides where as faster

* Corresponding author.
E-mail address: lojewskaj@uj.edu.pl (J. Łojewska).

4.6 Microscopic degradation markers of fibroin in silk through infrared spectroscopy

Appl. Phys. A (2014) 114:301–308
 DOI 10.1007/s00339-013-8143-z

Applied Physics A
 Materials Science & Processing

RAPID COMMUNICATION

Size exclusion chromatography for analyses of fibroin in silk: optimization of sampling and separation conditions

Dominika Pawcenis · Monika A. Koperska ·
 Jakub M. Mileczarek · Tomasz Łojewski ·
 Joanna Łojewska

Received: 2 July 2013 / Accepted: 5 November 2013 / Published online: 20 November 2013
 © The Author(s) 2013. This article is published with open access at Springerlink.com

Abstract A direct goal of this paper was to improve the methods of sample preparation and separation for analyses of fibroin polypeptide with the use of size exclusion chromatography (SEC). The motivation for the study arises from our interest in natural polymers included in historic textile and paper artifacts, and is a logical response to the urgent need for developing rationale-based methods for materials conservation. The first step is to develop a reliable analytical tool which would give insight into fibroin structure and its changes caused by both natural and artificial ageing. To investigate the influence of preparation conditions, two sets of artificially aged samples were prepared (with and without NaCl in sample solution) and measured by the means of SEC with multi angle laser light scattering detector. It was shown that dialysis of fibroin dissolved in LiBr solution allows removal of the salt which destroys stacks chromatographic columns and prevents reproducible analyses. Salt rich (NaCl) water solutions of fibroin improved the quality of chromatograms.

Abbreviations

A_2	Second virial coefficient in Rayleigh equation
c	Concentration of a solution, mg/ml
λ	Wavelength of incidental beam (in vacuum), nm
M_w	Weight average molar mass, derived from Rayleigh equation, g/mol
n_0	Refractive index of a solvent
N_A	Avogadro constant
dn/dc	Refractive index increment

$P(\theta)$	Form factor in Rayleigh equation
$R(\theta)$	Excess Rayleigh ratio, the difference between Rayleigh ratio for a solution and a pure solvent
g	Branching ratio
R_{lin}^2	Mean square radius of linear sample
R_{br}^2	Mean square radius of branched sample

1 Introduction

Silk fibres have been used for centuries in the textile industry due to their characteristic strength and beautiful lustre. Nowadays, thanks to its biocompatibility and biodegradability silk is finding numerous new applications in biotechnology [1] (i.e. wound dressing [2], tissue engineering [3], targeted drug delivery [4]).

The most direct information regarding the condition of the historical silk textiles or silk-based modern products could be obtained from measurements of the molecular weight distribution of the fibroin polymer—a major component of a silk fibre. Silk analysis by size exclusion chromatography (SEC) is, however, challenging. The difficulties arise mainly from a sample preparation method or more precisely the choice of a solvent, which in some cases could lead to degradation [5] and/or aggregation of fibroin [6]. Presented work focuses on the optimization of the sample preparation method and separation conditions to obtain reproducible and reliable results of molar mass of *Bombyx mori* silk fibroin.

Since there are no standards of fibroin of a given average molar mass, a thermal degradation can be applied to obtain a series of silk samples differing in mass. Thermal degradation effects can be classified into two groups: one involves purely physical (structural) changes in the fibre, whereas the other involves chemical changes. Thermal

D. Pawcenis (✉) · M. A. Koperska · J. M. Mileczarek ·
 T. Łojewski · J. Łojewska
 Chemistry Faculty, Jagiellonian University, Ingardena 3,
 30-060 Kraków, Poland
 e-mail: pawcenis@chemia.uj.edu.pl



Degradation markers of fibroin in silk through infrared spectroscopy

M.A. Koperska^{a,*}, D. Pawcenis^a, J. Bagniak^b, M.M. Zaitz^a, M. Missoni^c, T. Lojewski^a, J. Lojewska^a^a Jagiellońska University, Chemistry Faculty, Ingardena 3, 30-060 Kraków, Poland^b Jan Matejko Academy Of Fine Arts, 43 Matyja Square, 31-157 Kraków, Poland^c Istituto del Seta e Seta Composita, Consiglio Nazionale delle Ricerche, Via Salaria km 29.300, 00015 Monterotondo Scalo, Roma, Italy

ARTICLE INFO

Article history:

Received 26 February 2014

Received in revised form

15 April 2014

Accepted 16 April 2014

Available online 24 April 2014

Keywords:

Fibroin

ATR–FTIR spectroscopy

UV/Vis spectroscopy

XRD

SEC

Degradation estimators

ABSTRACT

Infrared spectroscopy (FTIR) is a commonly available tool in laboratories dealing with both degradation of materials and conservation of art objects to evaluate their condition. In this paper FTIR was engaged to study degradation of fibroin included in silk samples (*Bombyx mori*) artificially aged at various conditions (oxygen, water vapor and volatile organic products) at temperature of 150 °C. The results collected by Attenuated Total Reflectance/Fourier Transform Infrared Spectroscopy (ATR/FTIR) were validated by UV/Vis, XRD and SEC analyses. Based on the results, the degradation estimators were verified and classified as: (1) crystallinity defined as ratio of absorbance at 1620 and at 1656 cm⁻¹, A_{1620}/A_{1656} [1], or at 1620 and 1699 cm⁻¹, A_{1620}/A_{1699} [2]; or ratio of areas under fitted curves of band at 1261 and 1230 cm⁻¹, P_{1261}/P_{1230} [3]; (2) oxidation – A_{1620}/A_{1656} and (3) depolymerization – P_{1261}/P_{1230} . Degradation gauges defined in such a way indicate that upon artificial aging water vapor and oxygen has the most profound impact on the progress of silk degradation. It also indicates that oxygen-lean conditions stabilize silk at elevated temperature.

© 2014 Elsevier Ltd. All rights reserved.

1. Introduction

From sometime before the middle of the 3rd millennium BC, people have spun silk into threads and from these they produced textiles [4]. Silk can be found in garments, upholstery, banners or rugs and thus is abundantly present in museum collections all over the world. In 21st century, silk has been rediscovered and it is being extensively exploited for new material engineering especially for biomedical applications [5]. Unfortunately with time, silk loses its appealing properties like strength and lustre, becomes brittle and yellows, comes to be hard to handle, exhibit and use. Thus fought-through preservation of cultural heritage imprinted, painted or woven into a silk fabric is impossible without thorough understanding of the mechanisms that triggers silk degradation processes. Understanding mechanisms of long-term degradation can also contribute to understanding silk for material development purposes.

Silk can be regarded as a semi-crystalline biopolymer with highly organized nanocrystals surrounded by amorphous matrix

[6] as shown in Fig. 1. The mulberry silk (in contrast to the non-mulberry one) is synthesized by the glands of a silkworm *Bombyx mori*, in a form of a fiber, to form a protective cocoon. Silk fibers are composed of two main proteins: fibroin (around 66 wt%) and sericin (about 26 wt%) [6–8], however, the latter together with impurities is removed from the thread during the manufacture processes in textile industry. Fibroin macro fibrils (width of up to 6.5×10^3 nm) consist of helically packed nanofibrils 90–170 nm in diameter [9], which in turn are built of heavy and light polypeptides of ~350 kDa and ~25 kDa, respectively [6,7]. The protein tertiary structure is stabilized by: van der Waals bonds – between the segments of the peptide; hydrogen bonds – at a distance of 0.5 nm from the –C=O and –N–H groups of an adjacent peptide; and disulphide cross-links – covalent bonds between two cysteine amino acids of neighboring chains or within a single one [10].

The most important amino acids found in fibroin primary structure are: glycine (44.6%), alanine (29.4%), serine (12.1%), tyrosine (5.1%), valine (2.2%), aspartic acid (1.3%), leucine (1.2%), glutamic acid (1.0%), threonine (0.9%), arginine (0.5%), proline (0.4%), phenylalanine (0.4%), lysine (0.3%), cysteine (0.2%), histidine (0.1%) and tryptophan (0.1%) [7]. But their distribution throughout the protein varies. Some regions are constructed of patterns only made of the simplest amino acids ((–Gly–Ala–Gly–Ala–Gly–Ser–Gly–Ala–Ala–Gly–[Ser–Gly–(Ala–Gly)₂]³–Tyr) [10]) arranged

* Corresponding author. Tel.: +486132087.

E-mail addresses: mkoperska@gmail.com, monika.koperska@uj.edu.pl (M.A. Koperska).<http://dx.doi.org/10.1016/j.polydegstab.2014.04.008>

0141-3910/© 2014 Elsevier Ltd. All rights reserved.

5. Evaluating degradation of fibroin by ATR-FTIR: case study of historic textiles from Polish collections

Spectrochimica Acta Part A: Molecular and Biomolecular Spectroscopy 135 (2015) 576–582



Contents lists available at ScienceDirect

Spectrochimica Acta Part A: Molecular and
Biomolecular Spectroscopy

journal homepage: www.elsevier.com/locate/saa

Evaluating degradation of silk's fibroin by attenuated total reflectance infrared spectroscopy: Case study of ancient banners from Polish collections

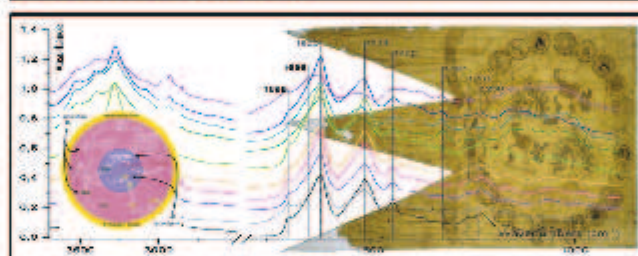
M.A. Koperska^{*}, T. Łojewski, J. Łojewska

Jagiellonian University, Chemistry Faculty, Ingardena 3, 30-060 Kraków, Poland

HIGHLIGHTS

- ATR-FTIR estimators to describe crystallinity and oxidation of fibroin were chosen.
- A new, proposed estimator E_{COOH} monitors the hydrolysis of fibroin.
- ATR-FTIR estimators were classified as primary and secondary structure estimators.
- Primary and secondary structure estimators help in museum objects' risk assessment.
- Estimators can discriminate surfaces directly exposed to ex humidity, pollution.

GRAPHICAL ABSTRACT



ARTICLE INFO

Article history:

Received 31 December 2013
Received in revised form 12 May 2014
Accepted 13 May 2014
Available online 8 July 2014

Keywords:

Fibroin
ATR-FTIR spectroscopy
Degradation estimators
Historic silk samples

ABSTRACT

In this study a part of research where artificially aged model samples were used as a guideline to the mechanism of degradation is presented. In previous work Bombyx Mori silk samples were exposed to various environments such as different oxygen, water vapour and volatile organic products content, all at the temperature of 150 °C [1]. Based on those results gathered with by Attenuated Total Reflectance/Fourier Transform Infrared Spectroscopy (ATR-FTIR) the degradation estimators were proposed and classified as follows:

(1) Primary functional groups estimators

$E_{\frac{A_{1650/1630}}{A_{1520}}}$ – intensity ratios of Amide I C=O stretching vibration to Amide II N–H in-plane bending and C–N stretching vibrations A_{1650}/A_{1520}
 E_{COOH} – band 1318 cm^{-1} integral to band integral of CH_3 bending vibration band located at 1442 cm^{-1}
 P_{1318}/P_{1442}

(2) Secondary conformational estimators

$E_{\text{C}=\text{O}}$ – intensity ratios within Amide I C=O stretching vibration of parallel β -sheet to antiparallel β -sheet A_{1620}/A_{1630}

In this work estimators were verified against estimators calculated from spectra of silk samples from 8 museum objects: 3 from 19th, 2 from 18th, 1 from 17th and 2 from 16th century including 3 banners from the storage resources of the Wawel Royal Castle in Kraków, Poland.

© 2014 Elsevier B.V. All rights reserved.

^{*} Corresponding author.

E-mail addresses: mkoperska@gmail.com, monika.koperska@uj.edu.pl (M.A. Koperska).

6. Conclusions and guidelines for conservators

The main achievement of the work is the determination of different degradation estimators describing crystallinity, depolymerisation and oxidation states in fibroin silk by a single, spectroscopic method (ATR-FTIR). The FTIR derived estimators were validated by the independent analytical methods (XRD, SEC, UV/VIS). Both primary functional group ($E_{\text{AmideI/II}}$, E_{COOH}) and secondary conformational estimators ($E_{\text{C}=\text{O}1}$, $E_{\text{C}=\text{O}2}$, $E_{\text{C}-\text{N}}$) were justified and their meaning correctly recognised. It has been shown that peptide bond estimator ($E_{\text{AmideI/II}}$) shows mostly the oxidation effects of degradation (confirmed by UV-Vis analysis), and newly proposed by our group estimator (E_{COOH}) focuses primarily on the development of bicarboxylic groups created during hydrolysis (confirmed by mean molar mass calculated from SEC). It is worth noting that SEC analysis technique had to be carefully investigated and procedure of dialysis improved before obtaining reliable mean molar mass results for fibroin. XRD analysis proved to be helpful in choosing the crystallinity estimator that followed the crystallinity change despite the severe oxidation of degraded fibroin samples. What is important the chosen estimators allow to trace down the degradation progress of artificially aged model silk samples at different atmospheres.

The estimators were also evidenced to be useful for the evaluation of the condition of historic objects obtained from the museums. Indeed, crystallinity, oxidation and hydrolysis estimators based on non-destructive ATR-FTIR analyses can be successfully used to describe the condition of the historical silk textiles and thus help conservators with risk assessment for more efficient restoration planning. Also thanks to estimators, monitoring textile surfaces directly exposed to destructive factors like humidity and pollution, outer side of garments were confirmed to suffer greater degradation state than the ones hidden from such influences. Basing on the values of crystallinity and oxidation estimators a straight forward “age of sample” cannot be approximated but some indication of correlation of estimator with age of the sample was shown by hydrolysis estimator E_{COOH} .

Moreover some macroscopic estimators such as mass loss, tensile strength, colour change (in the CIEDE 2000 colour space), viscosity and pH, especially interesting from the point of view of silk end-users, were put under scrutiny. It was shown that mass loss is a sensitive and discriminative indicator of silk degradation especially when it comes to changes induced by hydrolysis. Colour change ($L^*a^*b^*$, ΔC^* and Δh^* parameters) on the other hand is helpful to monitoring the appearance of new functional groups that evolve during especially the oxidation pathway of silk degradation. The change in tensile strength is resulting of a complexity of all degradation reactions and thus its ability to differentiate between different

reaction pathways is low. It was reported that pH values bear such complex information drawn from measurement of electrode in contact with silk fibres and such high uncertainty that it would be rather risky to draw any solid conclusions from it. The polypeptide masses calculated from viscosity seem to follow the trend of oxidation rather than hydrolysis and thus are hard to interpret. The usage of carefully and thoroughly prepared SEC analysis seems to give more reliable results to viscosity possibly due to salt pollution.

What stems from the results is that the most detrimental variables affecting fibroin depolymerisation and oxidation is humidity and keeping silk textiles in dry conditions can be crucial for ensuring its longevity. Volatiles can also accelerate the degradation process, especially the oxidation path thus purging any enclosed silk storing compartments is very advisable. Effects of the oxygen-lean conditions are only shown when some humidity is involved, but one must remember that model samples were not dyed, and anoxic environment is especially important in colour preservation of dyed materials [21]. These conclusions can be beneficial for art conservations when planning storage of historic, silk based objects and are already considered by leading museums in Poland as Wawel Castle Museum in Cracow.

Bibliography

1. The Silk Road: A Very Short Introduction (Very Short Introductions) by James A. Millward, oxford University Press, ISBN: 0199782865, 2013;
2. Global Silk Industry: A Complete Source Book by Rajat K. Datta, Mahesh Nanavaty, Universal-Publishers, ISBN: 1581124937, 2005;
3. <http://wawel.krakow.pl/pl/zalaczniki/Chor%C4%85gwie%20w%20zbiorach%20ZKW.pdf>;
4. Dziesięciolecie Polski odrodzonej 1918-1928, edited by Marian Dąbrowski, Kraków-Warszawa, ISBN: 8390306581, 1928;
5. Encyclopaedia Britannica, ed. Charles Van Doren, pub. Encyclopedia Britanica Inc.
6. A text book of fibre science and technology, Mishra (principal of Institute of Textile Technology), New Age International, ISBN 8122412505, 2000;
7. Chemical principles of textile conservation by Ágnes Tímár-Balázs and Dinah Eastop, ISBN: 0750626208, 2011;
8. Handbook of fiber chemistry, Lewin, CRC PRESS, ISBN 0824725654, 2006;
9. Historic textile and paper material, Becker B., III ASC symposium series 410, vol. 95. American Chemical Society; 1989.
10. Spider Silk Aging: Initial Improvement in a High Performance Material Followed by Slow Degradation, Agnarsson, Boutry, Journal of experimental zoology, Vol. 309A, 494-504, 2007;
11. Weighted silk: history and conservation, Hacke, Reviews in Conservation, No. 9, 3-15, 2008;
12. General Effects of ageing on textiles, R. Bresee, JAIC, Vol. 25, Number 1, 1986.
13. Conservation Science, first ed., edited by E. May, M. Jones, RSC Publishing, 2006.
14. Photochemical behavior of natural silk I-III, Baltova, Vassileva, Polymer Degradation and Stability, Vol 60, 1998.
15. Photodegradative changes in chemical structures of silk studied by pyrolysis-gas chromatography with sulfur chemiluminescence detection, Tsuge, Yokoi, ishida, Ohtani, Becker, Polymer degradation and stability, Vol. 69, 223-227, 2000.
16. Thermal behaviour of regenerated *Antheraea pernyi* silk fibroin film threated with aqueous methanol, Kweon, Park, 2000; Structural and thermal characteristics of antheraea silk fibroin/chitosan blend film, Kweon, Park, Polymer, Vol. 41, 7361-7367, 2000;
17. The inherent acidic characteristics of aged silk, Kim, Zhang, Wyeth, Preservation, Vol. 5, 41-48, 2008;
18. Degradation markers of fibroin in silk through infrared spectroscopy., Monika A. Koperska, Dominika Pawcenis, Jacek Bagniuik, Mauro Missori, Tomasz Łojewski, Joanna Łojewska, Polym Degrad Stab 2014;105:185-196.

19. Scientific analysis of ancient and historic textiles informing preservation display and interpretation. Wyeth PR, editor, Archetype Publications; pp. 137-42, 2004.
20. Fourier Transform Raman and Fourier Transform infrared spectroscopy studies of silk fibroin. Shao J, Zheng J, Liu L, Carr MC. *J Appl Polym Sci*, 96(6):1999-2004, 2005;
21. Vibrational spectroscopy techniques to study degradation of natural dyes. Assessment of oxygen free cassette for safe exposition of artifacts Monika Koperska, Tomasz Łojewski, Joanna Łojewska, *Analytical and Biochemical Chemistry*, Volume 399, Issue 9, pp 3271-3283, 2011.

List of figures

Figure 1 XVI and XVIIth century silk banners from Wawel Castle Museum.

Figure 2. Left - unit cell of fibroin *Bombyx mori* and right – structure of long-chain polymers exhibiting crystalline and amorphous regions “fringed micelle” structure.

Figure 3. Typical degradation paths of silk

Figure 4. Analytical strategy scheme

Figure 5. Historical silk storage in Wawel Castle Museum magazines.

Figure 6. Tg experiments of silk model sample performed in flow of air and argon.

Figure 7. ATR-FTIR spectra of MS aged at different temperatures in closed and open reactor after 7 days of aging.

List of tables

Table 1. Silk producing animal's scientific classification

Table 2. Composition of silk proteins depending on the origin.

Table 3. Average humidity and temperature in Wawel Castle Museum according to seasons.

Table 4. Table 4. Texture of model samples of silk– A. photographic image, B. 10x magnification, C. 40x magnification in optical microscope and D. texture specification

Table 5. Colour change expressed by ΔE for 5 model silk samples aged for 7 days at 50 °C, 150 °C and 200 °C

Table 6. Table 6. Crystallinity indexes $E_{C_{C-N}}$ and $E_{C_{C=O1}}$ and relative tyrosine content E_{TR} calculated from the ATR-FTIR spectra for aged in different temperatures MS samples.

Abbreviations

$E_{Amide\ I/II}$ - intensity ratios of Amide I C=O stretching vibration to Amide II N-H in-plane bending and C-N stretching vibrations A_{1620}/A_{1514} (symbol A stands for maximum absorbance of a band);

E_{COOH} - band 1318 cm^{-1} integral to band integral of CH₃ bending vibration band located at 1442 cm^{-1} P_{1318}/P_{1442} (symbol P stands for integral absorbance of a band);

$E_{C=O\ 1}$ - intensity ratios within Amide I C=O stretching vibration of b-sheet to a-helix/random coil motifs A_{1620}/A_{1656} ;

$E_{C=O\ 2}$ - intensity ratios within Amide I C=O stretching vibration of parallel b-sheet to antiparallel b-sheet A_{1620}/A_{1699} ;

E_{C-N} - area under fitted curves of Amide III C-N stretching and N-H bending vibration of b-sheet band to area under of the same vibration of a-helix/random coil motifs band P_{1261}/P_{1230} ;

ATR-FTIR – Attenuated Total Reflectance Fourier Transformed Infrared Spectroscopy;

SEC – Size Exclusion Chromatography;

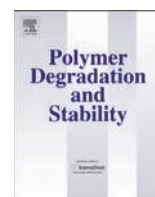
UV-Vis – UV-Vis spectroscopy;

XRF – X-ray fluorescence spectroscopy;

XRD – X-ray diffraction;

MS – model sample;

VOCs – volatile organic compounds.



Fibroin degradation – Critical evaluation of conventional analytical methods



Monika A. Koperska, Dominika Pawcenis, Jakub M. Milczarek, Andrzej Blachecki, Tomasz Łojewski, Joanna Łojewska*

Jagiellonian University, Faculty of Chemistry, Ingardena 3, 30-060 Krakow Poland

ARTICLE INFO

Article history:

Received 25 March 2015
Received in revised form
2 July 2015
Accepted 6 July 2015
Available online 15 July 2015

Keywords:

Fibroin
Artificial ageing
Viscosity
Tensile strength
Colour
CG-MS
pH
Degradation

ABSTRACT

Due to their practical importance and widespread application in the studies of polymer degradation, the analytical methods: viscometry, colour and mass change, pH, mechanical strength were selected in this work so as to provide a macroscopic view of silk condition. The aim of the current work is to critically discuss the results obtained by these methods and confront them with the silk structure and degradation mechanism. They were differentiated with several criteria such as chemical (structural) information they bear, sensitivity to the changes induced by environment and their discriminative power. The results show that tensile strength before colour change and viscosity is the most sensitive method to measure silk degradation at various conditions. Significant colour change is typical of oxygen rich degradation atmosphere and was correlated with oxidation products of fibroin. Viscosity was shown to be hard to interpret in terms of mere changes of molecular mass as the most profound effects were observed in oxygen-rich conditions. Detailed research showed that oxygen plays an important role in silk degradation but it is only when combined with closed and humid conditions that results in catastrophic change.

© 2015 Elsevier Ltd. All rights reserved.

1. Introduction

Silk fibres have been used for centuries in the textile industry due to their characteristic strength and lustre and thus can be found in many collections in museums and galleries [4]. Nowadays, thanks to its biocompatibility and biodegradability the scientific world is rediscovering silk, using it for new applications in biotechnology and biomedicine (i.e. wound dressing [5], tissue engineering [6], targeted drug delivery [7–11]). But with time silk becomes lighter, yellows and loses its strength making it hard to use and handle. The aim of this paper is to: i) critically evaluate commonly used methods of testing silk properties such as change in viscosity, tensile strength, pH and mass and ii) confront the results with the silk structure and with theory describing the mechanism of silk degradation.

Silk unique properties derive from a semi crystalline biopolymer structure, with highly organized nanocrystals surrounded by amorphous matrix [12]. The nanocrystals are organised into the secondary structure of β -sheets chains of smaller amino acids

(glycine (44.6%), alanine (29.4%) and serine (12.1%)). They build up to 70% of entire fibroin structure in *Bombyx mori* silk [13]. Packed structure is quite resistant to chemical attack and that is why it is understood that degradation starts in easy to access amorphous regions [14]. Composed of both small and large amino acids (like: tyrosine (5.1%), valine (2.2%), aspartic acid (1.3%), leucine (1.2%), glutamic acid (1.0%), threonine (0.9%), arginine (0.5%) proline (0.4%), phenylalanine (0.4%), lysine (0.3%), cysteine (0.2%), histidine (0.1%), and tryptophan (0.1%) [12]) amorphous regions take on a secondary structure of α -helix and/or random coil arrangements.

The research on silk structure and chemical properties dates back to first half of twentieth century [15]. The study on silk degradation is, however, rather scarce and incomprehensive. Critical evaluation of spectroscopic diffraction and chromatography methods on silk structure determination has been presented in our previous work [1–3]. Amino acid chains of fibroin degrade following the hydrolysis and oxidation pathways simultaneously which results in significant drop of unorganised fibroin domains that leaves silk fibre richer in crystalline regions. Hydrolysis is triggered by water reaching the peptide bond resulting in formation of carbonyl and amine groups [16]. Slower alkali hydrolysis progresses mostly from the ends of the polypeptides whereas faster

* Corresponding author.

E-mail address: jlojewska@uj.edu.pl (J. Łojewska).

acidic hydrolysis is more random and can affect not only primary but also secondary and tertiary structure (results in breaking of hydrogen and disulphide bonds) [14]. Oxidation pathway proceeds through radical reactions [14]. Oxygen radicals (induced by light especially from the UV range or heat) first attack the most reactive aromatic amino acids like: tryptophan, tyrosine and phenylalanine [16] in amorphous regions resulting in silk yellowing [17,18]. Radicals can also accelerate: a) cleavage of neighbouring peptide bonds producing α -keto-acids and dicarboxylic amino groups [17]; b) breaking of S–S bonds between Cys–Cys and then Met–Met (that underlie the secondary and tertiary structure of fibroin) [19]; c) crosslinking of the o-quinone products of tyrosine oxidation [20].

Measuring sample's viscosity and pH could be found among the first popular methods used to describe silk's fibroin in the 20's of the last century [15], mainly because simplicity and availability of the instruments and relatively simple analytical protocols. Before analysis samples had to be dissolved and thus the first problem addressed was the low solubility of fibroin in most of solvents. It was only in 1964 that the official norm of measuring the intrinsic viscosity was issued [21]. According to the norm fibroin should be dissolved in the solution of lithium bromide, although some research on weighted or aged by UV light samples showed dissolution difficult [22,23] and thus reached out for an alternative salt solution (zinc chloride) [23]. Nevertheless, if possible it is recommended to use lithium bromide solution as it does not provoke changes in fibroin chain after dissolution [13]. Viscosity measurements have proved to be a useful tool when assessing degradation of sample as reported for those artificially aged with visible [23] or gamma light [24], or treated with high temperature (150 °C in dry conditions) [23], cleaned with laser light [18] as well as those aged naturally in museum conditions [22]. Silk acidity parameter expressed by pH can be found useful to assess fibroin's degradation state. Lately, drop in the pH has been found to correlate with tensile strength loss for aged in high temperature samples (100–150 °C in dry and humid conditions) [25–27] and with viscosity decline for both historical and aged samples (by light and temperature of 150 °C in dry conditions) [8].

Amongst the methods for assessment the mechanical properties of silk the most commonly used next to bending deformation, abrasion resistance and shear stiffness are tensile properties [12]. They reflect the changes due to forces or deformations applied along the axis of a fibre and are good indicators of handling properties of the textile [28]. It seems important to highlight here the fact that silk is the strongest natural fibre with tensile strength at about 360 N/m² (but degumming drops the value by approx. 40%) [12]. However, there have been numerous publications reporting correlation between diminish in tensile strength values and historical samples age [22,29]. A good correlation has also been observed between tensile strength and time upon exposure to different agents such as light, ozone [30], hydrogen peroxide [30], high temperature [25–27].

Besides mechanical strength colour is also often regarded as a parameter describing textile endurance. It is especially important for heritage value objects as silk's yellowing tendency makes information written or painted on silk objects illegible. Therefore colour change of silk is often expressed in form of the yellowness index (integral of UV/Vis spectra) as described for the samples aged upon light [17] or ozone [30]. Rarely some more sophisticated than yellowness index parameters, as for example L*a*b* parameters derived from the CIEDE 2000 colour space, can be found. First described and used in some publications printed in the 80's, hue (Δh^*) and chroma (ΔC^*) estimators were recently found to be helpful in research dedicated to light degradation processes of silk degradation [18]. The favoured radical mechanism of both light-a thermo-induced reactions justifies applying these estimators to

analysis held in this research.

Monitoring the mass change is one of more obvious methods applied for the assessment of fibroin degradation state. It has been used for both naturally aged samples [24] and those oxidised by ozone or hydrogen peroxide [30]. Mass loss can be utilised to study kinetic aspects of silk degradation to express degradation progress. Information about the mass becomes more informative when combined with monitoring the volatile products of ageing. There is only one publication that tackles into this problem presenting basic analysis of VOCs liberated from naturally aged (over 4 years) spider silk samples and reporting ammonia detection upon ageing [31]. This is why in this paper we have also attempted to scrutinise the VOCs liberated by fibroin sample during thermo-ageing.

Beside their practical importance and widespread application, the analytical methods were selected in this study as to provide a macroscopic view of silk condition as opposed to microscopic and structural assessment of silk condition by spectroscopic (in situ ATR-FTIR, Raman), diffraction (XRD) or chromatographic (SEC) analyses reported in our previous survey [1–3]. The focus of the current work is to present a possibly comprehensive picture of macroscopic changes of silk samples by means of simple analytical tools and combine them with known degradation mechanisms. It is achieved by thorough design of ageing conditions that rely on different combinations of degradation agents applied at high temperature and reactor types. Through such combinations it is possible to discriminate (to a high extent) among hydrolytic, structural or autocatalytic (induced by degradation products) degradation pathways. A practical question to answer is how and to what extent the exposure conditions affect the chosen macroscopic features of the material and whether these simple analytical tools can be used in designing process of proper storage facilities especially in the context of museum collections.

2. Materials and methods

2.1. Textile samples

In this work plain weave silk textile was used as a model sample. Degummed and bleached *B. mori* silk textile (35 g/m²) was purchased from China by Sailong, Warsaw, Poland. Silk textile (0.075 mm thick) was cut in squares of about 5 × 4 cm resulting in samples weighing c.a. 0.070 g.

It is a common practise to use plain weave textiles during the conservation treatments of silk artefacts and similar conservation material are used by leading museums in Europe [20].

2.1.1. Ageing conditions

During artificial ageing tests silk samples were hanged in the ageing chamber (open reactor) or in closed vials (closed reactor) and heated up to 150 °C in various composition of gaseous atmosphere (aged at 3 different humidity levels: dry and in absolute humidity (AH) at 0.724 kg/m³ and 1.690 kg/m³; and in 2 different atmospheres: air and nitrogen). The detailed description of the ageing procedure and the results of previous research is described in Table 1 below and elsewhere [1]. Examples of silk samples aged from 1 to 14 days in various ageing conditions are depicted in Fig. 1.

2.2. Measurements

2.2.1. Colour

The colour measurements were performed with HUNTERLAB, ColorQuest XE apparatus with diffuse/8° geometry and 15.2 cm sphere. To assess the colour change the L*, a* and b* parameters values collected based on the CIEDE 2000 model [32]. Each value was measured as an arithmetical mean from 3 series of aged

Table 1

Conditions of artificial ageing tests in several environments (variables) influencing fibroin degradation at 150 °C has been studied from single to multivariable systems.

Ageing method label	Reactor type	Gaseous atmosphere	Environment (variables)	Expected degradation effect
O ₂	Open reactor	Air	O ₂	Oxidation
O ₂ /VOCs	Closed reactor	Air	O ₂ , VOCs	Oxidation, autodegradation
VOCs	Closed reactor	Nitrogen	VOCs	Autodegradation
O ₂ /VOCs/AH = 0.7	Closed reactor	Air, water vapour AH = 0.7 kg/m ³	O ₂ , VOCs H ₂ O (AH = 0.7)	Oxidation, hydrolysis, autodegradation
VOCs/AH = 0.7	Closed reactor	Nitrogen water vapour AH = 0.7 kg/m ³	VOCs H ₂ O (AH = 0.7)	Hydrolysis, autodegradation
O ₂ /VOCs/AH = 1.7	Closed reactor	Air, water vapour AH = 1.7 kg/m ³	O ₂ , VOCs H ₂ O (AH = 1.7)	Oxidation, hydrolysis, autodegradation
VOCs/AH = 1.7	Closed reactor	Nitrogen water vapour AH = 1.7 kg/m ³	VOCs H ₂ O (AH = 1.7)	Hydrolysis, autodegradation

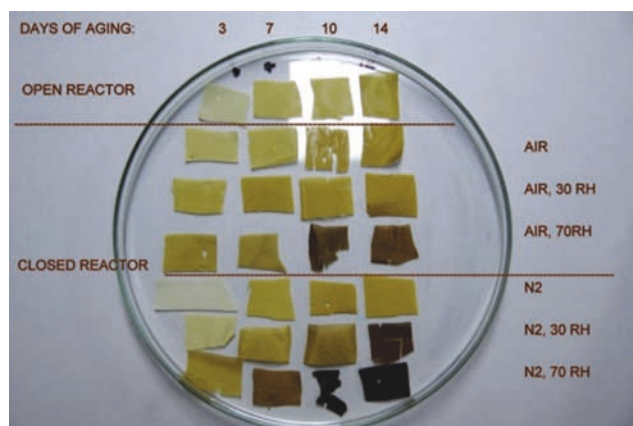


Fig. 1. Examples of silk samples after two weeks of ageing at 150 °C in 7 different atmospheres: O₂; O₂/VOCs; VOCs; O₂/VOCs/AH = 0.7; VOCs/AH = 0.7; O₂/VOCs/AH = 1.7; VOCs/AH = 1.7 (Table 1).

samples, were each sample was analysed in 3 random places and each place colour measured 3 times.

2.2.2. Viscosity

Prior to viscosity measurements the silk samples were dissolved in saturated lithium bromide water solution following the procedures developed by the Swiss Standards Association [21], 5 ml of lithium bromide was added to 110 mg of aged silk and left in a water bath at 60 °C for 3 h to fully dilute. Such solutions of fibroin were filtered through a glass filter G3 causing foaming and thus some sample loss. Calculated amount of 65 w.% glycerol was added to the sample's solution to obtain final solution ready for viscosity tests.

The relative viscosity (η_r) is a quotient of viscosity of measured substance to viscosity of reference substance. In practice it is obtained from flow time of measured (t_x) sample related to flow time of reference sample (t_0) (see Equation (1)).

$$\eta = \frac{\rho_x t_x}{\rho_0 t_0} \quad (1)$$

As densities of the samples were unknown, comparative method was used and both flow times, of LiBr solution and glycerol solution, were measured. By comparison of the flow time of glycerol measured on two Ostwald viscometers: 1 ml analysis one and 2 ml comparative one, the calibration constant (h) was calculated (Equation (2)):

$$h = \frac{t_{LiBr}^{2ml} \cdot t_{glycerol}^{2ml}}{t_{glycerol}^{1ml}} \quad (2)$$

Therefore the relative viscosity of fibroin in LiBr solution could be expressed by following Equation (3):

$$\eta_r = ht_x \quad (3)$$

During experiments, temperature of the viscometer was maintained at a constant temperature of 20.0 ± 0.1 °C. The measurements collected for 3 series of independently aged silk samples were repeated 3 to 5 times for each sample (depending on amount of sample), thus an arithmetical mean of the gathered data was calculated and taken for further analyses.

2.2.3. pH

The acidity of silk samples was determined using a flat-membrane electrode – electrode for pH measurement on surfaces. Water mili-extract was measured with Metrohm electrode using Metrohm Titrino 809 device following the TAPPI procedure (TAPPI T 529 om-09). The measurements collected for 3 series of independently aged silk samples were repeated 3 times for each sample allowing arithmetical mean to be calculated.

2.2.4. Mass loss

Each of the 3 series of samples was weighted before and after ageing on METTLER-TOLEDO (XP205) micro-analytical balance. Before weighting each sample was conditioned in dry conditions for 2 days. The quality of the VOCs eliminated from the samples during thermos-degradation was analysed by the means gas chromatography equipped with the sensitive to up to 1050 Da quadruple mass spectrometry detector (THERMO/Finnigan TRACE DSQ) and thermodesorber (PERKIN-ELMER/Turbomatrix 300TD) (TD-GC/MS). VOCs were sampled during the whole period of degradation using Thermal Desorption Tubes with Tenax filling (Sigma–Aldrich) enclosed in closed reactor. Desorption tubes were thermo-cleaned (up to 250 °C) before each ageing and conditioned before analysis.

2.2.5. Tensile strength

Mechanical properties of samples were measured on test strips of dimensions c.a. 200 × 50 mm and were acquired on an Universal Material Testing Machine (Lloyd instr.) adapting the standard method for fabric strips BS EN ISO 139341:1999. The stress–strain curve was recorded for two pieces of each sample from one series of samples aged in 7 different conditions and a mean tensile strength value calculated for each time of ageing in appropriate atmosphere.

For all measurements the statistical uncertainty was assessed as the average of the absolute deviations of data point from their arithmetic mean.

3. Results and discussion

3.1. Fibroin colour changes in CIEDE 2000 colour space

During thermo-degradation silk samples undergo visible colour change due to the formation of chromophores upon polymer oxidation. Colour analysis in CIEDE 2000 colour space revealed these phenomena to be a two stage process. For most conditions

initial colour coordinates: $L^* = 92.66 \pm 0.62$, $a^* = -0.37 \pm 0.09$, $b^* = 2.05 \pm 0.28$ change in two distinctive stages. In the first stage change can be observed mostly in the b^* values towards yellow with only a slight change in a^* towards green and decrease in L^* towards grey (see Fig. 2).

This stage takes up to 3 days for dry conditions (oxidation, see Table 1) and 1 day for all conditions where water was introduced (oxidation and hydrolysis). Only for VOCs induced degradation (1.7 AH condition) different colour fluctuations occur. Beginning with a rapid change in a^* values towards magenta and accompanied by smaller but constant rise in b^* values, colour steady decrease in L^* towards an overall reach of brown. For the VOCs, 1.7 AH conditions after 7th day second stage entails drop in b^* values towards blue together with rapid drop in L^* and rise in a^* value, ending up with more black-brown colour.

The two stage colour change is also visible in the overall colour difference parameter ΔE calculated with the CIEDE 2000 corrected model (see Fig. 3). Used equation takes into account detailed aspects of changes in lightness, chroma and hue [33] so as to replicate the intricate mechanism of colour vision and perception. After only one day of ageing ΔE of silk samples is distinguishable for average human eye (about $\Delta E = 10$ [32]), reaching a value of over 20 for fibroin aged in VOCs, 1.7 AH conditions.

Further analysis of colour change components proves to be sensitive enough to reflect chemical changes in fibroin. According to previous findings, ΔC^* reflects an increase in the abundance of polar function groups (as $-\text{OH}$ and $-\text{NH}_2$) adjacent to delocalized conjugated systems [18] that could be found among oxidation products of fibroin polypeptide (like carboxylic groups: α -keto-acids and dicarboxylic amino acids [1]). On the other hand an increase in hue angle Δh^* is found to reflect on the production of increasingly conjugated systems (like abundant in light aged silk cross linked tyrosine derived quinones systems [18]). Colorimetric measurements, applied to the thermo-aged samples, show an increase in both ΔC^* and Δh^* (see Fig. 4.). However hue angle changes are up to 80 times smaller which indicates that artificial degradation under

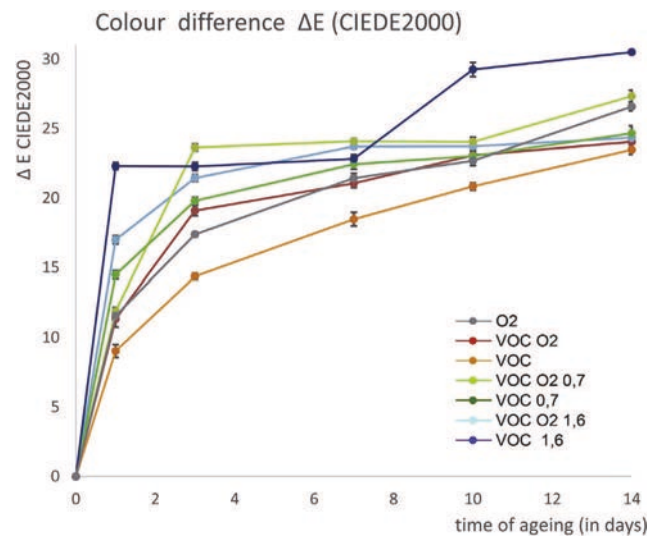


Fig. 3. Colour difference calculated with CIEDE2000 equation within two weeks of ageing at 150 °C in 7 different atmospheres.

influence of temperature (and water vapour) favours α -keto-acids and dicarboxylic amino acids formation. Increase in quinone conjugated systems is more dominant (although still disfavoured) among samples aged in high humidity (VOCs, O_2 , 0.7 AH) and especially in oxygen lean conditions (VOCs, 1.7 AH).

3.2. Peptide length by viscosity

Smallest decline of relative viscosity in 14 day ageing perspective was noted for samples aged in air open reactor (oxidation) and was analysed to be at the 63% of initial value (2.796 ± 0.004) (see Fig. 5). The appearance of VOCs (VOCs, O_2 and VOCs conditions) among ageing agents clearly accelerates breaking of the peptide

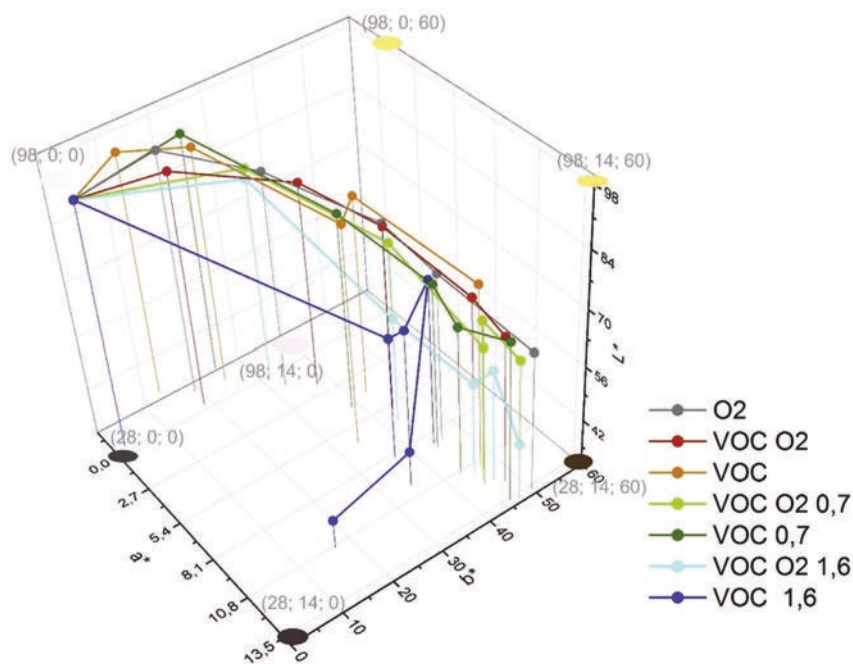


Fig. 2. Colour change represented in CIEDE 2000 colour space within two weeks of ageing at 150 °C in 7 different atmospheres: O_2 ; O_2/VOCs ; VOCs; $\text{O}_2/\text{VOCs}/\text{AH} = 0.7$; VOCs/ $\text{AH} = 0.7$; $\text{O}_2/\text{VOCs}/\text{AH} = 1.7$; VOCs/ $\text{AH} = 1.7$ (Table 1).

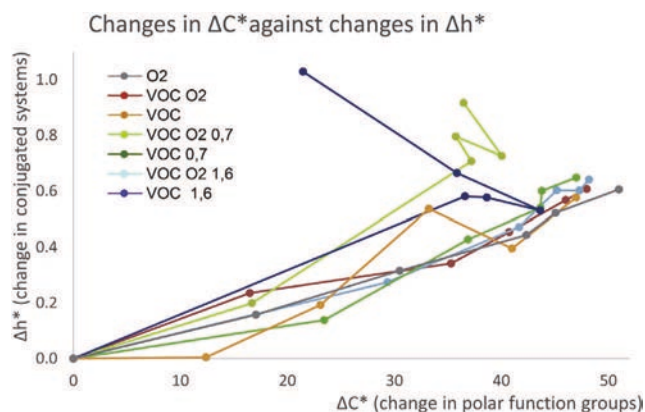


Fig. 4. Changes in Δh^* plotted against ΔC^* within two weeks of ageing at 150 °C in 7 different atmospheres (calculated using the CIEDE2000 equation for colour change).

chains thus causing the same degree of degradation in after just one day of examined thermo-ageing. After 1st day up to 14th day the relative viscosity changes not more than 9%. Major changes in relative viscosity in the first 24 h of ageing could be explained by rapid radical oxidation of fibroin (indicated by ΔE values above) that directly effects the polymer chain. This supports prior findings on molecular weight distribution drop upon thermos-ageing described elsewhere [3]. The overall influence of relative humidity on the degradation progress monitored by viscosity is rather low and noticeable also just after 1 day (about 7% gather decrease than in dry and closed reactor conditions). It is known from other studies [34] that both VOCs and water facilitate the radical oxygen formation thus accelerating oxidation. The influence of oxygen-lean conditions during ageing on the viscosity is minor (2–4% for values in all humidity variance). In all, oxygen in combination with volatile degradation products has a most profound effect on silk condition. The slightly higher value of relative viscosity in Fig. 5 for samples aged in VOCs, O₂, 0.7 AH and VOCs, 1.7 AH could be

explained by previously depicted in Fig. 4 increase in Δh^* , indicating crosslinking between tyrosine derived quinones.

3.3. Silk acidity by pH

Fibroin as a peptide is naturally rich in both $-\text{NH}_2$ and $-\text{COOH}$ groups. Therefore depending on the pH it will adopt an ionised basic or acidic form. Its isoelectric point is reached at pH of around 3.6 which is an indirect measure of the strength of acidic and basic groups [15]. Fibroin is reported to be most resistant to electromagnetic radiation at pH value close to 10 [15,35] and most prone to it around 6–8 [15]. The initial model sample's pH is at 5.32 ± 0.02 which indicates fibroin peptide prefers $-\text{COO}^-$ -end ionised form to the $-\text{NH}_3^+$ -ends one in the initial conditions.

During thermo-degradation the amount of basic and acidic end groups grows steadily throughout the degradation process (see Fig. 6). Due to the difference in dissociation equilibrium constant of both groups the increasing acidity of samples implies not only the formation of end groups but also additional acidic groups (both phenolic, carboxylic) on the polymer chains or light products of degradation of carboxylic character. They come from oxidation of alkyl or alcoholic fragments which oxidize to carboxyl groups and from aromatic rings. In this series of experiments the most significant changes of pH were observed without presence of oxygen (VOCs, H₂O (0.7 AH) and VOCs, H₂O (1.7 AH)). The resulting acidity of the peptides mix will thus depend on the equilibrium constants for the acidic groups (phenolic, carboxylic) and basic amino groups [35]. It would, however, be rather risky to draw any solid conclusions out of the pH values that bears a complex information included in the measurement of galvanic cell (electrode) in contact with fibres and also quite high experimental error.

3.4. Mass circulation

During ageing smaller and thus more volatile products of degradation can be liberated from the volume of the sample and

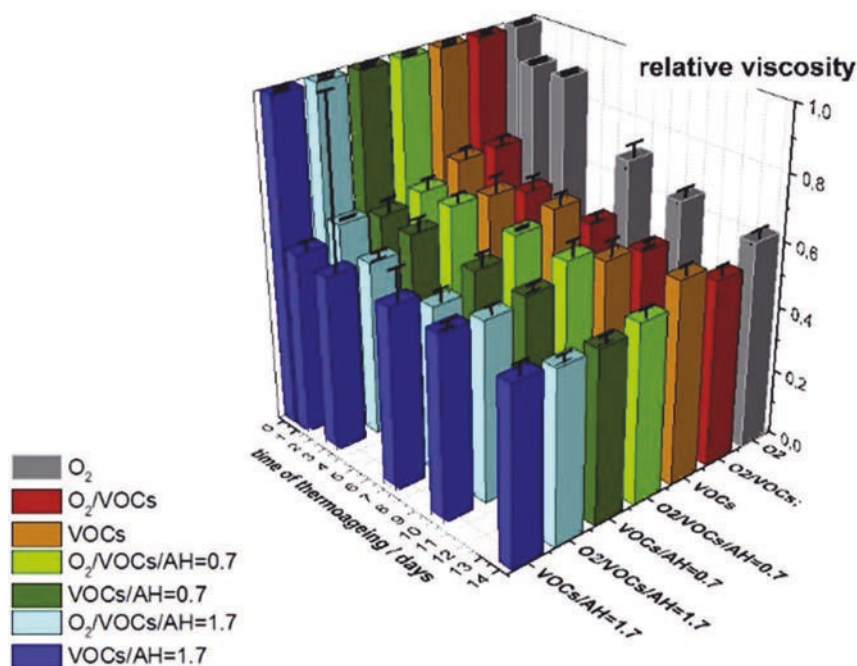


Fig. 5. Normalised relative viscosity changes within two weeks of ageing at 150 °C in 7 different atmospheres: O₂; O₂/VOCs; VOCs; O₂/VOCs/AH = 0.7; VOCs/AH = 0.7; O₂/VOCs/AH = 1.7; VOCs/AH = 1.7 (Table 1).

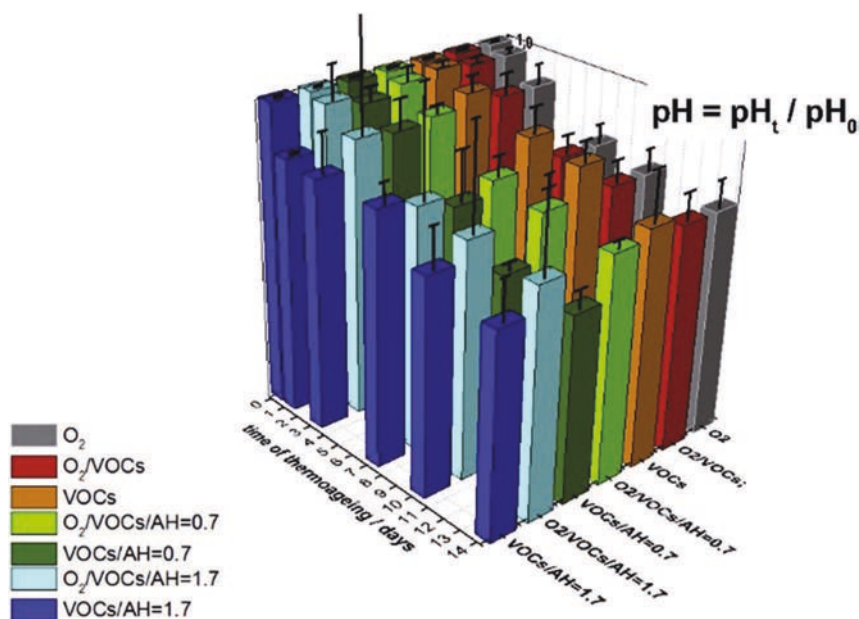


Fig. 6. Normalised pH decline within two weeks of ageing at 150 °C in 7 different atmospheres: O₂; O₂/VOCs; VOCs; O₂/VOCs/AH = 0.7; VOCs/AH = 0.7; O₂/VOCs/AH = 1.7; VOCs/AH = 1.7 (Table 1).

result in the change in its initial mass. These VOCs can in return facilitate the reactions taking place in the thermo-affected fibroin in the given volume of a closed reactor.

Based on the literature facts, it is justified to presume that amorphous regions undergo faster degradation, being more reachable to relatively small oxygen and water molecules that trigger fibroin deterioration, like another fibrous material – cellulose described in paper [36]. Also for the same reasons the VOCs are more probable to react or catalyse further reactions in non-organised regions of silk structure.

The analysis of VOCs composition by TD-GC/MS revealed its complexity. We managed to identify the following compounds (summarised in Table 2):

- ketones: butan-2-one, 5-methyl-2-hexanone, 5-methyl-3-hexanone;
- aromatic: benzene, ethylbenzene, benzaldehyde, 1,4-dimethylbenzene, methylbenzene;
- carboxylic acids: acetic acid, propionic acid;
- alcohols: n-propanol, n-butanol;
- (methyltrisulfanyl)methane and (methyldisulfanyl)methane;
- other: propyl acetate, pentane, 2-methylprop-2-enal and 1,4-dioxane.

Identified aromatic compounds may be the products of tyrosine oxidation or be the result of recombination generated by oxidation of the low molecular weight radicals (free radical thermal oxidation mechanism in Table 2). Dimethyl di- and tri-sulfide are probably the S–S bridges decomposition products. Ketones and acids could be derivatives of hydrolysed products of radical oxidation, thereby significantly shortened amino acid chains. Whereas acetic acid and propanoic acids are presumably the glycine and alanine oxidation products, an effect of the alkaline/acidic hydrolysis (see alkaline/acidic hydrolysis Table 2). It is just to presume that these liberated organic compounds will contribute to the further degradation of silk, catalysing acidic and alkaline reactions and recombining with radical products of thermal degradation.

Liberation of these gaseous compounds does leave its reminiscence in the aged sample and can be monitored by its mass loss (see

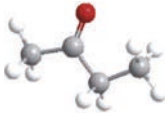
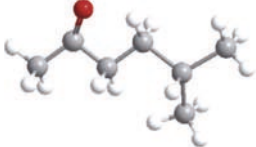
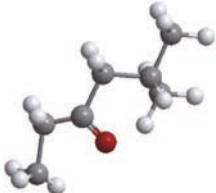
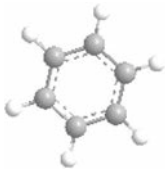
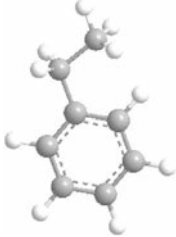
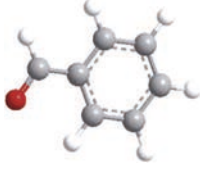
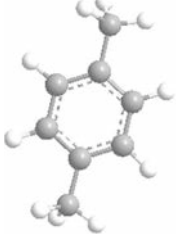
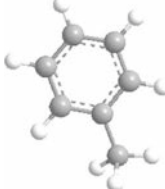
Fig. 7). Similarly to other results sample's mass drops gradually throughout the degradation process. But unlike in previous results the biggest factor on mass loss is water vapour present in the degrading atmosphere (the change is proportional to the water amount in ageing atmosphere). Thus the most profound effects were observed in simultaneous presence of 3 ageing agents: oxygen (not nitrogen), water vapour and VOCs in the reactor. That could be explained by the fact that most of the reactions triggering VOCs formation are the oxidation and hydrolysis. Water is a known oxygen radicals carrier and in this sense facilitates oxidation. On the other hand oxidation produces carboxylic groups (pH decreases) and in this way catalysis acidic hydrolysis. In this sense oxygen lean conditions or the lack of VOCs contribute to mass preservation.

3.5. Mechanical endurance

During the experiments, as the ageing process was executed, we have observed a tremendous failure in the tensile strength of the silk fabric (see Fig. 8). The results show the decreasing trend in both the load applied to the sample and its deformation ability with ageing time as can be concluded comparing the stress to strain values at rupture points (Fig. 8 (logarithmic scale)). After a few days most samples became so brittle and inelastic that it was difficult to handle them.

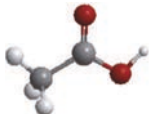
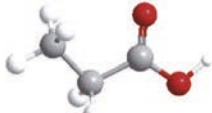
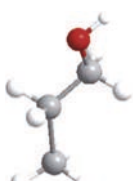
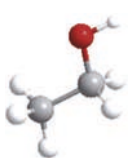
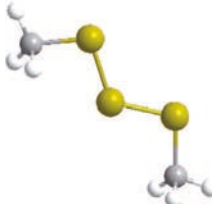
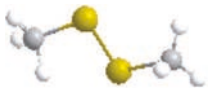
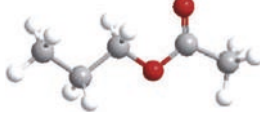

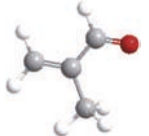
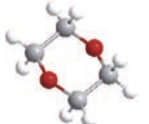
Tensile strength (TS), which is derived from the stress–strain curves obtained during a tensile test, gives an idea of the micro-structure of fibroin, or more precisely, of the combined strength of its fibres and bonding between them, which all undergo various changes with ageing time. In this way, a significant loss in tensile strength shown by aged samples can be accounted for by both the loss in the intermolecular forces, mostly hydrogen bonds, that connect together different polymer chains and by the decrease in polymerization degree. Both structural features, hydrogen bonding and polymerization degree are certainly affected in all degradation pathways including oxidation, hydrolysis and recrystallization. It is worth noting that all three degradation scenarios exert an effect on one another. The loss of elasticity and increase in brittleness is also the effect of the disappearance of amorphous regions that left the stiff and loosely connected crystalline arrangements behind. An

Table 2Table of dominant volatile organic compounds found by the GCMS analysis liberated from the silk sample aged in dry conditions in a closed reactor O₂/VOCs.

No.	Molecule scheme	IUPAC molecule name	Registered <i>m/z</i> of fragmented ions (from GC/MS analysis)
1		Butan-2-one	72, 57, 43, 29
2		5-methyl-2-hexanone	114, 81, 71, 58, 43
3		5-methyl-3-hexanone	114, 85, 57, 41
4		Benzene	78, 51, 39
5		Ethylbenzene	106, 92, 91
6		Benzaldehyde	106, 105, 78, 77
7		1,4-dimethylbenzene	106, 92, 91
8		Methylbenzene	92, 91

(continued on next page)

Table 2 (continued)

No.	Molecule scheme	IUPAC molecule name	Registered <i>m/z</i> of fragmented ions (from GC/MS analysis)
9		Acetic acid	60, 45, 43
10		Propionic acid	74, 73, 57, 55, 45, 29, 28, 27
11		n-butanol	73, 71, 57, 56, 43, 41, 31
12		n-propanol	60, 59, 42, 31
13		(methyltrisulfanyl)methane	128, 126, 111, 80, 79, 64
14		(methyldisulfanyl)methane	96, 94, 79, 64, 61, 47, 46, 45
15		Propyl acetate	73, 61, 43
16		Pentane	72, 57, 43, 42, 41
17		2-methylprop-2-enal	70, 41, 39
18		1,4-dioxane	89, 88, 58, 44, 43, 42

Typical degradation paths of silk [14]

Table 2 (continued)

No.	Molecule scheme	IUPAC molecule name	Registered m/z of fragmented ions (from GC/MS analysis)
Acidic hydrolysis			
Alkaline hydrolysis			
Free radical thermal oxidation			

increase in crystallinity upon degradation time has been evidenced in our previous work where the crystallinity estimator was verified with XRD investigation [1].

Tensile strength drops with degradation time and is sensitive to various changes in silk induced by ageing. The above interpretation of TS meaning explains why the TS drop depends on the number of

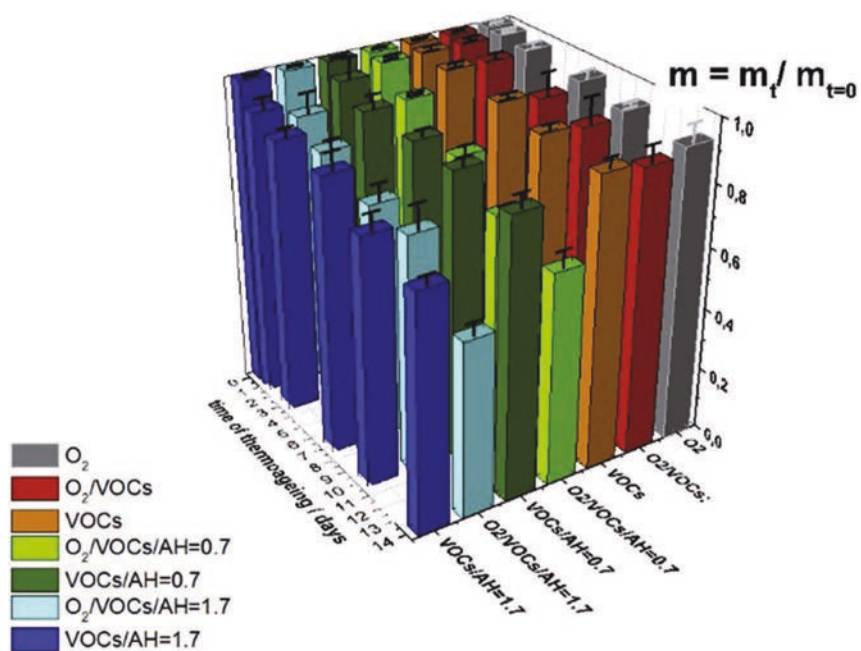


Fig. 7. Normalised mass change within two weeks of ageing at 150 °C in 7 different atmospheres: O_2 ; $O_2/VOCs$; $VOCs$; $O_2/VOCs/AH = 0.7$; $VOCs/AH = 0.7$; $O_2/VOCs/AH = 1.7$; $VOCs/AH = 1.7$ (Table 1).

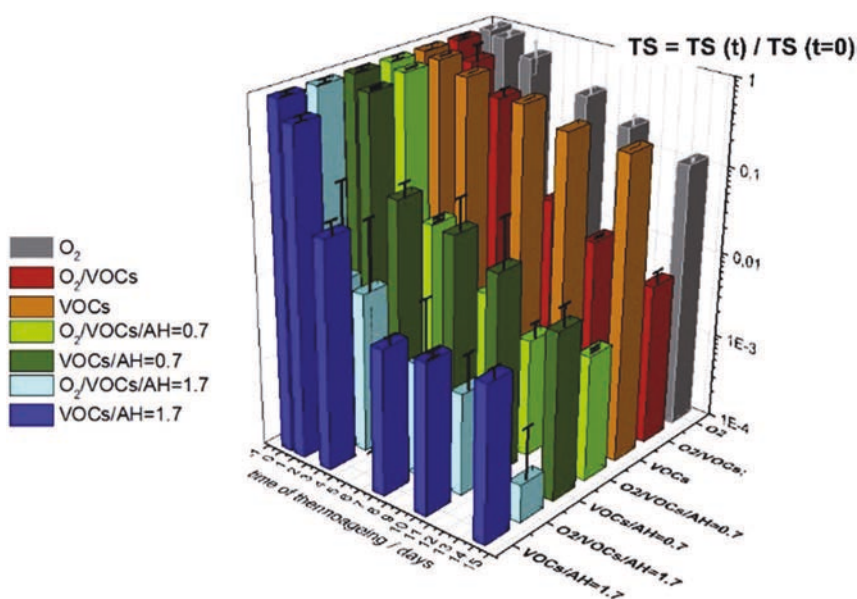


Fig. 8. Normalised tensile strength change within two weeks of ageing at 150 °C in 7 different atmospheres: O₂; O₂/VOCs; VOCs; O₂/VOCs/AH = 0.7; VOCs/AH = 0.7; O₂/VOCs/AH = 1.7; VOCs/AH = 1.7 (Table 1).

ageing agents used for sample conditioning and is the most profound for oxygen rich atmosphere with high humidity and VOCs. Gathered data also suggests that the best storing conditions are either dry or oxygen-lean (unavoidably in a closed container) or in completely open spaces.

4. Conclusions

Regarded in this work methods of evaluating silk condition chosen for their wide-spread availability and simplicity of usage have been critically evaluated for their ability of assessment the degradation stage of fibroin included in silk. Among them colour and mechanical endurance, are the most interested parameters describing material, from the point of view of silk end-users. The methods considered here have been discussed using several criteria such as chemical (structural) information they bear, sensitivity to the changes induced by environment and their discriminative power.

Even though the chemical information provided by tensile strength is rather tangled as it has been discussed in the previous section, it showing high sensitivity to the ageing conditions. Its ability to tell apart different reaction pathways is thus low (almost insensitive to the changes in O₂ and VOC), but the degradation progress followed by it depends on a number of chemical agents used in the ageing atmosphere.

A simple measurement based on the mass loss is a sensitive and discriminative indicator of silk degradation. It is most indicative of the changes induced by hydrolysis as the changes in mass depend on the water concentration (hydrolytic agent) during ageing. This complies with the evolution of VOC detected during mass loss experiments. The analysis of VOCs in return, just slightly approached in this work, can prospectively help analyse the pathways of fibroins degradation.

Other measured estimators, such as colour change, are able to monitor more selected pathways of fibroin degradation being more discriminative. Colour change is mostly due to oxidation to α -keto acids and dicarboxylic acids then caused by crosslinking of quinones as it has been shown in our previous work [1]. Both sets of parameters L*a*b* and ΔC^* and Δh^* can be connected with

chemical information on the appearance of new functional groups that evolve during degradation. In the light of our results the privileged chromophores are conjugated combinations of C=C bonds in quinones.

The information provided by viscosity measurements is not clear to interpret though it seems to be connected with the degree of polymerization of the polypeptide chains. Although relative viscosity is sensitive enough to detect changes in the polymer even after one-day ageing it seems to be less sensitive than other methods to ageing conditions. The changes in the polypeptide masses seem thus follow the trend of oxidative depolymerisation rather than hydrolysis.

The least sensitive parameter describing silk degradation is pH. Its low performance is mainly due to relatively high experimental uncertainty.

An important practical conclusion which can be drawn from the presented results is that oxygen plays an important role in silk degradation but only when combined with closed and humid conditions – that results in catastrophic change. The observation is very important for the design of the storage facilities for the culture heritage objects. The results of macroscopic changes indicate that silk textiles if framed should be put in dry, oxygen – lean conditions. What is important is the constant or periodical recirculation of gas of chosen atmosphere in the frame to eliminate accumulation of VOCs around sample.

Acknowledgements

The authors thank the Wawel Castle Museum and Anna Kli-sińska-Kopacz from Laboratory of Analysis and Nondestructive Investigation of Heritage Objects (LANBOZ), National Museum in Krakow, Poland for their help and support. Project was funded from the funds of NCN 2011/01/N/ST4/03604, FNP EX3/2012 and eea grants 11/III/2009/FWK.

References

- [1] M.A. Koperska, D. Pawcenis, J. Bagniak, T. Łojewski, J. Łojewska, Degradation markers of fibroin in silk through infrared spectroscopy, *Polym. Degrad. Stab.* 105 (2014) 185–196.

- [2] M.A. Koperska, T. Łojewski, J. Łojewska, Evaluating degradation of silk's fibroin by attenuated total reflectance infrared spectroscopy: case study of ancient banners from Polish collections, *Spectrochim. Acta A Mol. Biomol. Spectrosc.* 135 (2015) 576–582.
- [3] D. Pawcenis, M.A. Koperska, J.M. Milczarek, T. Łojewski, J. Łojewska, Size exclusion chromatography for analyses of fibroin in silk: optimization of sampling and separation conditions, *Appl. Phys. A Mater. Sci. Process* 114 (2) (2014) 301–308.
- [4] D. Hoiberg (Ed.), *Encyclopaedia Britannica*, 15th ed., 2010.
- [5] H. Teramoto, T. Kameda, Y. Tamada, Preparation of gel film from *Bombyx mori* silk sericin and its characterization as a wound dressing, *Biosci. Biotechnol. Biochem.* 72 (12) (2008) 3189–3196.
- [6] Y. Wang, H.J. Kim, G. Vunjak-Novakovic, D.L. Kaplan, Stem cell-based tissue engineering with silk biomaterials, *Biomaterials* 27 (36) (2006) 6064–6082.
- [7] E. Wenk, H.P. Merkle, L. Meinel, Silk fibroin as a vehicle for drug delivery applications, *J. Control. Release* 150 (2) (2011) 128–141.
- [8] S.C. Kundu, B. Kundu, S. Talukdar, S. Bano, S. Nayak, J. Kundu, B.B. Mandal, N. Bhardwaj, M. Botlagunta, B.C. Dash, C. Acharya, A.K. Ghosh, Invited review nonmulberry silk biopolymers, *Biopolymers* 97 (6) (2012) 455–467.
- [9] A.R. Murphy, P. St John, D.L. Kaplan, Modification of silk fibroin using diazonium coupling chemistry and the effects on hMSC proliferation and differentiation, *Biomaterials* 29 (19) (2008) 2829–2838.
- [10] S. Szela, P. Avtges, R. Valluzzi, S. Winkler, D. Wilson, D. Kirschner, D.L. Kaplan, Reduction-oxidation control of beta-sheet assembly in genetically engineered silk, *Biomacromolecules* 1 (4) (2000) 534–542.
- [11] Y. Hu, Q. Zhang, R. You, L. Wang, M. Li, The relationship between secondary structure and biodegradation behaviour of silk fibroin scaffolds, *Adv. Mater. Sci. Eng.* 2012 (2012) 1–5.
- [12] M. Lewin (Ed.), *Handbook of Fiber Chemistry*, third ed., CRC Press, 2006.
- [13] E.S. Sashina, A.M. Bochek, N.P. Novoselov, D. Kirichenko, Structure and solubility of natural silk fibroin, *Russ. J. Appl. Chem.* 79 (2006) 869–876.
- [14] E. May, M. Jones (Eds.), *Conservation Science*, first ed., RSC Publishing, 2006.
- [15] M. Harris, T.B. Johnson, Study of the fibroin from silk in the isoelectric region, *Ind. Eng. Chem.* 22 (5) (1930) 539–542.
- [16] A. Timar-Balazsy, D. Eastop (Eds.), *Chemical Principles of Textile Conservation*, Butterworth-Heinemann, 1988.
- [17] S. Baltova, V. Vassileva, E. Valtcheva, Photochemical behaviour of natural silk I – III, *Polym. Degrad. Stab.* 60 (2) (1998), 53–65 and 61(3):367–373.
- [18] M.M. Strlic, K. Lerber, S. Pentzien, W. Kautek, Laser cleaning of silk: a first evaluation, in: *Proceedings ICOM Committee for Conservation*, 2005, pp. 978–988.
- [19] S. Tsuge, H. Yokoi, Y. Ishida, H. Ohtani, M.A. Becker, Photodegradative changes in chemical structures of silk studied by pyrolysis–gas chromatography with sulfur chemiluminescence detection, *Polym. Degrad. Stab.* 69 (2) (2000) 223–227.
- [20] G.D. Kang, K.H. Lee, C.S. Ki, Y.H. Park, Crosslinking reaction of phenolic side chains in silk fibroin by tyrosinase, *Fibers Polym.* 5 (3) (2004) 234–238.
- [21] Swiss Standards Association, Silk viscosity test using lithium bromide, *Text. Rundscheu* 19 (1964) 80–83 (SNV 95595-1963).
- [22] J.E. Miller, B.M. Reagan, Degradation in weighted and unweighted historic silks, *JAIC* 28 (1989) 97–115.
- [23] X.M. Zhang, S.X. Yuan, Measuring quantitatively the deterioration degree of ancient silk textiles by viscometry, *Chin. J. Chem.* 28 (4) (2010) 656–662.
- [24] Y. Yanagi, Y. Kondo, K. Hirabayashi, Deterioration of silk fabrics and their crystallinity, *Text. Res. J.* 70 (10) (2000) 871–875.
- [25] P. Garside, P. Wyeth, Crystallinity and degradation of silk: correlations between analytical signatures and physical condition on ageing, *Appl. Phys. A Mater.* 89 (4) (2007) 871–876.
- [26] J. Kim, X. Zhang, P. Wyeth, The inherent acidic characteristics of aged silk, *e-PS* 5 (2008) 41–46.
- [27] P. Garside, P. Wyeth, X. Zhang, the inherent acidic characteristics of aged silk, part II – weighted silks, *e-PS* 7 (2010) 126–131.
- [28] L. Bratasz (Ed.), *Preservation of Historic Textiles*, Institute of Museology and Collections Protection, Krakow, 2011.
- [29] M.A. Becker, Y. Magoshi, T. Sakai, Chemical and physical properties of old silk fabrics, *Stud. Conserv.* 42 (1997) 27–37.
- [30] D. Sargunamani, N. Selvakumar, A study on the effects of ozone treatment on the properties of raw and degummed mulberry silk fabrics, *Polym. Degrad. Stab.* 91 (11) (2006) 2644–2653.
- [31] I. Agnarsson, C. Boutry, T.A. Blackledge, Spider silk ageing: initial improved in a high performance material followed by slow degradation, *J. Exp. Zool. A Ecol. Genet. Physiol.* 390 (8) (2008) 494–504.
- [32] D.H. Brainard, L.T. Maloney, Perception of color and material properties in complex scenes, *J. Vis.* 4 (9) (2004) ii–iv.
- [33] G. Sharma, W. Wu, E. Dalal, The CIEDE2000 Color-Difference Formula: Implementation Notes, Supplementary Test Data, and Mathematical Observations, vol. 30(1), 2005, pp. 21–30. Onlinelibrary.wiley.com.
- [34] M. Strlic, J. Kolar (Eds.), *Ageing and Stabilisation of Paper*, Chapter 7.5, first ed., National and University Library, 2005.
- [35] M. Harris, D.A. Jessup, The effect of pH on the photochemical decomposition of silk, *J. Res. Nat. Stand.* 7 (6) (1934) 1179–1184.
- [36] T. Łojewski, K. Zieba, A. Knapik, J. Bagniak, A. Lubanska, J. Łojewska, Evaluating paper degradation progress. Cross-linking between chromatographic, spectroscopic and chemical results, *Appl. Phys. A Mater* 100 (2010) 809–821.

Size exclusion chromatography for analyses of fibroin in silk: optimization of sampling and separation conditions

Dominika Pawcenis · Monika A. Koperska ·
Jakub M. Milczarek · Tomasz Łojewski ·
Joanna Łojewska

Received: 2 July 2013 / Accepted: 5 November 2013 / Published online: 20 November 2013
© The Author(s) 2013. This article is published with open access at Springerlink.com

Abstract A direct goal of this paper was to improve the methods of sample preparation and separation for analyses of fibroin polypeptide with the use of size exclusion chromatography (SEC). The motivation for the study arises from our interest in natural polymers included in historic textile and paper artifacts, and is a logical response to the urgent need for developing rationale-based methods for materials conservation. The first step is to develop a reliable analytical tool which would give insight into fibroin structure and its changes caused by both natural and artificial ageing. To investigate the influence of preparation conditions, two sets of artificially aged samples were prepared (with and without NaCl in sample solution) and measured by the means of SEC with multi angle laser light scattering detector. It was shown that dialysis of fibroin dissolved in LiBr solution allows removal of the salt which destroys stacks chromatographic columns and prevents reproducible analyses. Salt rich (NaCl) water solutions of fibroin improved the quality of chromatograms.

Abbreviations

A_2	Second virial coefficient in Rayleigh equation
c	Concentration of a solution, mg/ml
λ	Wavelength of incidental beam (in vacuum), nm
M_w	Weight average molar mass, derived from Rayleigh equation, g/mol
n_0	Refractive index of a solvent
N_A	Avogadro constant
dn/dc	Refractive index increment

$P(\theta)$	Form factor in Rayleigh equation
$R(\theta)$	Excess Rayleigh ratio, the difference between Rayleigh ratio for a solution and a pure solvent
g	Branching ratio
R_{lin}^2	Mean square radius of linear sample
R_{br}^2	Mean square radius of branched sample

1 Introduction

Silk fibres have been used for centuries in the textile industry due to their characteristic strength and beautiful lustre. Nowadays, thanks to its biocompatibility and biodegradability silk is finding numerous new applications in biotechnology [1] (i.e. wound dressing [2], tissue engineering [3], targeted drug delivery [4]).

The most direct information regarding the condition of the historical silk textiles or silk-based modern products could be obtained from measurements of the molecular weight distribution of the fibroin polymer—a major component of a silk fibre. Silk analysis by size exclusion chromatography (SEC) is, however, challenging. The difficulties arise mainly from a sample preparation method or more precisely the choice of a solvent, which in some cases could lead to degradation [5] and/or aggregation of fibroin [6]. Presented work focuses on the optimization of the sample preparation method and separation conditions to obtain reproducible and reliable results of molar mass of *Bombyx mori* silk fibroin.

Since there are no standards of fibroin of a given average molar mass, a thermal degradation can be applied to obtain a series of silk samples differing in mass. Thermal degradation effects can be classified into two groups: one involves purely physical (structural) changes in the fibre, whereas the other involves chemical changes. Thermal

D. Pawcenis (✉) · M. A. Koperska · J. M. Milczarek ·
T. Łojewski · J. Łojewska
Chemistry Faculty, Jagiellonian University, Ingardena 3,
30-060 Kraków, Poland
e-mail: pawcenis@chemia.uj.edu.pl

treatment of silk fibroin leads to the changes in its amino acids composition and to the scissions in protein chains, which results in the changes in molar mass distribution. It is worth noting here that non-crystalline areas are more affected by heat than the crystalline ones [7].

2 State of the art in SEC analysis of silk fibroin

Traditionally, the extent of degradation of silk fabrics has been measured by the loss of its mechanical endurance [8, 9], colour [10], crystalline structure by x-ray diffraction [11, 12], and viscosity [13, 14]. However, today these have been replaced by more advanced analytical methods involving:

- solid-state ^{13}C NMR for amino acid sequences [15, 16],
- Sodium dodecyl sulphate polyacrylamide gel electrophoresis (SDS-PAGE) to measure molecular weight of silk subunits [17],
- SEC to determine molecular weight distribution [10, 14].

The latter method, size exclusion chromatography, is most commonly applied for the analysis of polymers, but fibroin problems associated with its dissolution and the stability of the obtained solution substantially limit its use.

Silk originated fibroin solutions can be obtained by two methods. In the first approach, the liquid silk secreted in the silk gland is directly dispersed in water. The other way is to use chemical agents to dissolve previously degummed silk fibroin and this technique is most often used for sample preparation for SEC analysis of silk [10, 14, 18–20]. It must be highlighted that degumming applies only to fibroin coming from extruded silk of cocoons. The degumming process is utilized to remove sericin coating from silk fibre. Dissolution of silk fibres can be processed in aqueous solutions of chaotropic salts [21] like: LiSCN [10, 14,], LiBr [6, 20, 22–25]; mixed solvents like: $\text{CaCl}_2/\text{EtOH}/\text{H}_2\text{O}$ [26] or $\text{Ca}(\text{NO}_3)_2/\text{MeOH}$ [27] and in non-aqueous solvents, e.g. hexafluoroisopropanol [18], *N*-methylmorpholine *N*-oxide [28] and *N*-methylmorpholine *N*-oxide with addition of protic solvents like DMSO [29].

Amongst the solutions of salts surveyed by Sashina et al. [21] the most popular were concentrated solutions of lithium salts such as for example LiSCN and LiBr. Aqueous solutions of lithium thiocyanate as well as lithium bromide are very good solvents for fibroin, which is assigned to the nucleophilicity of anion attacking hydroxy, amide and amino groups. Since, solvency of lithium cations is of the greatest efficiency, lithium salt solutions are the most common solvents, used for dissolution of silk fibres. The conclusion is, however, that dependently on the applied measurement technique, removal of lithium bromide

should be considered to improve the separation conditions. For various applications, dialysis appears as a method that allows easy removal of a salt from a fibroin solution. It is worth mentioning that lithium bromide in water is used as a solvent for viscosity measurements in accordance to “Silk Viscosity Test Using Lithium Bromide” standard [24].

Except LiBr, lithium thiocyanate is often used as aqueous solvent. Thiocyanate anion has slightly higher nucleophilic properties comparing to bromide anion [21]. Kim and Wyeth [10] and Tse and Dupont [14] presented relatively broad studies on silk fibroin dissolved in saturated LiSCN. Calculation of molecular weights required in both cases, subtraction of LiSCN peaks from SEC chromatograms, which could lead to systematic errors, especially for degraded silk of low molar mass. In addition, applicability of this solvent for routine SEC analyses is questionable, since typically used columns (i.e. silica-based Biosep from Phenomenex) require salt concentrations to be kept below 1 M and its pH below 7.5. Saturated LiSCN solutions (>10 M) of high pH could drastically shorten service lifetime of columns. Another obstacle is that precipitation from concentrated salt solution may cause clogging inside pipes in the chromatographic system, particularly the columns, which generally makes it difficult to conduct SEC analyses with saturated solutions.

Mixed solvent systems such as $\text{CaCl}_2/\text{EtOH}/\text{H}_2\text{O}$ or $\text{Ca}(\text{NO}_3)_2/\text{MeOH}$ seem to be superior to the single salt solutions mentioned above due to low costs and good solvency, which lead to higher concentrations of silk fibroin. Unfortunately, in these systems the loss of molecular weight of fibroin molecules is observed [20].

A simple method of sample preparation via direct dissolution of freshly spun spider silk in mobile phase of hexafluoroisopropanol (HFIP) was also described in the literature [18]. HFIP is transparent to UV light and has low refractive index (RI) which makes this solvent convenient for analyses with UV or RI detection. HFIP is also commonly used in biochemistry to monomerize β -sheet protein aggregates, thus this particularly raises its applicability in molecular weight determination which would be undisturbed by formation of aggregates.

N-methylmorpholine *N*-oxide (MMNO) was proved to be efficient solvent of silk fibroin [28], also in combination with aprotic solvents like DMSO [29]. Dissolution by MMNO occurs in the crystal regions of a protein, which are more homogeneous and contain mainly glycine and alanine amino acids. Freddi et al. [28] investigated degrading influence of MMNO on silk fibroin. Observed decrease in measured intrinsic viscosity values indicated depolymerisation of fibroin chains. Moreover, MMNO has oxidative properties, which sometimes might be an eliminating factor. For these reasons, MMNO cannot be used for investigation of silk fibroin degradation.

According to our knowledge, there were only a few approaches to silk textile analyses by SEC that consider silk fibroin degradation. It can be due to difficulties in sample preparation, proper choice of dissolving agent and its influence on separation process. In previously described studies [10, 14] of fibroin dissolution in saturated LiSCN, no further separation of dissolved fibroin and LiSCN was used which leads to the problems described above. In light of literature findings there is a need for improvement in the sample preparation method, avoiding degradation and aggregation of fibroin and that would allow analyses of fibroin fractions of low molecular weight from highly degraded silk and at the same time would not be detrimental to the SEC set-up.

In this paper, we focus on optimization of the procedure of sample preparation to obtain accurate and reproducible analyses of the molecular weights distribution of silk fibroin, also for highly degraded samples. From available options: a silk fibroin solvent and an agent for further dialysis, aqueous solution of 9.3 M lithium bromide, were chosen.

3 Experimental

3.1 Samples

3.1.1 Accelerated ageing of silk fibroin samples

Commercial degummed Chinese *B. mori* silk (35 g/m²) was used in all experiments. Prior to accelerated ageing, the samples were cut into pieces (c.a. 0.07 g), dried for 15 min at 110 °C, sealed in glass vials (acting as ageing vessels) and aged at 150 °C for 1 and 336 h (14 days). Moisture content in ageing vessels was adjusted to obtain contrasting conditions—dry, semi-humid and humid, with RH values equal, correspondingly, to 0 % RH, 30 % RH and 70 % RH as calculated for 293 K and 1,013 hPa.

3.2 Size exclusion chromatography

3.2.1 Sample preparation

Approximately 0.07 g of silk textile was dissolved in 9.3 M lithium bromide, as proposed by Swiss Standard for viscosity test of silk textiles [24]. Solutions were thermostated in water bath for 3 h at 60 °C until samples completely dissolved. Dissolution was followed by dialysis in a cellulose membrane tube (molecular weight cut-off 12.8 kDa, Sigma) against pure water (Millipore)

for 3 days. The dialysis solution was exchanged every 12 h to remove LiBr. A parallel set of fibroin samples was prepared with NaCl addition. The solutions were prepared by mixing one volume of 0.4 M NaCl solution with three volumes of each sample to obtain silk fibroin in 0.1 M NaCl. Prior to SEC analyses, samples were filtered using RC syringe filters 0.45 µm (Sartorius). For the reason that the silk fibroin solutions were transparent and had no visible insoluble residues we omitted the centrifugation step. However, it is known from the literature [30] that in the case of the silk fibroin solutions in pure water, SEC analysis has to be performed soon after dialysis due to gelation of silk fibroin after prolonged storage. Regarding NaCl influence on silk, according to our experience the samples treated with NaCl solution can be stored for much longer time with no gelation than the samples that have not been treated with NaCl. Samples used in this experiment remained liquid after 4 months of storage in a fridge. Nevertheless, due to microbial growth, it is not recommended to run SEC analysis of samples stored for long period [31], as microorganisms present in both sample and mobile phase may lead to increasing noise in the MALLS detector.

The protein concentration for dn/dc determination was measured using Bradford standard assay procedure [32].

3.2.2 Analyses

The SEC system consisted of the following items: Waters 1515 isocratic pump, Waters 717+auto sampler, a column oven, a multi angle laser light scattering detector Dawn Heleos (Wyatt Technology) and a differential refractive index detector Optilab T-rEX (Wyatt Technology), acting as a concentration sensitive detector. Both detectors, MALLS and RI, worked at the same wavelength (658 nm). In the literature [33, 34] such a SEC configuration for protein analyses is well described.

Chromatographic separation was performed on silica-based column BioSep SEC S-4000 from Phenomenex (packed 5 µm, 300 × 4.6 mm), maintained at 30 °C (the same temperature as in RI detector), a downstream guard column was used (Phenomenex, 300 × 4.6 mm). Water (HPLC grade, Carl Roth) was used as a mobile phase, with a flow rate of 0.30 ml/min. Silk fibroin samples were injected in volumes ranging from 50 to 100 µl. Each sample was analysed six times—three injections from two solutions prepared from separate pieces of fabric aged under the same conditions.

The specific refractive index increment of fibroin was determined in batch mode using differential refractive index detector Optilab T-rEX and calculated in Astra 6.0.2 software (Wyatt Technology).

4 Data processing/calculations

4.1 Chromatographic results

The determination of absolute values of molecular weights using size exclusion chromatography with MALLS detection is based on Rayleigh equation:

$$\frac{k \cdot c}{R(\theta, c)} = \frac{1}{M_w P(\theta)} + 2A_2 c \tag{1}$$

where k is a combined constant including the refractive index increment dn/dc :

$$k = \left(2\pi^2 n_0^2 \left(\frac{dn}{dc} \right)^2 \right) \left(\frac{1 + \cos^2 \alpha}{N_A \lambda_0^4} \right) \tag{2}$$

There are several parameters that have to be known to apply Rayleigh equation: fibroin concentration c , its specific refractive index increment dn/dc and second virial coefficient A_2 .

Concentration values came from differential refractive index detector (concentration sensitive). Specific refractive index value was obtained from four batch measurements of five different concentration of fibroin in water, ranging from 0.035 to 1.764 mg/ml and was equal to 0.171 ± 0.007 ml/g. In general, most proteins have a dn/dc value close to 0.170 ml/g independently of amino acid composition [35].

Second virial coefficient A_2 has not been successfully determined yet. On-line approach to A_2 calculation was performed. A phrase “on-line determination” may indeed seem a little odd, but it has been used in the literature before [36]. Thus, the on-line determination of A_2 means that it has been derived from the experiments performed by injecting a series of known concentrations of the fibroin in an ascending order to a SEC column. If the mass recovery from such experiments is 100 % than this approach can be used to construct Zimm’s plot. However, the values obtained in that procedure were ambiguous, probably due to co-elution of fibroin protein adsorbed on column during previous runs. This phenomenon is quite common for SEC of protein, especially when pure water as mobile phase is used. Co-elution was not observed during a standard SEC analysis probably due to long enough intervals between sample injections. However, we would like to admit that during the on-line A_2 determination, eluting peaks (in the interval c.a. 15 min) were slightly noisy and somewhat distorted. To avoid molar masses errors affected by the lack of second virial coefficient, very small concentrations of protein were injected to the column (order of 10^{-3} mg/ml).

Weight average molar mass from Rayleigh equation was calculated with the use of Debye’s model, which is

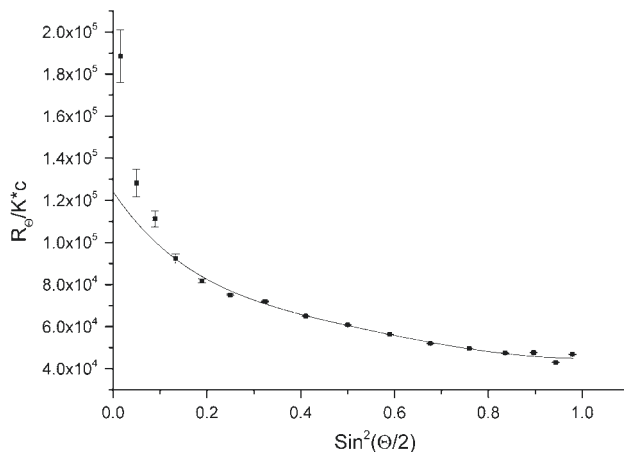


Fig. 1 Debye’s plot of angular dependence of scattered light for dialysed and separated silk fibroin (reference sample)

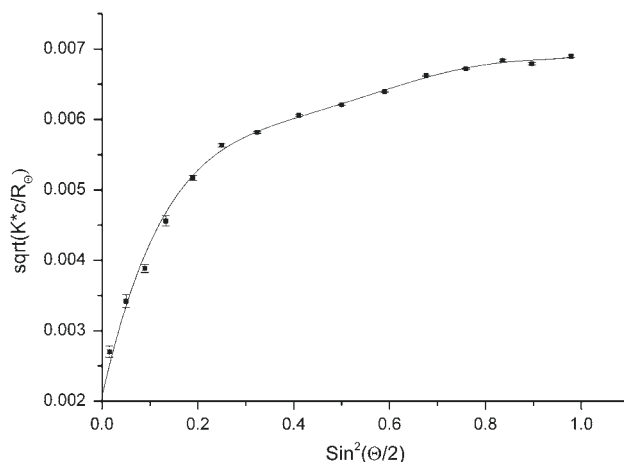


Fig. 2 Berry’s plot of angular dependence of scattered light for dialysed and separated silk fibroin (reference sample)

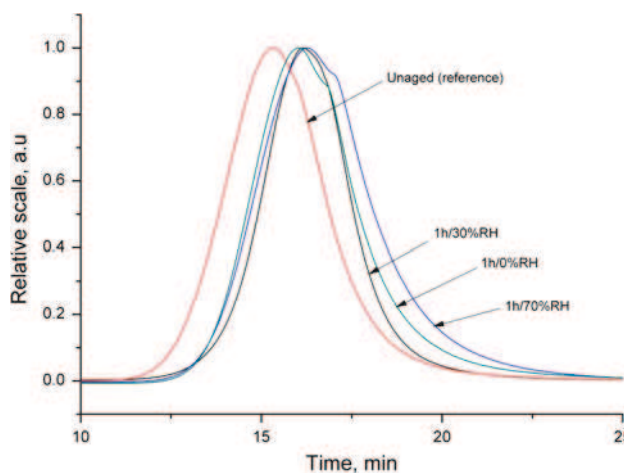


Fig. 3 Elution profile (light scattering detector) for silk samples aged for 1 h, with NaCl included in the solvent

recommended for large molecules [37]. A plot of $R_\theta/k \times c$ versus $\sin^2(\theta/2)$ was constructed. The plot was fitted by a polynomial to obtain the intercept at zero angle and the slope at zero angle as well. In this study, the fit was of the fifth order, as there was highly pronounced curvature on Debye's plot, which is assigned to find the presence of aggregates [37–39]. This curvature was presented independently of the fitting model used (comparison presented on Berry's model, which is suitable for large molecules, too).

Calibration of MALLS detector requires determination of detector constant which is a proportionality factor

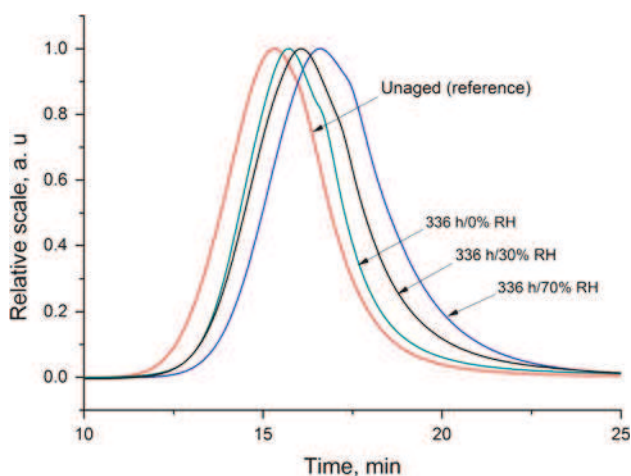
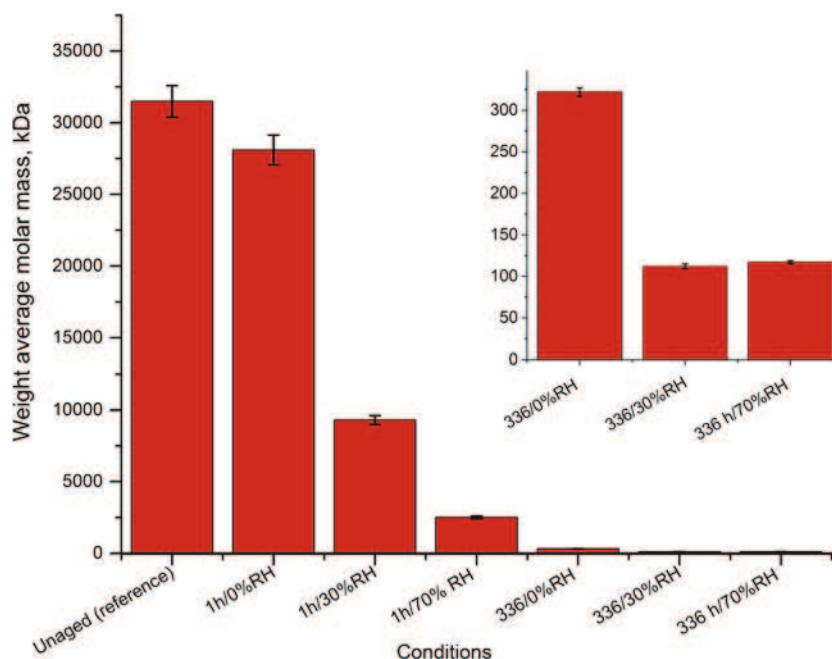


Fig. 4 Elution profile (light scattering detector) for silk samples aged for 336 h, with NaCl included in the solvent

Fig. 5 Weight average molar masses of silk fibroin before and after thermoaging, obtained by separation without NaCl addition



between the detector signal and the Rayleigh coefficient $R(\theta)$ for one photodiode (11th, on 90°). The detector constant determination was performed with toluene (HPLC purity) and was found to be $1.5511 \times 10^{-4} 1/V$. Further procedure includes normalization of other 17 photodiodes, which was done using a Pullulan standard (40 kDa, Fluka). Inter-detector delay was determined with the value of 0.9009 ml with the use of Pullulan (125 kDa, Fluka).

5 Results

5.1 Fitting model

As mentioned in section “Chromatographic results”, Debye's fitting method was applied for calculations of weight average molar mass. For all samples (reference-unaged silk, and aged samples), the curvature of Debye's plot was observed. Fitting method referring to Berry's formalism was also checked, but the difference in both results was negligible. The shapes of both plots from both methods showed curvatures (Figs. 1, 2).

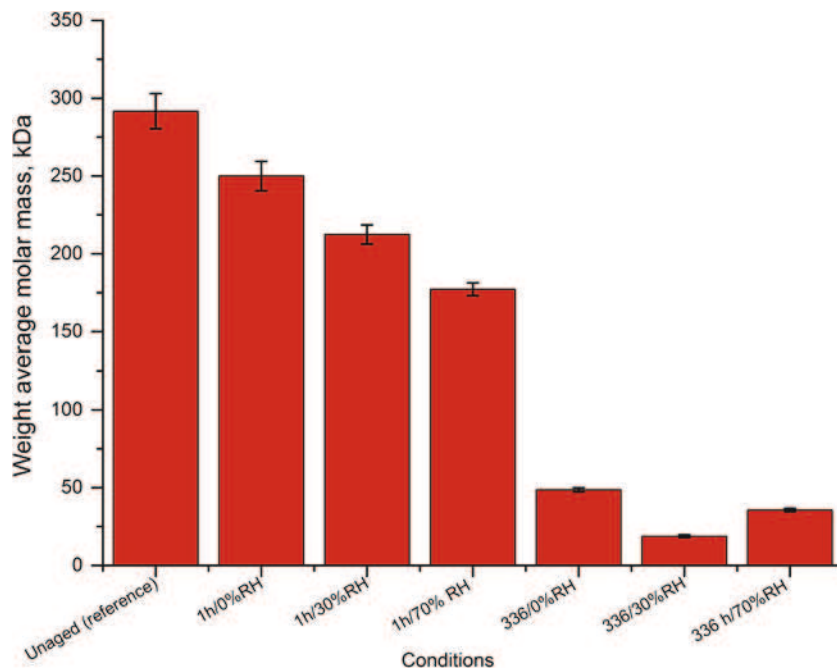
5.2 Molecular weight distribution of silk fibroin

Weight average molar mass was calculated from equation:

$$M_w = \frac{\sum H_i M_i}{\sum H_i} \quad (3)$$

We decided to use weight average molar masses, because a difference between M_w and M_v is very small

Fig. 6 Weight average molar masses of silk fibroin before and after thermoageing, obtained by separation with NaCl addition



(correlation of SEC and viscosity results for studied samples is in progress).

The elution profiles from the light scattering and refractive index detectors for the silk samples indicated a shoulder on the peak (Figs. 3, 4), coming from the occurrence of light and heavy chains in a fibroin fibre.

The observed peak can also be attributed to aggregation of fibroin molecules, taking into account the use of pure water as a mobile phase. To assess the influence of water as a mobile phase on the fibroin conformation the dependence of molar mass on root mean square radius, called a conformation plot analysis, has been obtained. Slopes derived from this relation provide the information on the conformation of a macromolecule in a given solvent. For the silk fibroin in pure water, the slopes values equal to 0.44 ± 0.08 indicate random coil conformation of a protein [40]. However, we are aware of the fact that more accurate determination requires the use of viscometric detector in SEC configuration which is not available in our laboratory.

Molecular weights obtained for experiments in which NaCl was not present may confirm aggregation phenomenon (Fig. 5). The values calculated for unaged silk textile are greater by up to 100 times in comparison with the samples where 0.1 M NaCl was added (Fig. 6). This result highlights the impact of salt presence on aggregation and separation efficiency of fibroin and supports the statement presented by Hagn et al. [41], where significant changes were observed in elution volumes of silk (specifically: N-terminal domain of spider dragline silk) when NaCl was used as an additive to the mobile phase. In addition, using dissolution in LiBr and dialysis of the silk solutions to

Table 1 Decrease in weight average molar masses with increasing ageing time compared for a set of samples with no NaCl and with NaCl

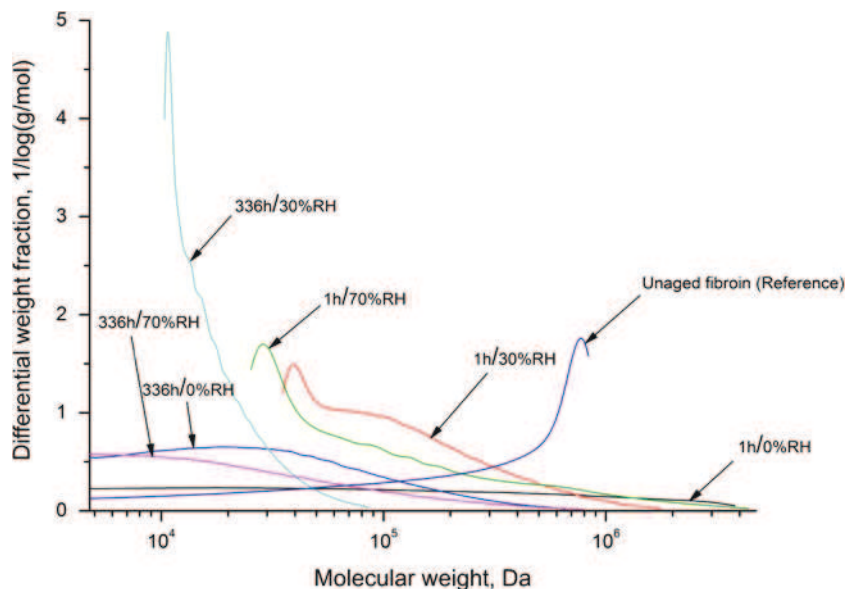
Sample	M_w [kDa] (in pure water)	σ [kDa]	M_w [kDa] (0.1 M NaCl added)	σ [kDa]
Reference (unaged)	31,490	1,100	292	11
1 h/0 %RH	28,095	1,040	250	10
1 h/30 %RH	9,296	317	212	6
1 h 70 %RH	2,506	98	177	4
336 h/0 %RH	322	5	49	1
336 h/30 %RH	112	3	19	1
336 h/70 %RH	117	2	36	1

prepare the samples overcomes the limitations of previous methods and ensures the chromatograms are not disrupted by LiSCN peaks.

The value of weight average molar mass of reference silk sample is close to the value determined with SDS-PAGE electrophoresis method (350 ± 25 kDa) [17]. Our experiments provided the value of 292 ± 11 kDa for unaged silk textile (Table 1). Thus, it supports the argument that dissolution in LiBr followed by dialysis does not cause serious depolymerisation of fibroin chain [17, 20].

It has been observed that with longer ageing time and increased relative humidity, molecular weight decreases, which is consistent with the results obtained for silk textiles artificially aged in experiments performed under other conditions than those used by authors [10, 14]. However, the measured decrease in M_w values is not linear and the greatest change is observed in first hour of ageing.

Fig. 7 Molecular weight distribution of all analysed samples (reference and thermoaged)



Molecular weight distribution curves (Fig. 7) demonstrate broad range with higher low M_w contributions for the 336 h aged samples. This may suggest a need for decreasing ageing temperature, as rapid and uncontrolled degradation of polypeptide chain can occur under these conditions. Moreover, each curve has bimodal distribution, which can be attributed both to disordered depolymerisation and simultaneous depolymerisation of light and heavy chains in fibroin.

For samples without the addition of NaCl (reference and aged for longer period of time in 70 % RH) branching ratio (g), calculated from Zimm–Stockmeyer’s Eq. (4), was lower than unity. No branching model fitted with a good accuracy, which suggests aggregation of fibroin molecules. This phenomenon is in agreement with the hypothesis stated in [6], where pronounced aggregation of silk fibroin molecules in pure water was observed. The Debye’s plot curvature mentioned above confirms this hypothesis.

$$g = \frac{R_{br}^2}{R_{lin}^2} \quad (4)$$

where R_{br}^2 and R_{lin}^2 are root mean square of a branched and linear molecule, respectively. The parameter g is also called the contraction factor. This ratio is equal to unity for linear polymers and decreases with increasing extent of branching [37].

The obtained branching ratio of a value lower than unity in this case indicates more protein aggregation rather than cross-linking, as only thermal degradation was simulated. Branching ratios for unaged fibroin and aged for 336 h were equal to 0.44 ± 0.08 and 0.83 ± 0.06 , respectively.

Cross-linking of fibroin via radical mechanism is possible under photo ageing in ultraviolet light [42].

6 Conclusions

Advantages of silk fibroin preparation involving removal of LiBr by dialysis followed by diluting with NaCl solution to obtain fibroin in 0.1 M NaCl are as follows:

- (i) No use of an agent that affects a column due to high value of pH (pH of LiBr exceeds range of pH for silica-based columns), which provides longer lifetime of columns,
- (ii) Elimination of protein molecules aggregation, which is likely to occur in LiBr and pure water,
- (iii) Good method to follow depolymerisation in fibroin, and consequently evaluating condition of historic silk textiles.

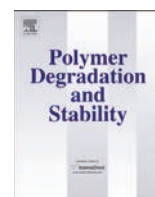
Notwithstanding the advantages presented above, a question whether the use of water as a mobile phase and addition of NaCl only to a sample is sufficient is still valid. Pure water used as a mobile phase is very convenient, as there is no need for system flushing, preparation of buffers and greater viscosity of mobile phase. However, the presence of salts in concentration up to 0.5 M is maintained to improve separation on a column and to prevent interactions between proteins in solution and proteins with column packing [43].

Acknowledgments The research was performed within SPB 811/N-COST/2010/0 from National Science Centre. Materials and chemicals were purchased thanks to financial support from National Science Centre project 2011/01/N/ST4/03604.

Open Access This article is distributed under the terms of the Creative Commons Attribution License which permits any use, distribution, and reproduction in any medium, provided the original author(s) and the source are credited.

References

1. C. Vepari, D.L. Kaplan, *Prog. Polym. Sci.* **32**, 991 (2007)
2. H. Teramoto, T. Kameda, Y. Tamada, *Biosci. Biotech. Biochem.* **72**, 3189 (2008)
3. Y. Wang, H.J. Kim, G. Vunjak-Novakovic, D.L. Kaplan, *Bio-materials* **27**, 6064 (2006)
4. E. Wenk, H.P. Merkle, L. Meinel, *J. Control. Release* **150**, 128 (2011)
5. K. Matsumoto, H. Uejima, T. Iwasaki, Y. Sano, H. Sumino, *J. Appl. Polym. Sci.* **60**, 503 (1996)
6. K.S. Hossain, N. Nemoto, J. Magoshi, *Langmuir* **15**, 4114 (1999)
7. Y. Yanagi, Y. Kondo, K. Hirabayashi, *Test. Res. J.* **70**, 871 (2000)
8. X. Zhang, I.V. Berghe, P. Wyeth, *J. Cult. Herit.* **12**, 408 (2001)
9. P. Garside, P. Wyeth, X. Zhang, *E. Preserv. Sci.* **7**, 126 (2010)
10. J. Kim, P. Wyeth, *E. Preserv. Sci.* **6**, 60 (2009)
11. A.C. Hermes, R.J. Davies, S. Greiff, H. Kutzke, S. Lahlil, P. Wyeth, C. Riekel, *Biomacromolecules* **7**, 777 (2006)
12. P. Garside, P. Wyeth, *Appl. Phys. A* **89**, 871 (2007)
13. X. Zhang, S. Yuan, *Chin. J. Chem.* **28**, 656 (2010)
14. S. Tse, A.L. Dupont, *Historic textiles, papers and polymers in museums*, in *Measuring silk deterioration by high performance size exclusion chromatography, viscometry and electrophoresis*, ed. by J.M. Cardamon, M.T. Baker (American Chemical Society, Washington, 2001)
15. T. Asakura, J. Yao, T. Yamane, K.E. Umemura, A.S. Ulrich, *J. Am. Chem. Soc.* **124**, 8794 (2002)
16. R. Chujo, A. Shimaoka, K. Nagaoka, A. Kurata, M. Inoue, *Polymer* **37**, 3693 (1996)
17. H. Yamada, H. Nakao, Y. Takasu, K. Tsubouchi, *Mater. Sci. Eng. C* **14**, 41 (2001)
18. C. Jackson, J.P. O'Brien, *Macromolecules* **28**, 5975 (1995)
19. W.A. Gaines, M.G. Sehorn, W.R. Marcotte, *J. Biol. Chem.* **285**, 40745 (2010)
20. H.J. Cho, C.S. Ki, H. Oh, K.H. Lee, I.C. Um, *Int. J. Biol. Macromol.* **51**, 336 (2012)
21. E.S. Sashina, A.M. Bochek, N.P. Novoselov, D.A. Kirichenko, *Russ. J. Appl. Chem.* **79**, 869 (2006)
22. K.S. Hossain, E. Ohya, A. Ochi, J. Magoshi, N. Nemoto, *J. Phys. Chem. B* **107**, 8066 (2003)
23. K. Sah, K. Pramanik, *Int. J. Environ. Sci. Develop.* **1**, 404 (2010)
24. Swiss Standards Association, *Silk viscosity test using lithium bromide*, textile Rundschau, **80**, 19 (1964)
25. B. Zuo, L. Liu, F. Zhang, *J. Appl. Polym. Sci.* **113**, 2160 (2009)
26. Y. Joo-Hong, L. Kwang-Gill, L. Yong-Wo, K. Sun Yeou, *Eur. Polym. J.* **39**, 1195 (2003)
27. A.B. Mathur, A. Tonelli, T. Tathke, S. Hudson, *Biopolymers* **42**, 61 (1997)
28. G. Freddi, G. Pessina, M. Tsukada, *Int. J. Biol. Macromol.* **24**, 251 (1999)
29. E.S. Sashina, N.P. Novoselov, K. Heinemann, *Russ. J. Appl. Chem.* **76**, 128 (2003)
30. A. Matsumoto, J. Chen, A.L. Collette, U.-J. Kim, G.H. Altman, P. Cebe, D.L. Kaplan, *J. Phys. Chem. B* **110**, 21630 (2006)
31. R. Scherrers, *Noise problems in SEC-MALS*, Wyatt Technology Europe GmbH 2009, support documents Wyatt Technology, <http://wyatt.eu/index.php?id=support-documents-hardware>. Accessed 3 Sep 2013
32. M.M. Bradford, *Anal. Biochem.* **72**, 248 (1976)
33. A. Oliva, M. Llabrés, J.B. Farina, *J. Pharm. Biomed. Anal.* **25**, 833 (2001)
34. K.S. Hossain, A. Ochi, E. Ooyama, J. Magoshi, N. Nemoto, *Biomacromolecules* **4**, 350 (2003)
35. J. Wen, T. Arakawa, J.S. Philo, *Anal. Biochem.* **240**, 155 (1996)
36. S. Girod, P. Baldet-Dupy, H. Maillols, J.M. Devoisselle, *J. Chromatogr. A* **943**, 147 (2002)
37. S. Podzimek, *Light scattering, size exclusion chromatography and asymmetric flow field flow fractionation* (John Wiley&Sons, Inc, Chichester, 2011)
38. P. Kratochvil, in *Light scattering from polymer solutions*, ed. by M.B. Huglin (Academic, New York, 1972)
39. A.J. Hyde, C. Wippler, *J. Polym. Sci.* **58**, 1083 (1962)
40. W.H. Fissell, C.L. Hofmann, R. Smith, N.H. Chen, *Am. J. Physiol. Ren. Physiol.* **298**, 205 (2010)
41. F. Hagn, C. Thamm, T. Scheibel, H. Kessler, *Angew. Chem. Int. Ed.* **50**, 310 (2011)
42. S. Baltova, V. Vassileva, *Polym. Degrad. Stab.* **60**, 53 (1998)
43. T. Arakawa, D. Ejima, T. Li, J.S. Philo, *J. Pharm. Sci.* **99**, 1674 (2010)



Degradation markers of fibroin in silk through infrared spectroscopy



M.A. Koperska^{a,*}, D. Pawcenis^a, J. Bagniak^b, M.M. Zaitz^a, M. Missori^c, T. Łojewski^a, J. Łojewska^a

^aJagiellonian University, Chemistry Faculty, Ingardena 3, 30-060 Krakow, Poland

^bJan Matejko Academy Of Fine Arts, 13 Matejko Square, 31-157 Krakow, Poland

^cIstituto dei Sistemi Complessi, Consiglio Nazionale delle Ricerche, Via Salaria km 29.300, 00015 Monterotondo Scalo, Rome, Italy

ARTICLE INFO

Article history:

Received 26 February 2014

Received in revised form

15 April 2014

Accepted 16 April 2014

Available online 24 April 2014

Keywords:

Fibroin

ATR–FTIR spectroscopy

UV/Vis spectroscopy

XRD

SEC

Degradation estimators

ABSTRACT

Infrared spectroscopy (FTIR) is a commonly available tool in laboratories dealing with both degradation of materials and conservation of art objects to evaluate their condition. In this paper FTIR was engaged to study degradation of fibroin included in silk samples (*Bombyx mori*) artificially aged at various conditions (oxygen, water vapor and volatile organic products) at temperature of 150 °C. The results collected by Attenuated Total Reflectance/Fourier Transform Infrared Spectroscopy (ATR/FTIR) were validated by UV/Vis, XRD and SEC analyses. Based on the results, the degradation estimators were verified and classified as: (1) crystallinity defined as ratio of absorbance at 1620 and at 1656 cm⁻¹, A_{1620}/A_{1656} [1], or at 1620 and 1699 cm⁻¹, A_{1620}/A_{1699} [2]; or ratio of areas under fitted curves of band at 1261 and 1230 cm⁻¹, P_{1261}/P_{1230} [3], (2) oxidation – A_{1620}/A_{1514} and (3) depolymerization – P_{1318}/P_{1442} . Degradation gauges defined in such a way indicate that upon artificial aging water vapor and oxygen has the most profound impact on the progress of silk degradation. It also indicates that oxygen-lean conditions stabilize silk at elevated temperature.

© 2014 Elsevier Ltd. All rights reserved.

1. Introduction

From sometime before the middle of the 3rd millennium B.C. people have spun silk into threads and from these they produced textiles [4]. Silk can be found in garments, upholstery, banners or rugs and thus is abundantly present in museum collections all over the world. In 21st century, silk has been rediscovered and it is being extensively exploited for new material engineering especially for biomedical applications [5]. Unfortunately with time, silk loses its appealing properties like strength and lustre, becomes brittle and yellows, comes to be hard to handle, exhibit and use. Thus fought-through preservation of cultural heritage imprinted, painted or woven into a silk fabric is impossible without thorough understanding of the mechanisms that triggers silk degradation processes. Understanding mechanisms of long-term degradation can also contribute to understanding silk for material development purposes.

Silk can be regarded as a semi crystalline biopolymer with highly organized nanocrystals surrounded by amorphous matrix

[6] as shown in Fig. 1. The mulberry silk (in contrast to the non-mulberry one) is synthesized by the glands of a silkworm *Bombyx mori*, in a form of a fiber, to form a protective cocoon. Silk fibers are composed of two main proteins: fibroin (around 66 wt.%) and sericin (about 26 wt.%) [6–8], however, the latter together with impurities is removed from the thread during the manufacture processes in textile industry. Fibroin macro fibrils (width of up to 6.5×10^5 nm) consist of helically packed nanofibrils 90–170 nm in diameter [9], which in turn are built of heavy and light polypeptides of ~350 kDa and ~25 kDa, respectively [6,7]. The protein tertiary structure is stabilized by: van der Waals bonds – between the segments of the peptide; hydrogen bonds – at a distance of 0.5 nm from the –C=O and –N–H groups of an adjacent peptide; and disulphide cross-links – covalent bonds between two cysteine amino acids of neighboring chains or within a single one [10].

The most important amino acids found in fibroin primary structure are: glycine (44.6%), alanine (29.4%), serine (12.1%), tyrosine (5.1%), valine (2.2%), aspartic acid (1.3%), leucine (1.2%), glutamic acid (1.0%), threonine (0.9%), arginine (0.5%), proline (0.4%), phenylalanine (0.4%), lysine (0.3%), cysteine (0.2%), histidine (0.1%) and tryptophan (0.1%) [7]. But their distribution throughout the protein varies. Some regions are constructed of patterns only made of the simplest amino acids ((–Gly–Ala–Gly–Ala–Gly–Ser–Gly–Ala–Ala–Gly–[Ser–Gly–(Ala–Gly)₂]⁸–Tyr) [10]) arranged

* Corresponding author. Tel.: +486632087.

E-mail addresses: mkoperska@gmail.com, monika.koperska@uj.edu.pl (M. A. Koperska).

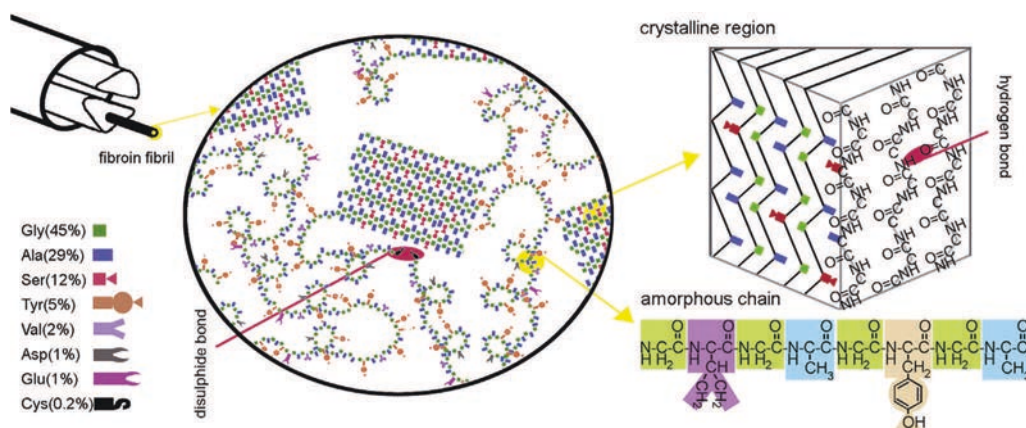


Fig. 1. Scheme of silk's fibroin primary and secondary structure.

into the crystalline regions (Fig. 1). Small functional groups such as methyl- or hydroxyl- allow chains of amino acids to be closed together making possible ordering into the secondary structure of β -sheets. Crystalline structure of *B. mori* fibroin can take up to 60–70% of entire fibroin structure [10]. Crystalline regions are surrounded by disordered chains, richer in heavier amino acids, called the amorphous parts. Ordered regions give silk its characteristic strength and non-ordered ones resilience [8]. It is the proportion of these two secondary structure states that can be manipulated by introduction of hydrophobic or hydrophilic side groups resulting in different crystallinity degree in purpose-designed material [11]. As the non-crystalline regions are more accessible to oxygen, water, enzymes and other agents there are reasons to believe that this is where the degradation processes starts and proceeds from.

Studies on the degradation of silk fibroin can be divided according to the accelerating factor, meaning biodegradation and physicochemical deterioration. Biodegradation is evaluated when various enzymes (like protease [12]) are introduced to silk solution; its effects are often monitored by the means of all IR and/or UV–Vis and XRD spectroscopies [5,12–16]. Several works show silk fibroin as a material for new cutting age technologies, especially in biomedical applications (like for bone, cartilage, adipose, and other tissue regeneration or drug delivery) due to its biodegradability and biocompatibility [5,11,14,17].

Physicochemical deterioration studies date back about 60 years [18], and include those where light as well as those where temperature (and humidity) was introduced to the experiment as the degradation triggering factor. The process of fibroin degradation induced by UV radiation enjoyed great interest among scholars. It is understandable that silk ages upon exposure to UV as it absorbs strongly in this region of radiation. In 1996, a series of publications investigating photo degradation process was published by Baltova et al. [19]. There, a model of radical oxidation of fibroin to α -keto-acids was proposed. Later Sashina et al. proposed the tyrosine oxidation mechanism that was leading to the dityrosine products that could explain the silk yellowing [10]. In 2004, Shao et al. published papers, in which experiments from FT-Raman and Attenuated Total Reflectance (ATR) FTIR spectroscopies served to prove that the contents of tyrosine and the degree of crystallinity decrease during UV evoked aging [3]. The authors also confirmed that the polymer length is reduced by breaking the C–N bonds in the peptide chain. It was also evidenced that ozone provoked degradation results in generation of amino and carboxylic groups that were later oxidized to keto-acids [20]. The first attempts to describe the long-term degradation of fibroin induced by high temperature can be assigned to year 1989. It is when Becker, during

a talk given for the American Chemical Society, proved that the temperature of 150 °C was the most suitable for the degradation of fibroin [18]. It is worth noting that his experiments were sketchy and the study was focused on numerous materials made of textiles and paper. From then infrared spectroscopic research devoted to long-term high temperature degradation of fibroin focuses on investigation of the C=O vibration regions of spectra [1,21]. Other studies have not been published in the English language (and are further discussed in Sections 3.3.1 and 3.4) [2]. XRD is one of the first methods to rich out for when trying to evaluate the crystallinity degree of silk samples [22]. UV/Vis spectroscopies have been reported to monitor biodegradation of solubilized silk [15,16] or to measure the yellowness index on UV irradiated samples [19], but rarely thermo-aged silk ones. After these years of studies a comprehensive description of silk degradation markers is still missing.

An additional aim of our work is to explore fibroin degradation by the means of the estimators and based on this look into the mechanism of silk degradation. The subject of this paper focuses only on the high temperature thermal aging therefore is restricted to only one of the mentioned above media that could artificially accelerate silk fibroin degradation processes. Motivated by the lack of comprehensive description of silk thermo-degradation markers recorded by FTIR we have attempted to test and evaluate four estimators that are quoted in publications on silk and one that we proposed on the basis of our own findings. Additionally, we want to verify what kind of physical properties the estimators can describe thus the data gathered by the means of ATR–FTIR was compared against other analytical methods like XRD, UV/Vis spectroscopies and SEC measurements. The study is hoped to provide a simple but reliable tool for assessment of silk materials condition for both textile conservators and material engineers dealing with textiles.

2. Experimental section

2.1. Initial model silk sample

In this work plain weave silk textile was used as a model sample. Degummed and bleached *B. mori* silk textile (35 g/m²) was purchased shipped from China by Sailong, Warsaw, Poland. It is a common practise to use plain weave textiles during the conservation treatments of silk artefacts [7]. Alike textiles can be found and is used by leading museums in Europe during the conservation processes.

Silk textile (0.075 mm thick) was cut in squares of about 5 × 4 cm resulting in samples weighing c.a. 0.070 g.

Table 1

Conditions of artificial aging tests performed – several environments (variables) influencing fibroin degradation at 150 °C has been studied from single to multivariable systems.

Aging method label	Reactor type	Gaseous atmosphere	Environment (variables)	Expected degradation effect
O ₂	Open reactor	Air	O ₂	Oxidation
O ₂ /VOC	Closed reactor	Air	O ₂ , VOCs	Oxidation, autodegradation
VOC	Closed	Nitrogen	VOCs	Autodegradation
O ₂ /VOC/AH = 0.7	Closed	Air, water vapor AH = 0.7 kg/m ³	O ₂ , VOCs H ₂ O(AH = 0.7)	Oxidation, hydrolysis, autodegradation
VOC/AH = 0.7	Closed	Nitrogen, water vapor AH = 0.7 kg/m ³	VOCs H ₂ O(AH = 0.7)	Hydrolysis, autodegradation
O ₂ /VOC/AH = 1.7	Closed	Air, water vapor AH = 1.7 kg/m ³	O ₂ , VOCs H ₂ O (AH = 1.7)	Oxidation, hydrolysis, autodegradation
VOC/AH = 1.7	Closed	Nitrogen, water vapor AH = 1.7 kg/m ³	VOCs H ₂ O(AH = 1.7)	Hydrolysis, autodegradation

2.2. Preparation of artificially aged samples

Silk molecular structure can undergo a glass transition transformation at temperatures above 170 °C [6]. A Thermal decomposition study of silk shows weight loss recorded in the regions 220–300 °C [23]. Taking all that under consideration thermo-aging must be performed in lower temperatures, so as not to induce additional processes that do not occur for the natural degradation changes. That is why the temperature of aging was set to 150 °C. Upon heating silk at that temperature both kinds of water molecules: adsorbed and bound in the fibroin structure can be removed together with volatile organic compounds (VOCs) liberating from the samples [23].

During artificial aging tests silk samples were hanged in the aging chamber (open reactor) or in closed vials and heated up to 150 °C at various content of gaseous atmosphere. By changing the reactor type and gaseous agent the influence of several environments (here called variables) influencing degradation were studied (Table 1). Artificial aging lasted 1, 3, 7, 10 and 14 days, allowing monitoring reasonably long time changes.

VOCs impact on silk degradation was considered by aging in closed reactors. Samples of c.a. 0.070 g of textile were put in c.a. 150 cm³ volume hybridization glass vials (acting as closed aging vessels) and were air tight locked. The amount of silk was calculated to leave access of oxygen in the vials to assure the possibility of a total oxidation of all N, C and S atoms in the fibroin molecule.

For high temperature and high humidity artificial aging, a precise amount of water was added to vials just before closing. The two partial pressures of water vapor inside vials were chosen to be smaller than the maximum saturated vapor pressure at the aging temperature (0.471 MPa at 150 °C): they were set to be 0.141 MPa and 0.330 MPa. That corresponds to the values of absolute humidity (AH) of 0.724 kg/m³ and 1.690 kg/m³, respectively. It is worth noting that above 100 °C water vapor takes a super-heated state form and relative humidity (RH) often used to describe conditions in museums is no longer valid. That is why the absolute value of humidity was calculated to describe conditions inside the chamber or a vial. Before closing the vials silk samples were dried for 15 min in 110 °C in order to desorb water, and in this way not to distort the calculated absolute humidity.

Additionally, a set of samples was aged under pure nitrogen to investigate the impact of oxygen-lean atmosphere on the fibroin degradation process (and the influence of VOCs). Oxygen-lean conditions were achieved by covering the bottom of the vial with liquid nitrogen and waiting for it to feel the interior before sealing the reactor.

2.3. Spectroscopic analysis of silk protein thermo-aged textiles

Infrared spectra were collected directly from the textile samples by means of the Fourier Transformed Infrared THERMO (Nicolet 5700) spectrometer equipped with Golden Gate attenuated total

reflection (ATR) device (MkII), with a diamond crystal. This device allows to apply a predefined and constant pressure between the sample and the ATR window.

Spectral intensities of samples having complex structure (paper, textile) may vary due to heterogeneity reasons. However, that does not represent a source of errors in this study because each estimator is obtained as a quotient of the intensities or integral of two bands. The signal was revealed by a mercury–cadmium–telluride detector (with detection range 11,000–400 cm⁻¹, and optical resolution of 4 cm⁻¹), interfaced to a personal computer. All spectra were acquired using the Omnic FTIR software averaging 200 scans.

Absorption values were calculated from baseline drawn from 1818 to 866 cm⁻¹. It is worth noting that all the samples were dried before the measurements at 110 °C for 15 min to remove the water vapor so that water vibration would not contribute to measured intensities. ATR was confirmed to be second best FTIR sampling technique for silk, proving to give more resolved spectra comparing to transmission spectroscopy or KBr disk technique, but less intense in signal to DRIFT technique [24].

FT-Raman measurements were performed with THERMO Nicolet 5700 spectrometer with Raman attachment (NXR FT-Raman, Thermo), equipped with 1064 nm Nd:YVO₄ laser and germanium NXR Genie Raman detector. Spectra were obtained with a resolution 4 cm⁻¹ and acquired using the Omnic Raman software.

X-ray diffraction (XRD) analysis was performed by means of a Bruker D2 Phaser X-ray powder diffractometer (30 kV, 10 mA) with a LYNXEYE detector using Cu K α radiation, 0.15418 nm at room temperature. The patterns were collected in the 2 θ range of 5–40 with step size of 0.02 and scan rate of 1 s.

Reflectance UV–Vis measurements (*R*) were carried out by using a THERMO Nicolet Evolution 600 spectrometer equipped with an integrating sphere (Labsphere, USA), with spectral range 190–1095 nm. Spectra were measured in the range of 190–900 nm with a resolution of 1 nm. Absorbance were calculated according to the Kubelka–Munk model, as $K/S = (1 - R)^2/2R^2$ [4].

The SEC system consisted of the following items: Waters 1515 isocratic pump, Waters 717 + auto sampler, a column oven, a multi angle laser light scattering detector Dawn Heleos (Wyatt Technology) and a differential refractive index detector Optilab T-rEX (Wyatt Technology), acting as a concentration sensitive detector. Both detectors, MALLS and RI, worked at the same wavelength (658 nm). Chromatographic separation was performed on silica based column BioSep SEC S-4000 from Phenomenex (packed 5 μ m, 300 \times 4.6 mm), maintained at 30 °C (the same temperature as in RI detector), a downstream guard column was used (Phenomenex, 300 \times 4.6 mm). Water (HPLC grade, Carl Roth) was used as a mobile phase, with a flow rate of 0.30 ml/min. Further details concerning sample preparation and molecular weight calculations were described in Ref. [25].

The spectra collected with FTIR and UV/Vis was measured for 3 separately aged silk samples and an arithmetical mean of the data

was calculated and taken for further analysis. The statistical error was calculated as the average of the absolute deviations of data point from their arithmetic mean.

3. Results and discussion

3.1. Vibrational bands assignment

The FTIR and Raman complementary spectra were collected for all initial and aged fibroin samples. Exemplary spectra of the initial fibroin sample are presented in Fig. 2. The Amide group in proteins, including fibroin, presents characteristic vibrational modes (called Amid modes) which are sensitive to protein conformation. In this way, Amid I band in 1700–1590 cm^{-1} region can be attributed to mostly C=O stretching vibrations, Amid II in 1590–1460 cm^{-1} region – to N–H bending and C–N bending vibrations, and Amid III in 1190–1280 cm^{-1} – to N–H bending and C–N stretching vibrations. As the arrangement of atoms and angles between bonds change in different secondary structure, the arrangements of polypeptide including β -sheet, α -helical, random coil, all Amid I–III bands are influenced by a local potential that arises from different conformations. In this way Amid bands become composed of vibrational modes of the same origin but of slightly different frequency [6,26–28]. Attribution of vibrations derived from the secondary structure of silk is well established in the literature and has been derived basing on the shifts upon deuteration or bands deconvolution and differentiation as summarized in Table 2.

Additionally to Amid bands the C–H bending vibrations (in the range 1460–1350 cm^{-1}), tyrosine or alanine C–N stretching vibrations (1164 cm^{-1} and 1083 cm^{-1} respectively) and C–C skeletal stretching (below 980 cm^{-1}) are present in the spectra in Fig. 2. These vibrations are relatively more intense on the Raman spectra due to the higher polarization potential, so a change in induced dipole moment upon electromagnetic radiation is higher for those particular vibrational modes [28].

3.2. Choosing thermo-degradation estimators from ATR–FTIR

Last two decades show growing interest in the following changes in the secondary structure of silk with FTIR spectroscopy [28]. Along techniques like XRD, Raman spectroscopy, ^{13}C CP/MAS NMR, XRD [29], data from FTIR are used to calculate markers for the crystalline and amorphous structure of fibroin. That finds

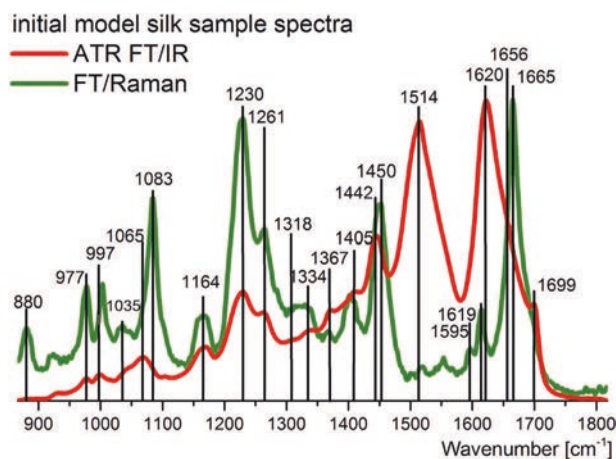


Fig. 2. ATR–FTIR and FT–Raman spectra of the model silk sample. Bands identified in Table 2 are marked with black vertical lines.

Table 2
Bands assignment of spectra shown in Fig. 2.

Wavenumber [cm^{-1}]	Attribution for fibroin [source]
1699	Amid I [peptide bond 80% C=O stretching, 10% C–N stretching, 10% N–H bending] [21,27,28,37]
1665	Amid I in antiparallel β -sheet conformation [3,37,40]
1656	Amid I in random coil and α -helical conformation [1,11];
1620	Amid I in parallel β -sheet conformation [21,27,28,31]
1595	C=C–C stretching in tryptophan [43]
1524	Amide II [peptide bond 60% N–H bending and 40% C–N bending] [11,21,31,43,35]
1442	CH ₂ , CH ₃ bending in alanine [1,3];
1405	CH ₂ bending in asparagine [12]
1367	C–H bending [12]
1334	C–H bending; phenylalanine [3]
1261	Amide III in β -sheet conformation [peptide bond 30% C–N stretching and 30% N–H bending, 10% C=O stretching/10% O=C–N bending/20% other] [3,11,21,26,35]
1230	Amide III in random coil conformation [11,21,26,35]
1164	C–N stretching in tyrosine [1,43]
1083	C–N stretching in alanine [3,39,43]
1065	CH ₃ rocking + C–N stretching [35,42]
1035	C–N stretching in phenylalanine [3,43]
997	'Gly–Ala' CH ₃ rocking [1,35]
977	'Gly–Gly' and 'Gly–Ala' C–C skeletal stretching [1,3,21,37]
880	C–C skeletal stretching, =C–H out-of-plane deformations in aromatic rings of tryptophan [3,42]

applications both for biomedical [5,12,13,29–31] and culture heritage fields [1–3,21,25,32,33].

ATR–FT/IR spectra of model silk samples aged at 150 °C for 14 days in different atmospheres described in Table 1 are depicted in Fig. 3. It is clear from the spectra that Amid I–III are those regions suffering the greatest change in relative absorption upon aging. Difference in relative intensities within Amid I band: shoulder at about 1656 and 1699 cm^{-1} appears, difference in relative

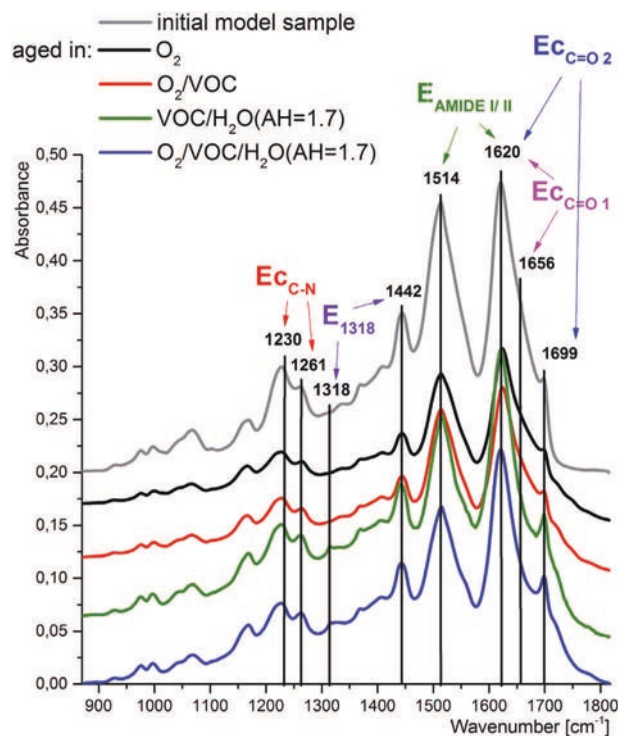


Fig. 3. ATR–FT/IR spectra of model silk samples aged in 150 °C for 14 days in different atmospheres: O₂; O₂/VOC; VOC/AH = 1.7; O₂/VOC/AH = 1.7 (Table 1).

intensities of Amid III bands and difference in relative intensities of Amid I–II bands are also visible. In addition, a new band developing at 1318 cm^{-1} is noticeable.

The literature records bands at 1620 or 1442 cm^{-1} used as an internal standard for the spectra normalization (attributed to Amide I and CH_2 , CH_3 bending in alanine) [3,13]. However, since during aging the molecules undergo structural modifications which influence bands intensities, this type of quantitative analysis was abandoned.

Instead, semi-quantitative approach was chosen by calculating relative intensities. In the literature, the ratio of two Amide I band intensities at 1615 and 1655 cm^{-1} has been considered a crystallinity index for fibroin as it reflects the relative proportion of the polymer in an organized β -sheet relative to α -helix or/and random coil arrangement [1,21,29,34]. Analogically, the Amid III bands at 1264 and 1230 cm^{-1} can lead to calculating crystallinity index basing on similar grounds [3,12,29,31,33]. Recently, a paper has been published comparing the two crystallinity indexes by Synchrotron FTIR Microspectroscopy and validating their applicability for various origin silk materials [29]. Ling et al. favored the estimators calculated from the Amid III band as Amid I can overlap with vibrations of water vapor (asymmetric water vapor deformation vibration at 1595 cm^{-1}) in the beam line. The growth of the band centered at 1699 cm^{-1} was reported during biological [30] and thermo-degradation [2] but the band's origin has been variously explained either by an increase of antiparallel β -sheet contribution or by formation of new carboxylic (COOH) groups.

Apart from secondary structure also the Amid I–II intensity ratios were considered. Monitoring this ratio allows calculation of metal uptake in polypeptide solution [35] or the N–H group formation during thermo-degradation [2].

Taking all into account ATR/FTIR of aged silk samples allowed calculating 3 crystallinity estimators (concentrated on the secondary structure of the protein), and 2 estimators looking at effects of the oxidation and hydrolysis on the primary structure of fibroin. They are defined as follows:

1. Primary functional groups estimators:

$E_{\text{Amide I/II}}$ – intensity ratios of Amide I C=O stretching vibration to Amide II N–H in-plane bending and C–N stretching vibrations A_{1620}/A_{1514} (symbol A stands for maximum absorbance of a band);

E_{COOH} – band 1318 cm^{-1} integral to band integral of CH_3 bending vibration band located at 1442 cm^{-1} P_{1318}/P_{1442} (symbol P stands for integral absorbance of a band).

2. Secondary conformational estimators:

$E_{\text{C=O } 1}$ – intensity ratios within Amide I C=O stretching vibration of β -sheet to α -helix/random coil motifs A_{1620}/A_{1656} ;

$E_{\text{C=O } 2}$ – intensity ratios within Amide I C=O stretching vibration of parallel β -sheet to antiparallel β -sheet A_{1620}/A_{1699} ;

$E_{\text{C-N}}$ – area under fitted curves of Amide III C–N stretching and N–H bending vibration of β -sheet band to area under of the same vibration of α -helix/random coil motifs band P_{1261}/P_{1230} .

The FTIR estimators were verified against calculations from other spectroscopies. The crystallinity change was reinvestigated with XRD analyses of the same samples; oxidation and hydrolysis products of degradation with UV/Vis spectroscopy (chromophores in form of conjugated double C=C groups and carbonyl groups) and size exclusion chromatography, respectively.

The crystallinity estimators from point 1 of the above mentioned list are found in the literature and were described

above. The carbonyl groups estimator from point 2 is proposed in this paper. Raman data collection for aged samples was found problematic due to absorption of 1064 nm laser light by aged, yellowed samples. Resulting fluorescence gave rise to baseline elevation and signal from sample diminished. Only the FTIR data were utilized for calculating degradation estimators.

3.3. Primary FTIR estimators for hydrolysis and oxidation assessment

3.3.1. $E_{\text{Amide I/II}}$ as an oxidation measure

$E_{\text{Amide I/II}}$ estimator (Section 3.2) was found in the literature to be used for describing the thermo induced degradation (the interpretation of the estimator is not clear as the article is in Chinese) [2] or as a tool in investigation of the binding mode of metal cations to chemically modified *B. mori* silk fibers [35].

In majority of aging conditions the general trends in $E_{\text{Amide I/II}}$ are increasing as depicted in Fig. 4. Only slight (within the upper limits of the 17% relative error) increase after 14 day aging was triggered in open and closed reactors for dry conditions. That observation stands in agreement with findings by Zhang and Yuan [2] and can be explained by radical oxidation pathway resulting in new carbonyl group formation. No significant changes were spotted by this estimator during aging at oxygen-lean conditions. $E_{\text{Amide I/II}}$ grows significantly with gradual increase of water vapor concentration (from AH = 0.7 to AH = 1.7) in aging atmosphere and rises by about 23% for samples aged in 1.7 kg/m^3 AH atmosphere.

Upon hydrolysis of peptide bonds the intensities of both bands of Amide I and II should decline. Due to significantly higher molar absorptivity (extinction coefficients) of C=O groups from the peptide bonds in comparison with the N–H groups we should observe a strong decreasing tendency of the $E_{\text{Amide I/II}}$ upon aging time [28], which is not the case at the majority of aging conditions. The $E_{\text{Amide I/II}}$ estimator seems thus to reflect more oxidation of polypeptide to ketones (also *o*-quinone), aldehydic or carboxylic groups rather than its hydrolysis. In our previous FTIR studies of cellulose oxidation the bands at around 1610 cm^{-1} have been assigned to conjugated ketones formed on glucopyranose rings [36]. Indeed, the vibrations of ketonic and aldehydic groups being observed in the wide range of frequencies between 1850 and 1600 cm^{-1} [37] can influence the intensity of the Amide I band at 1620 cm^{-1} .

The oxidation of fibroin explains an increase of the estimator during aging. Its fluctuations observed at dry aging conditions can

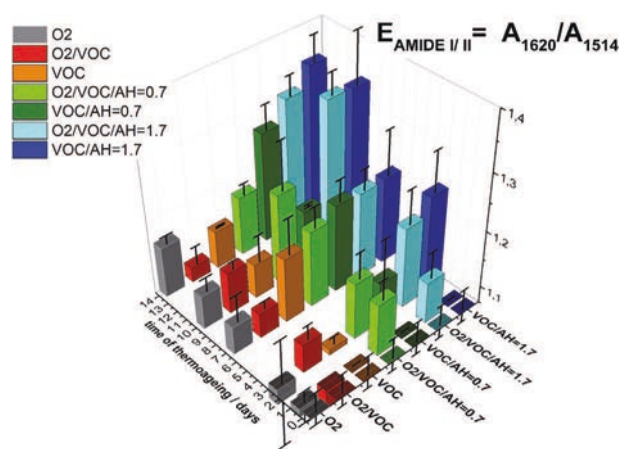


Fig. 4. Degradation estimator $E_{\text{Amide I/II}}$ (A_{1620}/A_{1514}) absorbance ratios of Amide I C=O stretching vibration to Amide II N–H in-plane bending and C–N stretching vibrations calculated for model silk samples aged in $150\text{ }^\circ\text{C}$ in 7 different atmospheres: O_2 ; O_2/VOC ; VOC ; $\text{O}_2/\text{VOC}/\text{AH} = 0.7$; $\text{VOC}/\text{AH} = 0.7$; $\text{O}_2/\text{VOC}/\text{AH} = 1.7$; $\text{VOC}/\text{AH} = 1.7$ (Table 1).

be accounted for by different contributions of hydrolysis and oxidation at degradation advancement. A rapid growth of $E_{Amide\ I/II}$ in humid atmosphere is due to catalyzing effect of, water molecules, that are a known source of radicals and active oxygen species [38], facilitate radical oxidation of polypeptide. Similar acceleration of oxidation at humid conditions has been observed during cellulose oxidation in the presence of water vapor like Strlič and Kolar et al. [38].

3.3.1.1. Correlations with UV/Vis results. The oxidation of fibroin was verified in the UV/Vis range of fibroin spectra. The peptide groups of the protein main chain absorb light in the high energy UV range (180–230 nm) [39]. This should be attributed to the bimodal band at 216 and 236 nm depicted on Fig. 5. Aromatic amino acids from the amorphous regions of the chains additionally absorb light in energy range 240–300 nm causing carbonyl and $\pi-\pi^*$ electron transitions. On the initial sample spectra asymmetric band centered at 280 nm can be attributed to Tyr, Trp, Phe, as these absorb at 275, 280, 258 nm respectively [11,39,40]. To understand the contribution of aromatic amino acids to this band it should be noted that although absorption coefficient of tryptophan is much higher than that of tyrosine and phenylalanine (in solution: 5500, 1490, 200 ($L\ mol^{-1}\ cm^{-1}$), respectively [39]), tyrosine is the most abundant in silk fibroin of the 3 amino acids (1.1, 51.7, 6.3 (g/1000 g fibrous protein), respectively [10]). Additionally, a shoulder band at 260 nm could be attributed to bonds that form between two Cys residues, so called disulphide bonds [39].

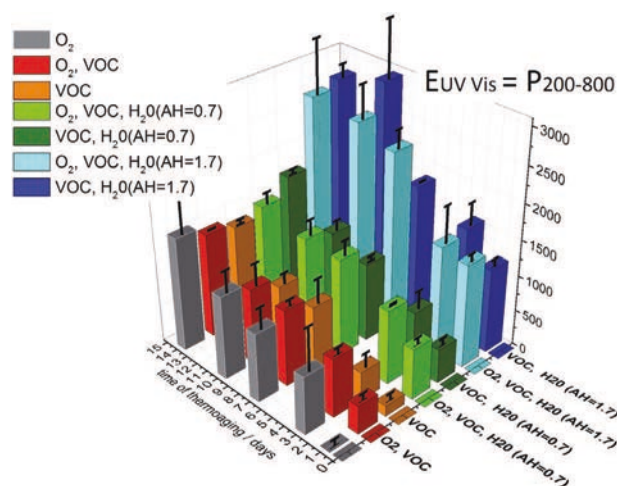


Fig. 6. Chromophores development in silk samples aged in 150 °C in different atmospheres (Table 1): evolution of integrated absorption in UV/Vis region $P_{200-800}$ calculated as an area under the spectra.

Upon thermo-aging a growth in 280 nm band can be spotted. The majority of intensification of absorbance in the 270–330 nm range should be attributed to α -keto-acids group formation and dicarboxylic amino group, formation of which was reported during the UV induced degradation by Baltova et al. [19]. A growing with

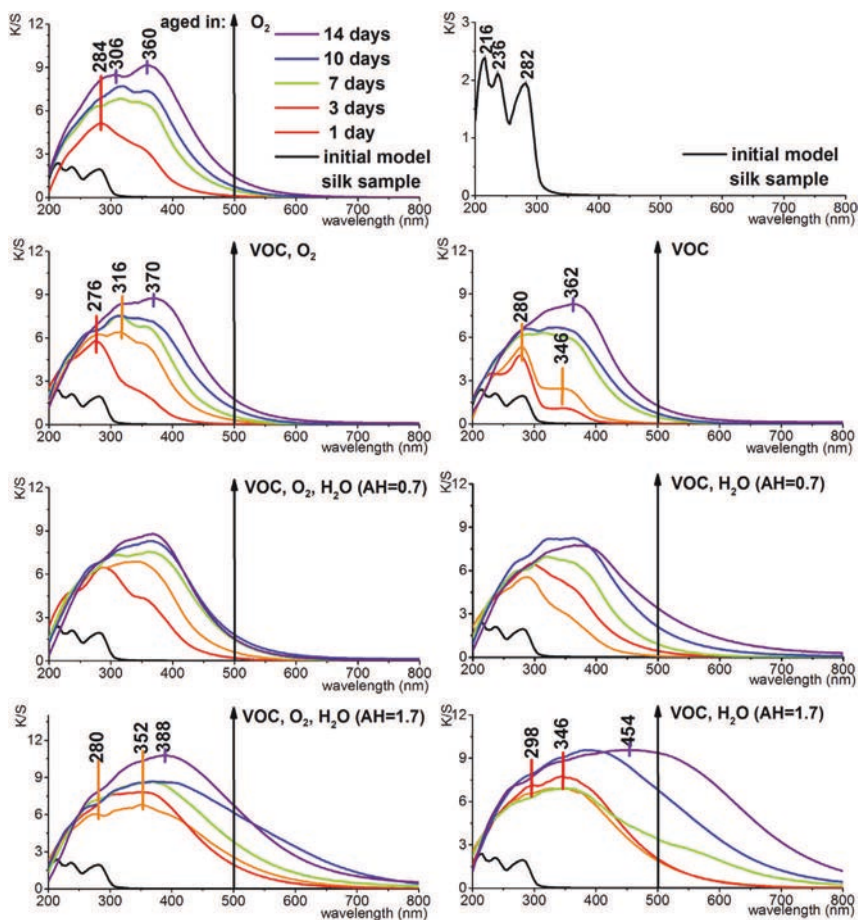


Fig. 5. UV/Vis spectra of model silk samples aged in 150 °C for 14 days in different atmospheres (Table 1). Absorbance values are given as K/S, according to the Kubelka–Munk model.

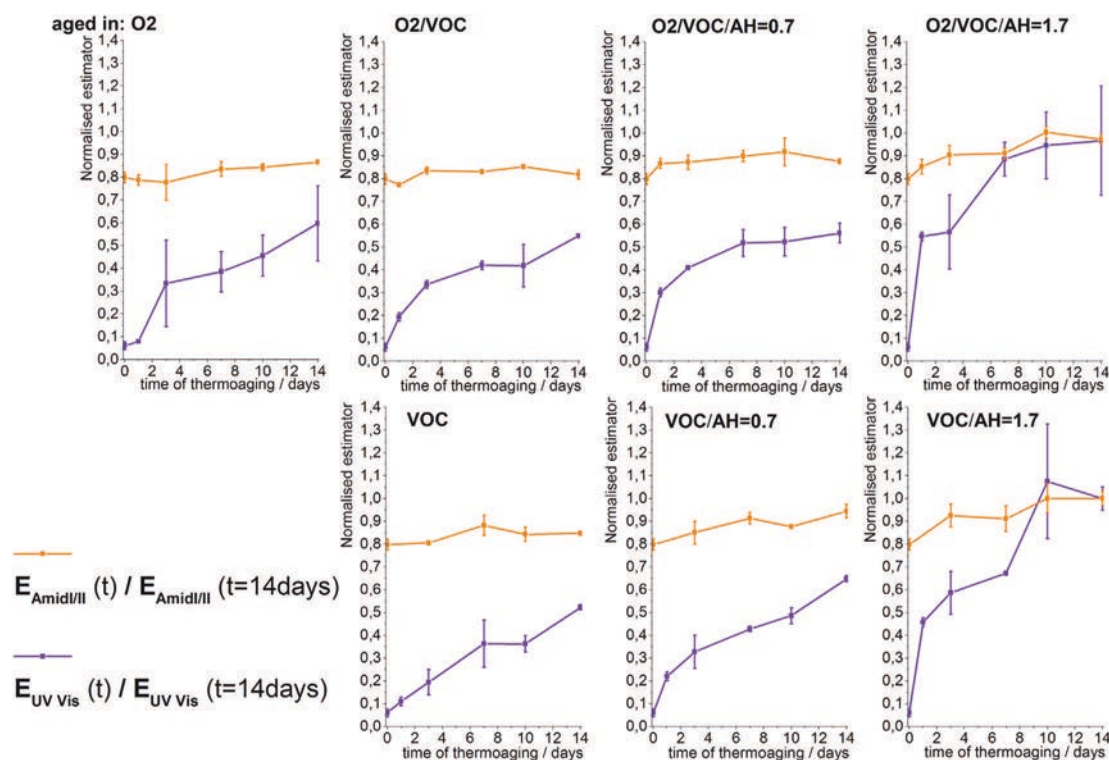


Fig. 7. Normalized oxidation estimators calculated for model silk samples aged over 14 days in 150 °C in different atmospheres.

time of thermo-aging bimodal band at 306 and 360 nm could be explained by *o*-quinone residues and *p*-cross-linked quinone, respectively [41]. *o*-quinones are the products of tyrosine oxidation and they can in turn react, with the amino group, in Michael-addition reaction forming *p*-cross-linked quinone. This mechanism was also supposed as one of the factors of photo yellowing of silk and enzymatic degradation by protease [42,43]. Increase of a band around 450 nm can be noticed for long-term degradation in high humidity atmosphere. Fluctuations in integrals of spectra in UV/Vis range over time of thermo-aging were monitored by the $E_{UV/Vis}$ estimator (Fig. 6). Estimator grows in all of monitored conditions from 6 times for O₂/VOCs conditions to up to 17 times in VOC/AH = 1.7. The data show that quinones formation is sensitive only to very humid conditions, otherwise increase is similar. Again no significant changes in carbonyl group content during oxygen-lean conditions aging were noticed comparing to changes in corresponding oxygen-rich aging condition.

Even though the two spectroscopic methods engaged to follow the oxidation state in fibroin are able to grasp slightly different oxidation products their general growing tendency with aging time and water vapor content is common for both of them. In general, the most active transitions upon UV/Vis irradiation occur for conjugated systems of double bonds, for all kinds of unsaturated hydrocarbons or for oxidation products of fibroin in form of carbonyl groups. A significant contribution of the latter is also due to a broad band at 1620 cm⁻¹ used for the evaluation of the oxidation state of fibroin by FTIR spectroscopy.

Normalized oxidation estimators from both FTIR and UV/Vis analyses are depicted together in Fig. 7. Data for calculating the oxidation estimator was normalized by dividing them with the value of the estimator at the 14 days aged sample in humid conditions. The steady growth calculated in this way $E_{UV/Vis}$ estimator on the surface incoherent with the slow escalations in $E_{Amide\ I/II}$ in fact, confirms hydrolysis contribution in its values as discussed above.

3.4. E_{COOH} as a hydrolysis gauge

New amino and carboxyl groups formed in hydrolysis and also in oxidation of fibroin during the thermo induced degradation should be confirmed by changes in the aged samples spectra. During aging simultaneous increase of shoulder bands at 1710, 1555 cm⁻¹, baseline escalation around 1220 cm⁻¹ and new band appearing at 1318 cm⁻¹ are visible on Fig. 3. Bands in these regions could correspond to deformation vibrations of –C–H groups in a free amino acid [37,44], or –C–H symmetric bending found in free dicarboxylic amino acids (COOH–NH–...–COOH) [37,45]. Following the trend of the band shift for –C–H deforming vibration: from acetic acid (1382 cm⁻¹) [46] glycine (1332 cm⁻¹) [45], hydroxy-acetic acid (1334 cm⁻¹) [45] and aspartic acid (1310 cm⁻¹)

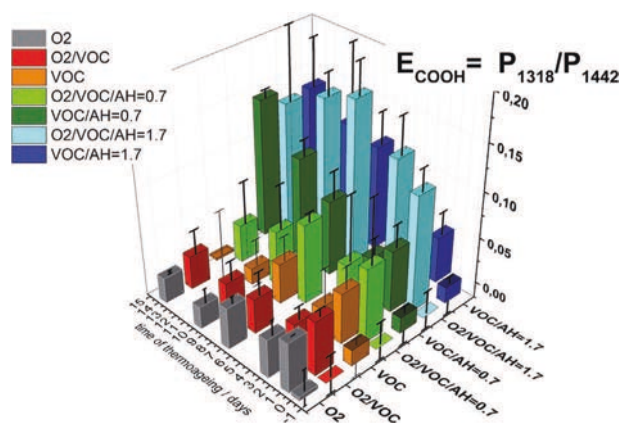


Fig. 8. E_{COOH} (A_{1318}/A_{1442}) estimator monitoring evolution of a new band at 1318 cm⁻¹, calculated from spectra of model silk samples aged at 150 °C in 7 different atmospheres: O₂; O₂/VOCs; VOCs; O₂/VOCs/AH = 0.7; VOCs/AH = 0.7; O₂/VOCs/AH = 1.7; VOCs/AH = 1.7 (Table 1).

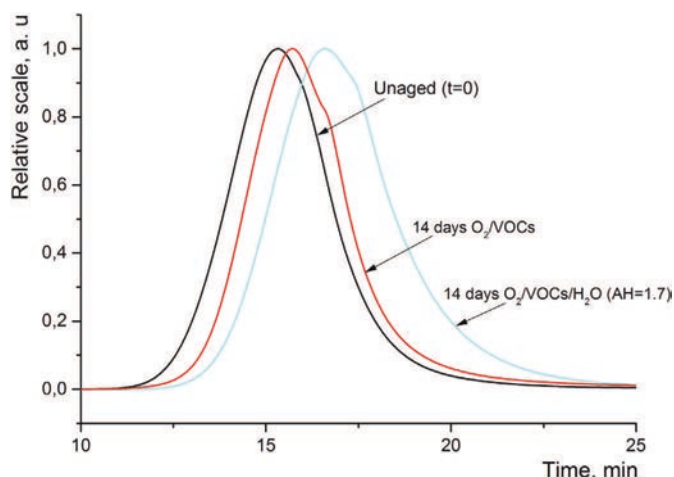


Fig. 9. Chromatograms of the model silk sample: initial and aged in 150 °C for 14 days in different atmospheres: O₂/VOCs; O₂/VOCs/AH = 1.7 (Table 1).

[45] it is clear that the observed band formation is due to strong shielding of –C–H band by –COOH groups.

The E_{COOH} degradation estimator, monitoring the development of the most resolved of above mentioned dicarboxylic amino acids vibration bands, the one centered at 1318 cm⁻¹, was calculated and depicted on Fig. 8. No significant (above the 50% of relative error) change after 14 days of aging was triggered in open reactor and in dry conditions and closed reactor. Again no significant changes were noted in E_{COOH} for oxygen-lean and oxygen-rich conditions during aging except opposite trends in compared 0.7 kg/m³ AH conditions.

E_{COOH} shows gradual growth upon introduction of water vapor to the atmosphere of aging. It doubles in O₂/VOCs/AH = 0.7 and almost 10 times then for the rest of the cases. This is consistent with the fact that water is a substrate for hydrolysis of peptide bonds and its increasing amount enhances carboxylic groups formation.

3.4.1. Validation by mean molar masses from SEC analyses

Depolymerization of fibroin due to hydrolysis of peptide bonds (and oxidation to some extent) is accompanied by both increase of a number of end carboxylic and amine groups, and the decrease of molar mass loss. If a number molar mass M_n is considered then the number of end groups is reversely proportional to M_n . To check the validity of the estimator E_{COOH} proposed to describe depolymerization the SEC analyses of the samples: unaged and aged for 14 days at the dry and humid conditions (O₂/VOCs and O₂/VOCs/AH = 1.7, Table 1), were performed (see Fig. 9). The number average molar masses were calculated following the method described in Ref. [47]. These are compared in Table 3.

According to our expectation the aging of fibroin results in a profound drop in mean molar mass of the polymer. The scission of the biopolymer is facilitated by the synergy of oxidation and hydrolysis. Thus it is justified to presume that there is a significant amount of dicarboxylic amino acids that are being formed during

the degradation and thereby supports the estimator E_{COOH} attribution.

3.5. Secondary FTIR estimators for crystallinity assessment

The trends of changes of E_{C=O 1} estimator value for samples aged in 7 different atmospheres (Table 1) is shown in Fig. 10A. No significant change after 14 day period of aging (above the 10% averaged statistical error calculated from the spectra of 3 series of aged samples) was triggered in O₂ (open reactor, Table 1) conditions under the influence of oxygen from air causing 8% drop in the E_{C=O 1}. In the other dry conditions (i.e. O₂/VOCs and VOCs) 9% and 7% drops were also observed, respectively. These results could correspond to findings reported by Garside and Wyeth [21] where almost no changes in this estimator after 14 days of aging at temperature of 125 °C were observed.

Introduction of water vapor into the atmosphere of aging (i.e. VOCs/AH = 0.7; O₂/VOCs/AH = 1.7 and VOCs/AH = 1.7) significantly increases E_{C=O 1} causing 17%, 23% and 24% changes in the intensities, respectively. Rise of E_{C=O 1} can be explained by profound disappearance of random coil regions which results in a relative gradual decrease of 1656 cm⁻¹ shoulder that distorts the estimator bands [34]. Thus the observation should be interpreted more as relative change in contribution of crystalline and random coil regions (supported by XRD) rather than absolute growth in the fibroin crystallinity. It is reasonable to presume that amorphous regions undergo faster degradation, as they are more reachable to relatively small water and oxygen molecules that trigger the decomposition mechanism. Similar findings were reported for another fibrous material as cellulose in paper [36]. As this process continues, the relative proportion of the abundance of the two phases changes and that might be reflected in the E_{C=O 1} change of trend.

The impact of oxygen on degradation of silk monitored by the E_{C=O 1} showed similar result for both O₂, VOCs and O₂, VOCs/H₂O (AH = 1.7) conditions. Only data collected in 0.7 AH show otherwise, suggesting acceleration of random coil degradation in oxygen-less atmosphere (VOCs/H₂O (AH = 0.7)) while in oxygen-rich conditions almost no change in the estimator was reported.

The other crystallinity estimator E_{C-N}, unlike that described above, calculated not from Amid I but from Amide III band, growths after aging at high temperature in all atmospheres (as depicted in Fig. 10B). Negligible (compared to 13% of statistical error) growth in the case of aging in dry open and closed reactor (O₂ – 6%; O₂/VOCs – 6% and VOCs – 6%) could indicate overall slight increase of crystallinity degree as more random coil structures undergo degradation. More profound increase in crystallinity is indicated for the conditions under which water vapor was introduced (VOCs/AH = 0.7–22%; O₂/VOCs/AH = 1.7–18% and VOCs/AH = 1.7–18%).

Our findings are in agreement with the work by Liu et al. where an intensification of E_{C-N} estimator in historical silks [33] was reported and with the work by Arai et al. where its escalation was correlated with the weight loss provoked by protease biodegradation [12]. A reduction in similarly calculated estimator was reported while aging by light and ozone [2] that evoke a different

Table 3

Number average molar mass for fibroin samples: unaged ($t = 0$ min) and aged at O₂/VOCs and in O₂/VOCs/H₂O (AH = 1.7) (Table 1) for 14 days.

Unaged ($t = 0$ min)			$t = 14$ days 150 °C in O ₂ /VOC			$t = 14$ days 150 °C in O ₂ /VOCs/H ₂ O (AH = 1.7)		
Number average molar mass								
M_n [kDa]	Stand. Dev [kDa]	Normalized value	M_n [kDa]	Stand. Dev [kDa]	Normalized value	M_n [kDa]	Stand. Dev [kDa]	Normalized value
150	28	1	26	1	0.2	18	1	0.1

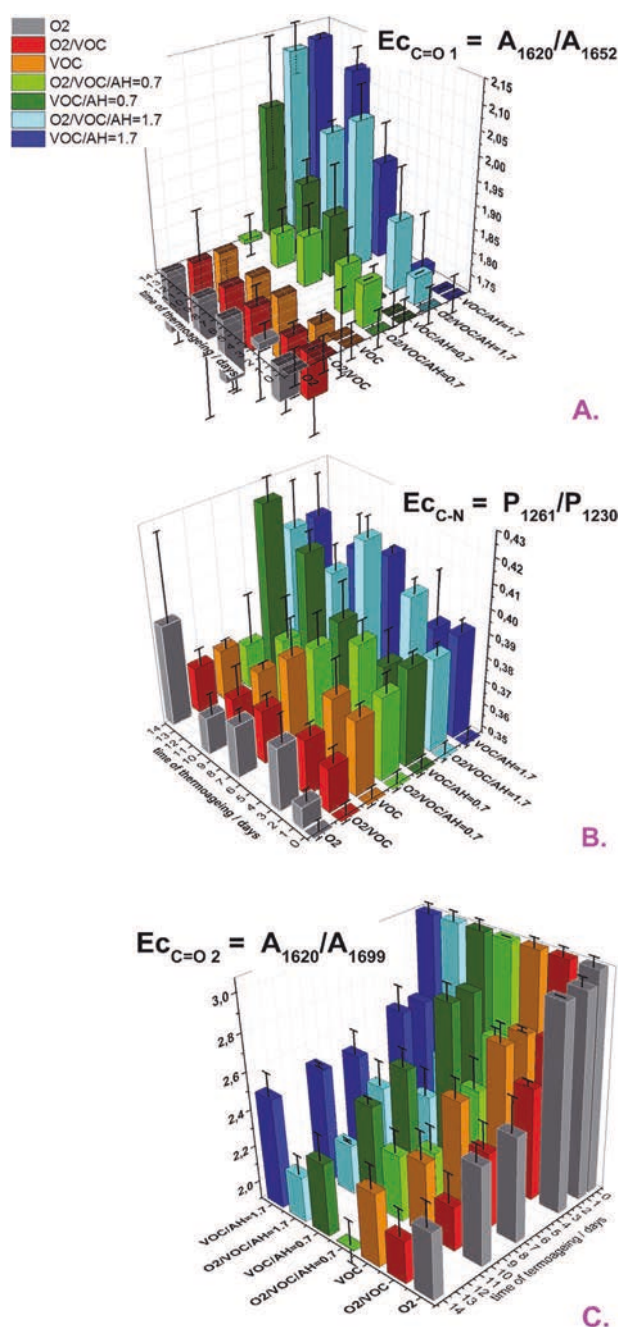


Fig. 10. Crystallinity degradation estimators: A. $E_{C=O 1}$ B. E_{C-N} C. $E_{C=O 2}$ calculated for model silk samples aged in 150 °C in 7 different atmospheres: O₂; O₂/VOCs; VOCs; O₂/VOCs/AH = 0.7; VOCs/AH = 0.7; O₂/VOCs/AH = 1.7; VOCs/AH = 1.7 (Table 1).

mechanism of degradation where the crystalline regions are equally accessible to the destructive agents as the amorphous ones.

The $E_{C=O 2}$ estimator declines after aging in all aging atmospheres (as depicted in Fig. 10C) by about 25–38% with statistical error of 11%. That can be attributed to a decrease of the antiparallel, in favor of parallel, arrangements of peptides in the crystalline region of the polypeptide [30]. However, a possibility that parallel arrangements vibrations are superimposed with stretching vibration of carboxyl groups formation during hydrolysis of peptide bond has to be kept in mind [2].

The impact of oxygen on degradation of silk at humid atmospheres is slightly different for very humid and humid conditions

(O₂, VOCs/H₂O (AH = 0.7) and (AH = 1.7)). That could be explained by overall greater carboxyl group formation in air filled with water vapor.

The trends of the crystallinity estimators upon aging are better visible for their standardized values as depicted together in Fig. 11. To obtain standardized values the estimators were normalized to their initial values measured for the unaged samples. In general, in dry atmosphere (O₂, O₂/VOCs Fig. 11) a maximum increase in the values of $E_{C=O 1}$ and E_{C-N} estimators do not exceed 20% of the initial value, while in the humid atmosphere an increase in the values of both parameters depends on the presence of oxygen and the water vapor partial pressure; the most profound effects having been observed at AH = 1.7 (O₂/VOCs/AH1.7 and VOCs/AH1.7 in Fig. 11). For the $E_{C=O 2}$ estimator, notwithstanding the conditions use, a reverse tendency with aging time can be noted with a maximum drop around 30%. Thus the question arises whether the phenomenon is either due to the differences in physical meanings of the estimators or due to wrong definition of one of them.

3.5.1. Validation of crystallinity degree by XRD

In order to verify the reliability of the secondary FTIR estimators – proposed in the literature crystallinity gauges, the X-ray diffraction analyses were carried out for the initial sample and the ones aged for 14 days in extreme conditions: O₂ and O₂, VOCs H₂O (AH = 1.7).

The typical diffraction peaks of the α -helix and random coil domains are $2\theta = 19.7^\circ$ (4.52 [Å], s), 24.72° (3.6 [Å], m), and 28.2° (3.16 [Å], m). On the other hand, those of antiparallel pleated β -sheet are $2\theta = 18.9^\circ$ (4.69 [Å], ms), and 20.7° (4.3 [Å], vs) [22]. The initial sample (black in Fig. 12) showed three diffraction peaks at 19.97° , 24.87° and 28.85° , attributed to the amorphous structure and peak at 20.87° attributed to the β -sheet structure. The diffractograms were resolved by fitting (summarized in Table 4) the four Gaussian curves [48]. Our analysis shows that upon very humid conditions (light blue in Fig. 12), the areas under the peaks around $2\theta = 24^\circ$ and 28° increase in favor of diminishing area under peaks located just above $2\theta = 19^\circ$. This can be interpreted as an increase of random coil content with proportional decrease of α -helix domains as the time of aging progresses.

To summarize briefly, the results of XRD analyses indicate the growing tendency of random coil concentration, decreasing trend in amorphous α -helix concentration and in crystalline β -sheet abundance in fibroin samples exposed to very harsh aging conditions including in O₂, VOCs and humidity at 150 °C for 14 days. The trends of XRD coincide with which expresses the β -sheets contribution. Since the trends of XRD results and the $E_{C=O 2}$ estimator coincide 4 scenarios can be assumed to interpret the infrared results:

- 1) Reorganization of β -sheets to antiparallel β -sheets;
- 2) Decrease in β -sheets with no changes in antiparallel β -sheets;
- 3) Increase in both β -sheets to antiparallel β -sheets when the extinction coefficient is lower for the first than for the latter;
- 4) Decrease in both β -sheets to antiparallel β -sheets when the extinction coefficient is higher for the first than for the latter.

Since, however, no changes in antiparallel β -sheets signal at 18.9° was observed by XRD analyses the 2nd possibility out of the four presented above seems to be the most plausible.

The other FTIR estimators E_{C-N} $E_{C=O 1}$ show a reverse trend to the XRD results for the samples aged at O₂/VOCs/AH (1.7) conditions for 14 days. Indeed, both estimators bear similar information on mutual changes in β -sheet, α -helix and random coil abundances, however, calculated from different feature of the fibroin FTIR spectra.

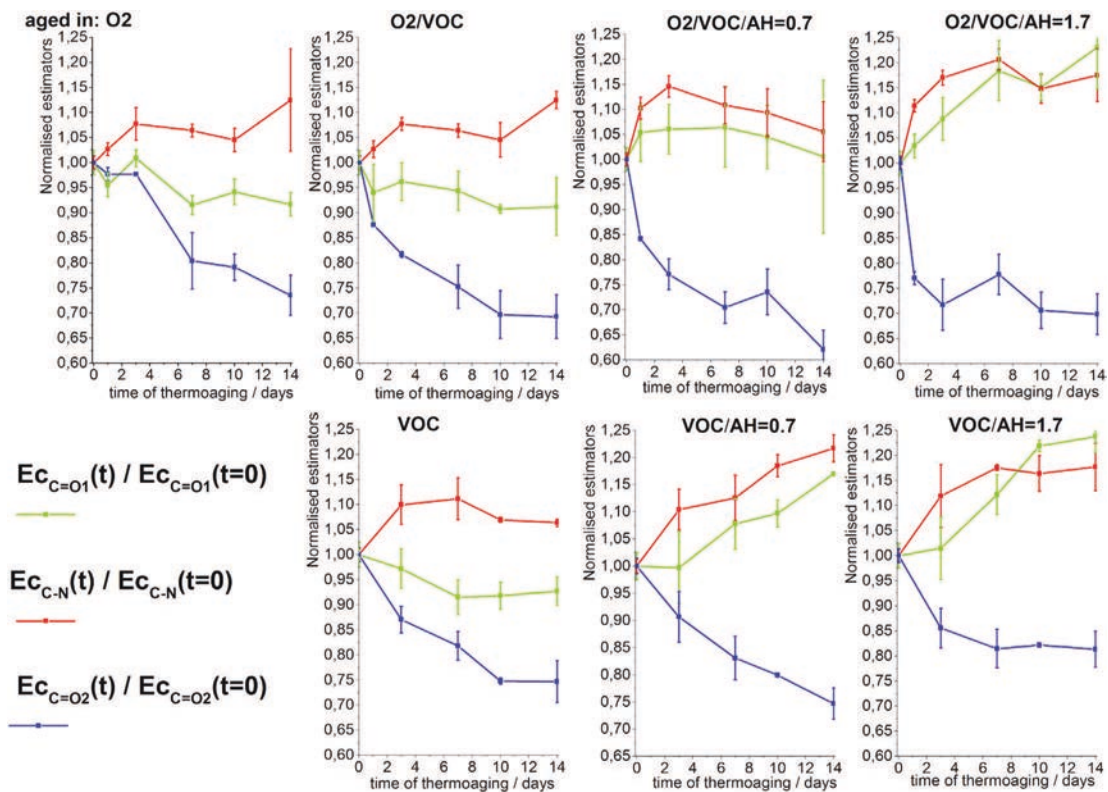


Fig. 11. Normalized crystallinity degradation estimators calculated for model silk samples aged over 14 days in 150 °C in 7 different atmospheres: O₂; O₂/VOCs; VOCs; O₂/VOCs/AH = 0.7; VOCs/AH = 0.7; O₂/VOCs/AH = 1.7; VOCs/AH = 1.7 (Table 1).

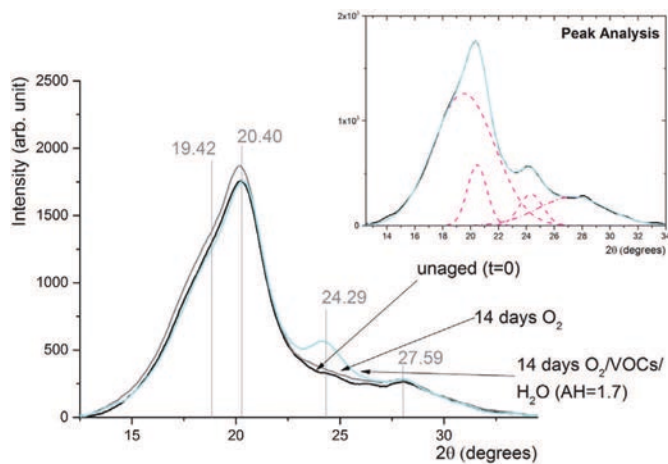


Fig. 12. XRD diffraction patterns of the model silk sample: initial and aged in 150 °C for 14 days in different atmospheres: O₂; O₂/VOCs/AH = 1.7. Inset: exemplary fitting results for O₂/VOCs/AH = 1.7 (Table 1).

In the light of the XRD analyses (Table 4), the growth in the values of both $EC_{C=O_1}$ and EC_{C-N} parameters which are both a function of three variables (β -sheets, random coil and α -helix concentrations) is only possible under one condition (see definition of the estimators in Section 3.2). The extinction coefficient of α -helix, whose concentration decreases with aging time according to XRD (Table 4), should be substantially greater the ones of both β -sheets (decrease with time), random coil (increase with time).

When analyzing these estimators we have to take into account that $EC_{C=O_1}$ and $EC_{C=O_2}$ values can also be influenced by the formation of carbonyl groups from fibroin oxidation, whose vibrations could appear in the vicinity of the maximum at 1620 cm⁻¹ (see Section 3.4.1).

4. Conclusions

The study poses a comprehensive approach to the interpretation of infrared spectra of degraded fibroin from silk samples. Spectroscopic data gathered for silk samples aged at various conditions lead to formulations of six degradation estimators that describe different properties of fibroin polymer: crystallinity,

Table 4

Fitting parameters for XRD results of fibroin samples: unaged ($t = 0$ min) and aged at O₂ and in O₂/VOCs/H₂O (AH = 1.7) (Table 1) for 14 days.

	Unaged ($t = 0$ min)			$t = 14$ days 150 °C in O ₂			$t = 14$ days 150 °C in O ₂ /VOCs/H ₂ O (AH = 1.7)		
	Peak Center [°]	Integ area %	FWHM	Peak Center [°]	Integ area %	FWHM	Peak Center [°]	Integ area %	FWHM
α -helix	19.42	70.69	5.12	19.33	70.74	5.26	19.52	67.44	5.21
β -sheet	20.40	10.50	1.70	20.36	10.55	1.70	20.46	9.82	1.64
Random coil	24.29	3.27	2.45	24.40	3.69	2.58	24.33	6.27	2.02
Random coil	27.59	15.53	5.84	27.64	15.01	5.75	27.30	16.48	5.84

polymerization degree, oxidation. Their physical meaning was validated by the other analytical methods such as XRD, UV/Vis and SEC.

The peptide bonds estimator based on the Amide I–II vibrations ($E_{\text{Amide I/II}}$) was verified by UV/Vis analyses. It has been evidenced that even though the estimator comprises the information on the cleavage of the peptide bonds it also has a profound contribution carbonylic groups vibrations coming from fibroin oxidation. The effect of oxidation prevails over hydrolysis in the estimator's values calculated for fibroin at various stages of its degradation.

A new estimator has been proposed in this study, E_{COOH} , that shows that development of bicarboxylic groups with characteristic influence on the frequency of bending vibrations of CH groups at 1318 cm^{-1} . This estimator has been shown to be selective for a hydrolytic degradation pathway during fibroin degradation and seems to be the most separated from other degradation effects. The trends in its values have been correlated with mean molar mass of fibroin measured by SEC.

It has been proved by independent XRD experiments that the FTIR index based on the intensity ratios within Amide I C=O stretching vibration of parallel β -sheet to antiparallel β -sheet (A_{1620}/A_{1699}) reflects the changes of the silk samples crystallinity. The information born by two other crystallinity indexes proposed in the literature (intensity ratios within Amide I C=O stretching vibration of β -sheet to α -helix/random coil A_{1620}/A_{1656} , and the area under Amide III C–N stretching and N–H bending vibration of β -sheet band to area under the same vibration of α -helix P_{1261}/P_{1230}) are not valid as crystallinity gauges due to the differences in physical meanings of the estimators.

Regardless of other factors, such as oxygen or volatile organic compounds (VOCs), water vapor contained in the atmosphere of reaction, has the greatest impact on the progress of degradation. This tendency is reflected by all the estimators as water vapor may facilitate both hydrolysis providing substrate for peptide bonds cleavage and oxidation being a source of oxygen radicals. The third function of water during degradation is also that it may act as a polymer plasticizer enhancing reorganization of fibroin chains towards random coil arrangements as shown by independent XRD analyses.

Effect of oxygen-lean conditions (VOCs influence) on aging silk itself is less significant to water and could only be indicated for AH = 0.7 conditions (Table 1). The absence of oxygen is noticeable on the impact of dicarboxylic amino acid formation in E_{COOH} and effectively distorts the $E_{\text{C=O}}$, $E_{\text{C-N}}$ estimator in oxygen-rich conditions and in wet conditions (AH = 0.7, see Table 1). In the rest of dry and very humid (closed reactors) conditions the oxygen has no significant impact on degradation process of silk fibroin.

Volatile organic compounds contribute to accelerating the degradation, because the degradation determines the parameters mentioned above. Some impact of VOCs can be viewed in the trend of $E_{\text{C=O}}$ supposing their special involvement in oxygenation path. This finding may be an indication for museum restorers or conservators for the advantageous use of hermetically sealed frames purged with nitrogen to store silk textiles of historical values.

In summary, our non-destructive diagnostic method provides a quantification of degradation of silk objects in terms of their crystallinity, oxidation and depolymerization stage all assess in one measurement from FTIR spectra. Such information is priceless when planning appropriate conservation strategies in museum all over the world and represents an important contribution to ensuring that collections will be enjoyed in the future.

Acknowledgments

The authors wish to thank the Wawel Castle Museum for their help and support.

Project was funded from the funds of National Science Centre 2011/01/N/ST4/03604 and Foundation For Polish Science EX3/2012. The authors are grateful to SPB 811/N-COST/2010/0 for sponsoring optical parts to Raman system. The XRD measurements were carried out with the equipment purchased thanks to the financial support of the European Regional Development Fund in the framework of the Polish Innovation Economy Operational Program (contract no. POIG.02.01.00-12-023/08).

References

- [1] Wyeth PR, editor. Scientific analysis of ancient and historic textiles informing preservation display and interpretation. Archetype Publications; 2004. pp. 137–42.
- [2] Zhang XM, Yuan S. Research on the infrared spectrometry of aging silk fabrics. *Chin J* 2004;24(12):1528–32.
- [3] Shao J, Zheng J, Liu L, Carr MC. Fourier Transform Raman and Fourier Transform infrared spectroscopy studies of silk fibroin. *J Appl Polym Sci* 2005;96(6):1999–2004.
- [4] Hoiberg D, editor. Encyclopedia Britannica. 15th ed. 2010.
- [5] Kundu SC, Kundu B, Talukdar S, Bano S, Nayak S, Kundu J, et al. Invited review nonmulberry silk biopolymers. *Biopolymers* 2012;97(6):455–67.
- [6] Lewin M, editor. Handbook of fiber chemistry. 2nd ed. CRC Press; 2006.
- [7] Landi S, editor. Textile conservator's manual. 2nd ed. Butterworth-Heinemann; 1998.
- [8] Timar-Balazsy A, Eastop D, editors. Chemical principles of textile conservation. Butterworth-Heinemann; 1988.
- [9] Putthanarat S, Striebeck N, Fossey SA, Eby RK, Adams WW. Investigation of nanofibrils of silk fibers. *Polymer* 2000;41:7735–47.
- [10] Sashina ES, Bochek AM, Novoselov NP, Kirichenko D. Structure and solubility of natural silk fibroin. *Russ J Appl Chem* 2006;79:869–76.
- [11] Murphy AR, St John P, Kaplan DL. Modification of silk fibroin using diazonium coupling chemistry and the effects on hMSC proliferation and differentiation. *Biomaterials* 2008;29(19):2829–38.
- [12] Arai T, Freddi G, Innocenti R, Tsukada M. Biodegradation of *Bombyx mori* silk fibroin fibers and films. *J Appl Polym Sci* 2004;91(4):2383–90.
- [13] Wray LS, Hu X, Gallego J, Georgakoudi I, Omenetto FG, Schmidt D, et al. Effect of processing on silk-based biomaterials: reproducibility and biocompatibility. *Appl Biomater* 2011;99(1):89–101.
- [14] Szela S, Avtges P, Valluzzi R, Winkler S, Wilson D, Kirschner D, et al. Reduction-oxidation control of beta-sheet assembly in genetically engineered silk. *Biomacromolecules* 2000;1(4):534–42.
- [15] Zhao C, Wu X, Zhang Q, Yan S, Li M. Enzymatic degradation of *Antheraea pernyi* silk fibroin 3D scaffolds and fibers. *Macromolecules* 2011;48(2):249–55.
- [16] Anghileri A, Lantto R, Kruus K, Arosio G, Freddi G. Tyrosinase-catalyzed grafting of sericin peptides onto chitosan and production of protein-polysaccharide bioconjugates. *J Biotechnol* 2007;127(3):508–19.
- [17] Hu Y, Zhang Q, You R, Wang L, Li M. The Relationship between secondary structure and biodegradation behavior of silk fibroin scaffolds. *Adv Mater Sci Eng* 2012;2012:1–5.
- [18] Becker B. Historic textile and paper material III in ASC symposium series 410, vol. 95. American Chemical Society; 1989.
- [19] Baltova S, Vassileva V, Valtcheva E. Photochemical behaviour of natural silk I–III. *Polym Degrad Stab* 1998;60:53–65. 61(3):367–373.
- [20] Sargunamani D, Selvakumar N. A study on the effects of ozone treatment on the properties of raw and degummed mulberry silk fabrics. *Polym Degrad Stab* 2006;91(11):2644–53.
- [21] Garside P, Wyeth P. Crystallinity and degradation of silk: correlations between analytical signatures and physical condition on ageing. *Appl Phys A Mater* 2007;89(4):871–6.
- [22] Lia M, Ogisob M, Minourab N. Construction and enzymatic degradation of multilayered poly-L-lysine/DNA films. *Biomaterials* 2003;24:357–65.
- [23] Motta A, Fambri L, Migliarese C. Regenerated silk fibroin films: Thermal and dynamic mechanical analysis. *Macromol Chem Phys* 2002;203(10–11).
- [24] Van Nimmen E, De Clerck K, Verschuren J, Gellynck K, Gheysens T, Mertens J, et al. FT-IR spectroscopy of spider and silkworm silks Part I. Different sampling techniques. *Vib Spectrosc* 2008;46(1):63–8.
- [25] Pawcenis D, Koperska MA, Milczarek JM, Lojewski T, Lojewska J. Size exclusion chromatography for analyses of fibroin in silk: optimization of sampling and separation conditions. *Appl Phys Mater Sci Process* 2014;114(2):301–8.
- [26] Teramoto H, Miyazawa M. Molecular orientation behavior of silk sericin film as revealed by ATR infrared spectroscopy. *Biomacromolecules* 2005;6(4):2049–57.
- [27] Bramanti E, Catalano D, Forte C, Giovanneschi M, Masetti M, Veracini CA. Solid state (^{13}C) NMR and FT-IR spectroscopy of the cocoon silk of two common spiders. *Spectrochim Acta A Mol Biomol Spectrosc* 2005;62(1–3):105–11.
- [28] Fabina H, Mantele W. Infrared spectroscopy of proteins. In: Handbook of vibrational spectroscopy. John Wiley & Sons; 2006.
- [29] Ling S, Qi Z, Knight DP, Shao Z, Chen XS. Synchrotron FTIR microspectroscopy of single natural silk fibers. *Biomacromolecules* 2011;12(9):3344–9.

- [30] Marelli B, Alessandrino A, Farè S, Freddi G, Mantovani D, Tanzi MC. Compliant electrospun silk fibroin tubes for small vessel bypass grafting. *Acta Biomater* 2010;6(10):4019–26.
- [31] Khan MMR, Morikawa H, Gotoh Y, Miura M, Ming Z, Sato Y, et al. Structural characteristics and properties of *Bombyx mori* silk fiber obtained by different artificial forcibly silking speeds. *Int J Biol Macromol* 2008;42(3):64–70.
- [32] Greiff S, Kutzke H, Riekel C, Wyeth P, Lahlil S. Signatures of ageing: correlations with behaviour. <http://eprints.soton.ac.uk/>.
- [33] Liu J, Guo D, Zhou Y, Wu Z, Li W, Zhao F, et al. Identification of ancient textiles from Yingpan, Xinjiang, by multiple analytical techniques. *J Archaeol Sci* 2011;38(7):1763–70.
- [34] Horan RL, Antle K, Collette AL, Wang Y, Huang J, Moreau JE, et al. In vitro degradation of silk fibroin. *Biomaterials* 2005;26(17):3385–93.
- [35] Taddei P, Monti P, Freddi G, Arai T, Tsukada M. IR study on the binding mode of metal cations to chemically modified *Bombyx mori* and Tussah silk fibres. *J Mol Struct* 2003;651–653(1–3):433–41.
- [36] Łojewski T, Zięba K, Knapik A, Bagniak J, Lubańska A, Łojewska J. Evaluating paper degradation progress. Cross-linking between chromatographic, spectroscopic and chemical results. *Appl Phys A Mater* 2010;100:809–21.
- [37] Socrates G, editor. Infrared and Raman characteristic group frequencies: tables and charts. 3rd ed. John Wiley & Sons; 2004.
- [38] Strlič M, Kolar J, editors. Ageing and stabilisation of paper, Chapter 7.5. 1st ed. National and University Library; 2005.
- [39] Schmid FX. Encyclopaedia of life sciences 2001. Macmillan Publishers Ltd, Nature Publishing Group; 2001.
- [40] Guo HL, Liu DY, Yu XD, Xia XH. Direct electrochemistry and electrocatalysis of hemoglobin on nanostructured gold colloid-silk fibroin modified glassy carbon electrode. *Sensors Actuators B Chem* 2009;139(2):598–603.
- [41] Kang GD, Lee KH, Ki CS, Park YH. Crosslinking reaction of phenolic side chains in silk fibroin by tyrosinase. *Fibers Polym* 2004;5(3):234–8.
- [42] Monti P, Freddi G, Sampaio S, Tsukada M, Taddei P. Structure modifications induced in silk fibroin by enzymatic treatments: a Raman study. *J Mol Struct* 2005;744:685–90.
- [43] Davidson RS. The photodegradation of some naturally occurring polymers. *J Photochem Photobiol B Biol* 1996;33(1):3–25.
- [44] Chen XG, Li P, Holtz JSW, Chi Z, Pajcini V, Sanford AA, et al. Resonance Raman examination of the electronic excited states of glycylglycine and other dipeptides: observation of a carboxylate → amide charge transfer transition. *J Am Chem Soc* 1996;118(40):9705–15.
- [45] Kumar S, Rai AK, Singh VB, Rai SB. Vibrational spectrum of glycine molecule. *Spectrochim Acta A Mol Biomol Spectrosc* 2005;61(11–12):2741–6.
- [46] NIST data base. www.nist.gov.
- [47] Łojewska J, Missori M, Lubanska A, Grimaldi P, Zieba K, Proniewicz LM, et al. Carbonyl groups development on degraded cellulose. *Appl Phys A Mater* 2007;89:883–7.
- [48] Lopez-Rubio A, Flanagan BM, Gilbert EP, Gidley MJ. A novel approach for calculating starch crystallinity and its correlation with double helix content: a combined XRD and NMR study. *Biopolymers* 2008;89:761–8.



Contents lists available at ScienceDirect

Spectrochimica Acta Part A: Molecular and Biomolecular Spectroscopy

journal homepage: www.elsevier.com/locate/saa

Evaluating degradation of silk's fibroin by attenuated total reflectance infrared spectroscopy: Case study of ancient banners from Polish collections



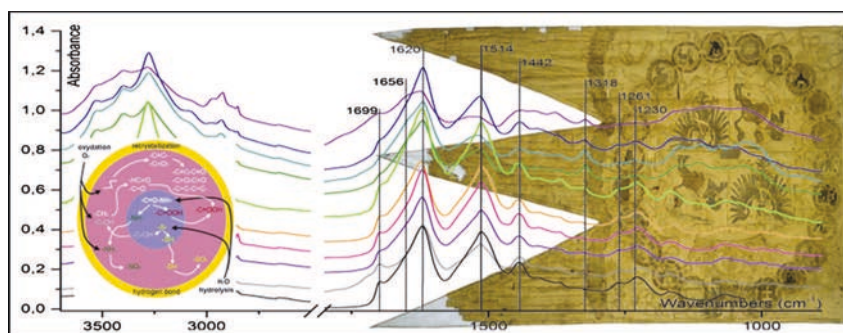
M.A. Koperska*, T. Łojewski, J. Łojewska

Jagiellonian University, Chemistry Faculty, Ingardena 3, 30-060 Krakow, Poland

HIGHLIGHTS

- ATR-FTIR estimators to describe crystallinity and oxidation of fibroin were chosen.
- A new, proposed estimator ECOOH monitors the hydrolysis of fibroin.
- ATR-FTIR estimators were classified as primary and secondary structure estimators.
- Primary and secondary structure estimators help in museum objects' risk assessment.
- Estimators can discriminate surfaces directly exposed to ex humidity, pollution.

GRAPHICAL ABSTRACT



ARTICLE INFO

Article history:

Received 31 December 2013
 Received in revised form 12 May 2014
 Accepted 13 May 2014
 Available online 8 July 2014

Keywords:

Fibroin
 ATR-FTIR spectroscopy
 Degradation estimators
 Historic silk samples

ABSTRACT

In this study a part of research where artificially aged model samples were used as a guideline to the mechanism of degradation is presented. In previous work *Bombyx Mori* silk samples were exposed to various environments such as different oxygen, water vapour and volatile organic products content, all at the temperature of 150 °C [11]. Based on those results gathered with by Attenuated Total Reflectance/Fourier Transform Infrared Spectroscopy (ATR-FTIR) the degradation estimators were proposed and classified as follows:

(1) Primary functional groups estimators

$E_{\text{AmideI/II}}$ – intensity ratios of Amide I C=O stretching vibration to Amide II N–H in-plane bending and C–N stretching vibrations A_{1620}/A_{1514} .

E_{COOH} – band 1318 cm^{-1} integral to band integral of CH_3 bending vibration band located at 1442 cm^{-1} P_{1318}/P_{1442} .

(2) Secondary conformational estimators

$E_{\text{C=O2}}$ – intensity ratios within Amide I C=O stretching vibration of parallel β -sheet to antiparallel β -sheet A_{1620}/A_{1699} .

In this work estimators were verified against estimators calculated from spectra of silk samples from 8 museum objects: 3 from 19th, 2 from 18th, 1 from 17th and 2 from 16th century including 3 banners from the storage resources of the Wawel Royal Castle in Cracow, Poland.

© 2014 Elsevier B.V. All rights reserved.

* Corresponding author.

E-mail addresses: mkoperska@gmail.com, monika.koperska@uj.edu.pl (M.A. Koperska).

Introduction

Silk can be regarded as a semi crystalline biopolymer with highly organized nanocrystals surrounded by amorphous matrix [1]. The crystalline structure is built by smaller amino acids: glycine (44.6%), alanine (29.4%), serine (12.1%). Small functional groups such as methyl- or hydroxyl- allow chains of amino acids to be closed together making ordering into the secondary structure of β -sheets possible. This crystalline structure (building up to 60–70% of entire fibroin structure in *Bombyx mori* [2]) is quite resistant to chemical attack [3]. It is understood that degradation triggers in easy to access amorphous regions [3]. These are understood as α -helix or/and random coil arrangements composed of larger amino acids (tyrosine (5.1%), valine (2.2%), aspartic acid (1.3%), leucine (1.2%), glutamic acid (1.0%), threonine (0.9%), arginine (0.5%) proline (0.4%), phenylalanine (0.4%), lysine (0.3%), cysteine (0.2%), histidine (0.1%), and tryptophan (0.1%)) [1].

The amino acid chain can be affected by both hydrolysis and oxidation (see Fig. 1). In high humidity water reaches the peptide bond in amorphous regions and causes forming of carbonyl and amine groups [4]. Water naturally bonds to hydrophilic silk (mostly tanks to the high content of polar – hydroxyl side groups) reaching up to 10% of its mass in 65% relative humidity [4]. Same research shows that strength of fibroin is preserved above 30–40% RH and rapidly falls over 60%RH, reaching the most brittle state after storage in 85% RH atmosphere [4,5]. Both acids and alkaline promote the hydrolysis, although the alkali hydrolysis progresses more slowly and mostly from the ends of the chains of peptides [3]. Acidic hydrolysis is more random and can affect not only primary but also secondary and tertiary structure through disrupting the hydrogen bonds and disulphide bonds.

Oxidation process in silk's fibroin takes place through radical reaction [3]. Usually light (especially from the UV region) or heat facilitates the oxygen radical formation. Oxygen radicals first attack the most reactive aromatic groups in amino acids like: tryptophan, tyrosine and phenylalanine [4]. The chromophores that are responsible for silk yellowing upon UV exposure are formed as products of these reactions. Radicals will also accelerate the cleavage of neighbouring peptide bonds producing α -keto-acids and dicarboxylic amino groups that contribute to weakening of the fibres [6]. Products of photo degradation are often prone to cross-linking (especially o-quinone products of tyrosine), which affects

the amorphous regions flexibility forcing the fibre to be more brittle [7]. Also the S–S bonds (that rule the secondary and tertiary structure of fibroin) undergo oxidation and break upon photo induced oxidation, the Cys–Cys bond are broken before the Met–Met are affected [8]. It is worth mentioning that water presence will facilitate the oxidation rate in both cases of photo and thermo oxidation. At high temperatures the presence of light is not required for oxygen radical formation therefore ageing in elevated temperature tents the free-radical thermal oxidation to occur [3].

Since about two decades and with the introduction of non-destructive sampling techniques (as photo-acoustic and attenuated total reflectance) infrared spectroscopy has been used for monitoring microstructural change caused by degradation processes occurring in historical objects build from silk [9,10,13–18]. The amount of information that can be deducted from the silk historical textile infrared spectra was first very scarce and based on juxtaposing the spectra of newly produced and historic samples [9]. With practice and time same few degradation markers derived from IR spectra of artificially aged model silk samples have been proposed in the literature.

The primary structure of historic silks can be monitored by the Amid I (at 1621 cm^{-1}) to Amid II (at 1514 cm^{-1}) intensity ratios [10]. From our previous research of artificially aged samples this estimator has been proved to be a promising tool for looking at the oxidation products in silks structure [11]. Our previous work also lead to proposing an estimator with view to monitoring the hydrolysis effect. It invigilates a band centred at 1318 cm^{-1} attributed to the vibration of C–H bond shielded by –COOH groups from bicarboxylic acids formed upon peptide bond breaking [12].

Lately also FTIR spectroscopy has been reported to be used for sericin detection (second to fibroin protein that composes silk, often lost during silk processing). Zhang et al. proposed 3 estimators facilitating sericin recognition in silk fibres from historical samples [13].

The secondary structure of silk concerns primary its crystallinity. In the literature, the ratio of two Amide I band intensities at 1615 and 1655 cm^{-1} has been considered a crystallinity index for historic silk fibroin as it reflects the relative proportion of the polymer in an organised β -sheet relative to α -helix or/and random coil arrangement [14–16]. Analogically, the Amid III bands at 1264 and 1230 cm^{-1} can lead to calculating crystallinity index basing on similar grounds [17]. The growth of the band centred at 1699 cm^{-1} was reported during biological [18] and thermo degradation [10] but the band's origin has been variously explained either by an increase of antiparallel β -sheet contribution or formation of new carboxylic (COOH) groups. In our previous work all of these literature three crystallinity estimators and their changes upon thermo aging in humid and dry conditions were taken under scrutiny and validated by X-ray diffraction (XRD) results [11]. The conclusion was that only the one taking into the account the 1699 cm^{-1} band can be considered reliable for crystallinity assessment [11]. The ambiguity of the other two is caused by the rise of the oxidation products vibrations bands at around 1700 – 1600 cm^{-1} that overlay with the Amid I band at 1620 cm^{-1} .

Few works on the subject of crystallinity change in historical samples spectra investigated both by FT IR and XRD techniques can be found [16–19]. The XRD patterns and FTIR spectra analysed by Greiff et al. indicate the continuous presence of crystalline domains in silk structure, but their almost complete disorientation in historic samples [16]. The findings of Zhang et al. gathered by the same techniques show both rise and fall of crystallinity in ancient samples [17]. WAXS experiments performed by Hermes et al. and ATR-FTIR by Arai et al. clearly indicate the loss of the connecting amorphous network. That with time produces break at a nanofibrils level of a fibre and causes the loss of mechanical strength [18,19].

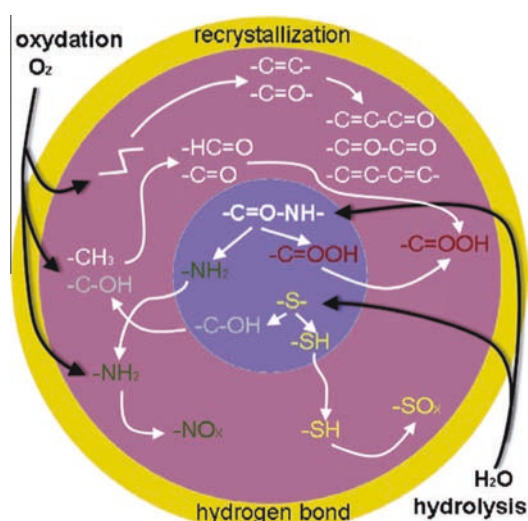


Fig. 1. Silk's (fibroin's) degradation pathway scheme, primary structure change is depicted on pink and blue background. (For interpretation of the references to colour in this figure legend, the reader is referred to the web version of this article.)

The aim of this work is to implement previously chosen primary and secondary structure estimators on to the analysis of state of degradation of historic silk samples. The change in the primary structure of fibroin was examined by hydrolysis and oxidation estimator calculated from ATR-FTIR spectra whereas the secondary change was studied by the change of one estimator derived from ATR-FTIR spectra that was previously verified with XRD experiments [11].

Materials and methods

Initial model silk sample and artificial ageing

In this work degummed and bleached *Bombyx mori* silk (35 g/m² of basis weight that is grams per square metre) was purchased from Chinese retailer (Sailong, Warsaw, Poland) and in this paper will be referred to as the model silk sample (MS). It is a common practise to use plain weave textiles during the conservation treatments of silk artefacts [4]. Alike textiles can be found and is used by leading museums in Europe during the conservation processes.

During artificial aging tests silk samples were hanged in the aging chamber (open reactor) or in closed vials and heated up to 150 °C at various content of gaseous atmosphere (aged at 3 different humidity levels and in 2 different atmospheres: air and nitrogen) (closed reactor). The detailed description of the ageing procedure and the results of previous research is described elsewhere [11]. In this work by “aged sample” authors mean the one aged for 14 days in the most harsh conditions (aged MS): closed reactor with water vapour partial pressures inside the vials set to 0.330 MPa (maximum saturated vapour pressure equals to 0.471 MPa at 150 °C) which corresponds to the value of absolute humidity (AH) equal to 1.690 kg/m³.

Historical silk samples

Thanks to the courtesy of the Museum of Wawel Castle in Cracow, Poland samples from 16th to 19th century silks were gathered. These included: Stanisław Barzi's Funeral Banner from 16th century (FB, see Fig. 2a), Court Banner from 16th century (CB, see Fig. 2b); 2 different coloured samples from Inscription Banner from 17th century (IB, see Fig. 2c); samples from 3 different conservation material from XIXth century (CM1, 2 & 3, see Fig. 2e–g) Thanks to the courtesy of Lodz University of Technology 3 samples

from chasuble from 17/18th century (C, see Fig. 2d) were added to the group of samples. All historic samples with their details about date and place of origin are listed in Table 1. Historical samples from objects C and CM were in very good condition, whereas the banner samples FB, CB, and IB (both samples green and red) were in a very brittle state. Both sets of samples were stored in magazines of Wawel Castle Museum for last few decades, unmoved. Also all samples except the Inscription Banner (made in Turkey, part of Asia at the time of manufacture) were manufactured in Europe.

Infrared spectroscopic analysis of silk samples

Infrared spectra were collected directly from the textile samples by the means of the Fourier Transformed Infrared THERMO (Nicolet 5700) spectrometer equipped with Golden Gate attenuated total reflection (ATR) device (MkII), with a diamond crystal. This device allows to apply a predefined and constant pressure between the sample and the ATR window.

Spectral intensities of samples having complex structure (paper, textile) may vary due to heterogeneity reasons. However, that does not represent a source of errors in this study because each estimator is obtained as a quotient of the intensities or integral of two bands. The signal was revealed by a mercury–cadmium–telluride detector (with detection range 11,000–400 cm⁻¹, and optical resolution of 4 cm⁻¹), interfaced to a personal computer. All spectra were acquired using the Omnic FTIR software averaging 200 scans.

Absorption values were calculated from baseline drawn from 1818 to 866 cm⁻¹. It is worth noting that all the samples were dried before the measurements at 110 °C for 10 min to remove the water vapour so that water vibration would not contribute to measured intensities. The spectra collected with ATR-FTIR was calculated as an arithmetical mean of the data for 4 different spots of an historical sample.

ATR-FTIR of historic silk samples allowed calculating: 2 estimators looking at the primary structure of fibroin (effects of the oxidation and hydrolysis) and one concentrated on the secondary structure of the protein (crystallinity estimator). They are defined as follows:

- (1) Primary functional groups estimators
 $E_{\text{AmideI/II}}$ – intensity ratios of Amide I C=O stretching vibration to Amide II N–H in-plane bending and C–N stretching vibrations A_{1620}/A_{1514} ;

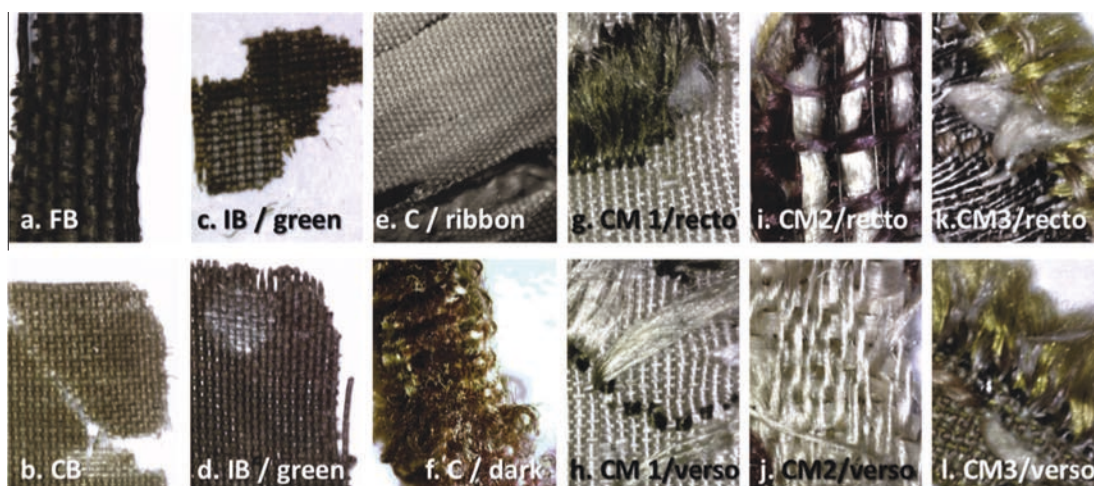


Fig. 2. Historical samples from 16th to 19th century, Europe: a. Stanisław Barzi's Funeral Banner 16th century, Poland, b. Court Banner 16th century, Poland, c and d. Inscription Banner 17th century (c. green and d. red sample), Turkey, e and f. samples from chasuble 17/18th century (e ribbon, f. dark chasuble), Poland, g–l. conservation material 19th century, Poland (recto and verso). (For interpretation of the references to colour in this figure legend, the reader is referred to the web version of this article.)

Table 1

Historic silk samples from 16th to 19th century, with full name and short name (abbreviation) used in this work.

Sample – short name (used in this paper)	Sample – full name	Date of manufacture [centuries]	Place of manufacture
FB	Stanisław Barzi's Funeral Banner	16th	Poland
CB	Court Banner	16th	Poland
IB/red	Inscription Banner/part dyed with red dye	17th	Turkey
IB/green	Inscription Banner/part dyed with green dye	17th	Turkey
C/ribbon	Chasuble's ribbon	17/18th	Poland
C/light	Chasuble light violet	17/18th	Poland
C/dark	Chasuble dark violet	17/18th	Poland
CM 1	Conservation material 1	19th	Poland
CM 2	Conservation material 2	19th	Poland
CM 3	Conservation material 3	19th	Poland

E_{COOH} – band 1318 cm^{-1} integral to band integral of CH_3 bending vibration band located at 1442 cm^{-1} P_{1318}/P_{1442} .

(2) Secondary conformational estimators

$E_{\text{C=O2}}$ – intensity ratios within Amide I C=O stretching vibration of parallel β -sheet to antiparallel β -sheet A_{1620}/A_{1699} .

$E_{\text{AmideI/II}}$ and $E_{\text{C=O2}}$ were found in the literature. E_{COOH} was proposed by our group based on previous work done on thermo-aged **MS** [11].

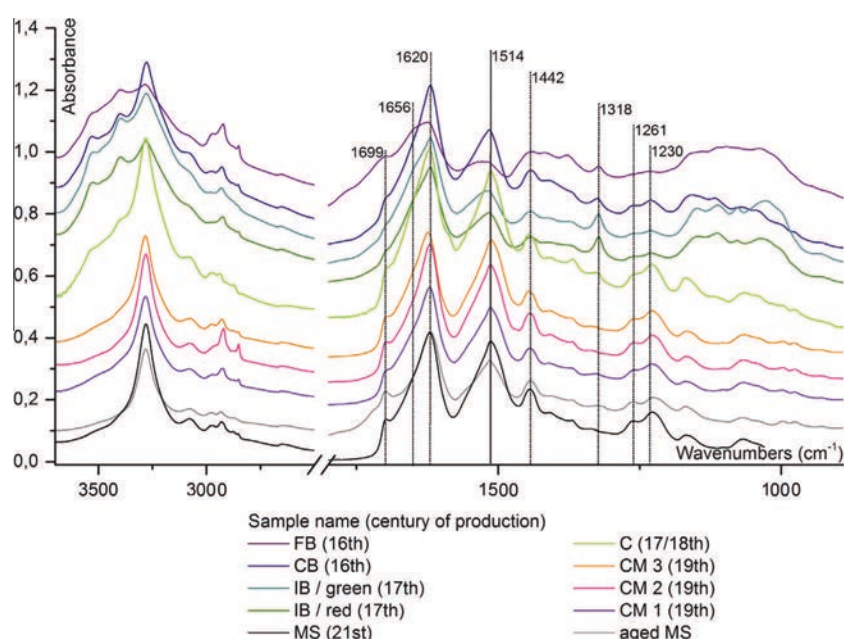
Results*ATR-FTIR spectra for historical material juxtaposed with model unaged and artificially aged samples*

The amide group in proteins, including fibroin, presents characteristic vibrational modes (called Amid modes). In this way, Amid I band in $1700\text{--}1590\text{ cm}^{-1}$ region can be attributed to mostly C=O stretching vibrations, Amid II in $1590\text{--}1460\text{ cm}^{-1}$ region – to N-H bending and C-N bending vibrations, and Amid III in $1190\text{--}1280\text{ cm}^{-1}$ – to N-H bending and C-N stretching vibrations. Fig. 3 depicts spectra gathered for historical samples (Section 'Historical silk samples') with means of ATR-FTIR, were oldest historical samples are located at the top of the figure, and the earliest at the bottom (as assigned in Section 'Historical silk samples') with

model silk samples at the very bottom part of the picture (aged in grey and unaged in black). The most evident change on spectra as we move to the top of the figure is the decrease in Amid I, II and III intensities, indicating the loss of peptide structure with the samples age. The more detailed analysis of Amid I to Amid II proportion change among the samples is discussed in Section 'Oxidation estimator' in terms of oxidation.

In Fig. 3 we can also distinguish new band formation centred at 1318 cm^{-1} and changes in band centred at 1699 cm^{-1} . The new band is attributed to deformation vibrations of -C-H groups in a free amino acid [12,20], or -C-H symmetric bending found in free dicarboxylic amino acids (COOH-NH-...-COOH) [12,21]. The rise of that band was noticed in aged **MS** and historical samples and was monitored by the hydrolysis estimator E_{COOH} in Section 'Hydrolysis estimator'. The changes in intensity of the band centred at 1699 cm^{-1} were monitored in relation to Amid I band in Section 'Secondary structure – crystallinity estimator' as the $E_{\text{C=O2}}$ crystallinity estimator.

Other changes in spectra presented in Fig. 3 are noticeable in the high wavelength range were bands centred at 3530 and 3400 cm^{-1} are emerging for old historical samples. These can be attributed to primary aliphatic amines N-H asymmetric and symmetric stretching vibrations (usually occurs at $3550\text{--}3330\text{ cm}^{-1}$ and $3450\text{--}3250\text{ cm}^{-1}$, respectively [12]). Therefore it is sound to presume that the decomposition of fibroin peptide in over 4 centuries silk samples produces primary aliphatic amines. That is

**Fig. 3.** ATR-FTIR spectra gathered for unaged and aged model samples and historical samples (as described in Table 1).

supported by appearance of wide band in the 1240–1020 cm^{-1} region that can be attributed to C–N stretching vibrations of primary aliphatic amines for banners from 16th and 17th century.

Primary structure degradation estimators

Hydrolysis estimator

E_{COOH} hydrolysis estimator was calculated from the spectra in Fig. 3 and depicted in Fig. 4. Its growing tendency for historical samples is consistent with the findings for the artificially aged MS [11]. It indicates peptide bond cleavage through acidic hydrolysis and grave radical oxidation.

The trend of the growth of E_{COOH} can be correlated with estimated age of the historic samples with exclusion of the one manufactured in Turkey, meaning that it could have been treated with

different chemical agents during processing and dyeing. This aged dependence tendency should be treated very cautiously as handling during usage and storage conditions having the most impact on silk degradation, differ gravely for all historical samples.

Oxidation estimator

The oxidation state of the silk sample was monitored by $E_{\text{Amide I/II}}$ estimator calculated from spectra in Fig. 3 and depicted in Fig. 5. Again the growth of the age of the historical samples reflects the tendency predicted the oxidation estimator derived from spectra of artificially aged fibroin and correlates with the age of sample with an exception of Turkish banner. All this clearly indicates that time causes the oxidation of peptide bond and aliphatic and aromatic side groups disrupting the silk fibroin peptide primary structure.

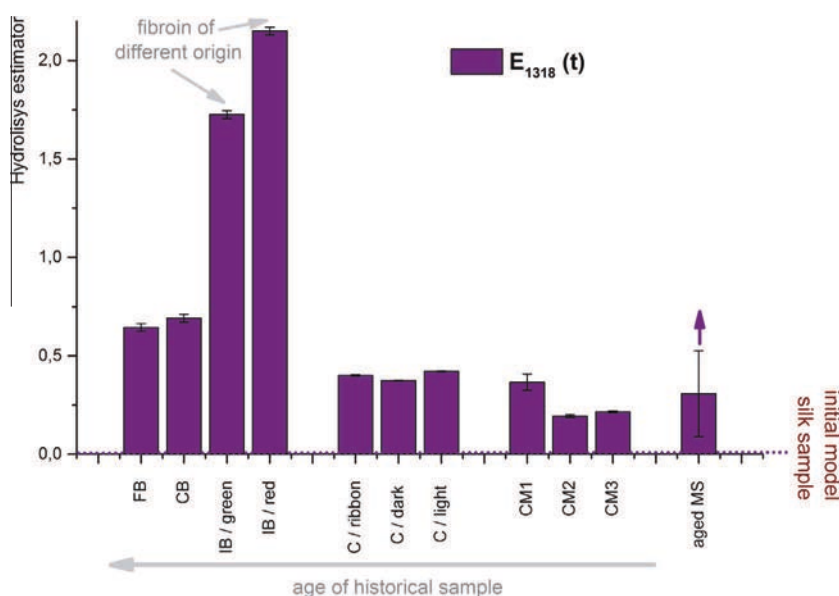


Fig. 4. Hydrolysis estimator calculated for unaged and aged model samples and historical samples (as described in Table 1).

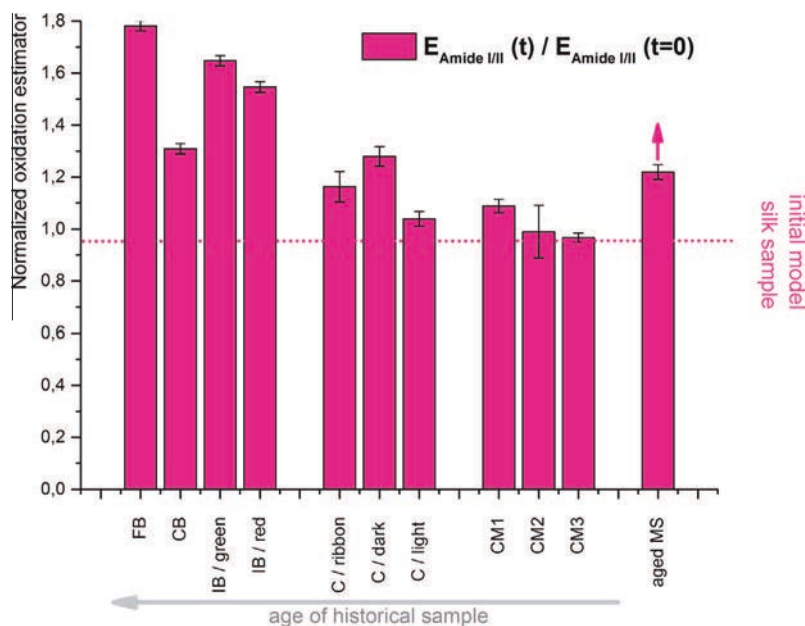


Fig. 5. Normalised oxidation estimator calculated for unaged and aged model samples and historical samples (as described in 'Section 'Historical silk samples').

Secondary structure – crystallinity estimator

The secondary structure of silk samples was monitored by crystallinity estimator $E_{C=O2}$; estimators were calculated from spectra gathered in Fig. 3 and depicted in Fig. 6. Although for artificially aged samples crystallinity drops with ageing time (verified by XRD experiments in previous work [11]), historical samples show different results. This can be accounted for by different time frames of artificially and naturally aged samples. For samples **CM 1–3**, **C/ribbon** and **FB** the estimator indicates drop of crystallinity. During natural ageing of these, not only easily accessible, non-ordered regions but also ordered ones underwent degradation. For samples **CB**, both **IB** (red and green) and both **C** (dark and light) $E_{C=O2}$ rises which indicated the rise of crystallinity. That can be explained by the loss of amorphous regions that causes overall rise in crystallinity. In these cases the degradation processes (hydrolysis and oxidation) alters only amorphous parts, leaving crystalline ones intact.

The loss of orientation of crystalline domains can be expected in these cases [15].

Degradation estimators – avers and revers recognition

In order to investigate the environmental influence (light triggered oxidation, humidity triggered hydrolysis and pollutant influence) on the rate of silks fibroin degradation two sides of the historical samples: verso and recto were analysed with ATR-FTIR spectroscopy and results compared. The obtained spectra are depicted in Fig. 7. Here dotted line indicates the verso spectra and straight line its recto. For samples from banners such experiment was pointless as the reverse side is covered with conservation treatment material – glue that once supported objects to its backing. The difference in primary amine $-N-H$ bands is clearly visible with the greater amine formation in avers of **C** and **CM1**. For **CM2** and **CM3** the opposite is observed spectra indicate graver

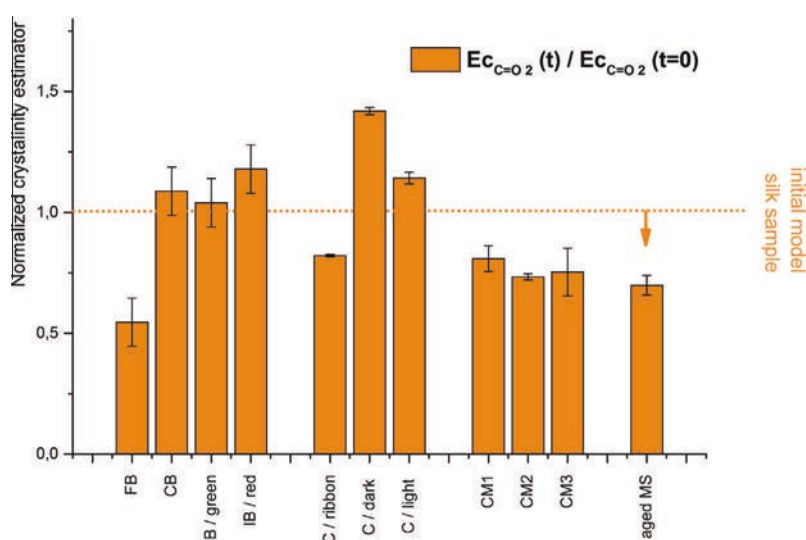


Fig. 6. Normalised crystallinity estimator calculated for unaged and aged model samples and historical samples (as described in Table 1).

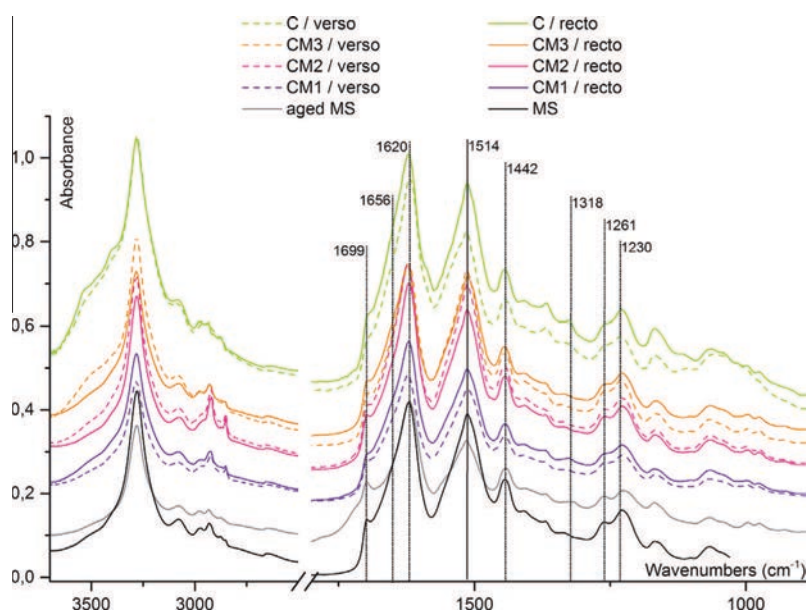


Fig. 7. ATR-FTIR spectra for unaged and aged model samples and historical samples (described in Table 1): recto (continuous line) and verso (dotted line).

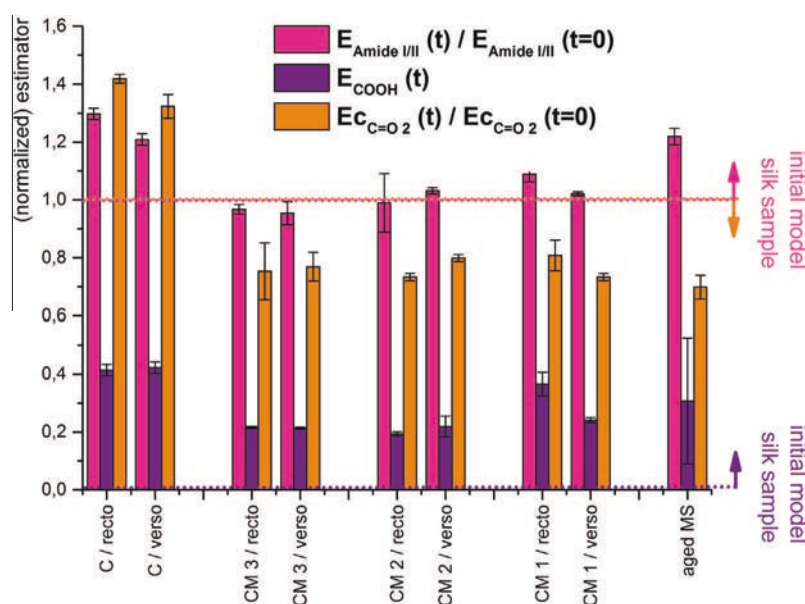


Fig. 8. Estimators calculated for unaged and aged model samples and historical samples (as described in Table 1).

verso degradation. This might have been caused by the storage conditions which are uncertain and has never been properly documented over centuries. Also for samples **CM** the period in which they were exposed towards one or the other side (as a tapestry for example) is unknown. Also the recto and verso sides (picture 2 g^{-1}) of **CM 2** and **CM 3** vary strongly in threads composition and it could be argued if they should be compared as such.

The primary and secondary structure degradation estimators were calculated from spectra in Fig. 7 and depicted in Fig. 8, where oxidation parameter is indicated in pink, hydrolysis and purple and crystallinity in orange. Suspicions from the visual analysis of ATR-FTIR spectra are reflected in calculations. As can be expected for **CM 1** sample estimators indicate more profound oxidation and hydrolysis for recto and for **CM 2** and **CM 3** slightly for verso side of the textile. Also, for defined recto and verso side **C** sample, verso is less oxidised and has lower crystallinity but the hydrolysis estimator is raised and not sensitive to the side of the textile. In the case of chasuble **C** both sides have suffered from oxidation and hydrolysis degradation, but it was probably due to the photo-oxidation (induced by the heavy violet dye on recto side) that made the recto side more degraded.

Conclusions

The crystallinity, oxidation and hydrolysis estimators based on non-destructive ATR-FTIR analyses can be successfully used to describe the condition of the historical silk textiles. Also thanks to estimators, monitoring textile surfaces directly exposed to destructive factors like humidity and pollution, outer side of garments were confirmed to suffer greater degradation state than the ones hidden from such influences.

Such defined estimators allow for simple risk assessment of museum objects and can facilitate future conservation planning pointing out these fabrics were the depolymerisation or oxidation is more advanced and amorphous regions decomposition more radical.

We have to admit that basing on the values of crystallinity and oxidation estimators a straight forward “age of sample” cannot be approximated as the historical objects were manufactured differently, stored at different conditions and thus influenced by differ-

ent production and degradation processes. Some indication of correlation of estimator with age of the sample was shown by the newly proposed by our group hydrolysis estimator E_{COOH} [11].

Acknowledgements

The authors thank the Wawel Castle Museum and Politechnika Łódzka for their help in gathering historic samples. Project funded from the funds of NCN 2011/01/N/ST4/03604 and FNP EX/04/2012. The authors are grateful to SPB 811/N-COST/2010/0 for sponsoring optical parts to spectrometers.

References

- [1] M. Lewin, Handbook of Fiber Chemistry, In: Lewin M. (Ed.), second ed., CRC Press, 2006.
- [2] E.S. Sashina, A. M Bochek, N.P. Novoselov, D. Kirichenko, Russian J. Appl. Chem. 79 (2006) 869–876.
- [3] E. May, M. Jones, Conservation Science, first ed., RSC Publishing, 2006.
- [4] A. Timar-Balazsy, D. Eastop, Chemical Principles of Textile Conservation, first ed., Butterworth-Heinemann, 1988.
- [5] D. Howell, ICOM Committee for Conservation 11th Triennial Meeting Edinburgh, Preprints London: James and James 2 (1996) 692–698.
- [6] S. Baltova, V. Vassileva, E. Valtcheva, Polym. Degrad. Stab. 3 (1998). 60, 53–65 and 61, 367–373.
- [7] G. D Kang, K. H Lee, C.S. Ki, Y.H. Park, Fibers Polym. 5 (2004) 234–238.
- [8] Tsuge, Toki, Ishida, Ohtani, Becker, Polym. Degrad. Stab. 69 (2000).
- [9] J.E. Miller, B.M. Reagan, J. Am. Inst. Conserv. 28 (1989) 97–115.
- [10] X.M. Zhang, S. Yuan, Spectrosc. Spectral Anal. 24 (2004) 1528–1532.
- [11] M.A. Koperska, D. Pawcenis, J. Bagniak, M.M. Zaitz, M. Missori, T. Łojewski, J. Łojewska, Polym. Degrad. Stab. 10.1016/j.polymdegradstab.2014.04.008.
- [12] G. Socrates, Infrared and Raman Characteristic Group Frequencies: Tables and Charts, third ed., John Wiley & Sons, 2004.
- [13] X.M. Zhang, P. Wyeth, Sci. China Chem. 53 (2010) 626–631.
- [14] P. Wyeth, AHRB research centre for textile conservation and textile studies, in: First Annual Conference, Winchester, UK, 2004.
- [15] P. Garside, P. Wyeth, Appl. Phys. A 89 (2007) 871–876.
- [16] S.Greiff, H. Kutzke, C. Riekell, P. Wyeth, S. Lahli, <http://eprints.soton.ac.uk/>.
- [17] X.M. Zhang, Spectrosc. Spectral Anal. 30 (2010) 262–265.
- [18] A.C. Harmes, R.J. Davies, S. Greiff, H. Kutzke, S. Lahli, P. Wyeth, C. Riekell, Biomacromolecules 7 (2006) 777–783.
- [19] T. Arai, J. Appl. Polym. Sci. 91 (2004) 2383–2390.
- [20] X.G. Chen, P. Li, J.S.W. Holtz, Z. Chi, V. Pajcini, A.A. Sanford, L.A. Kelly, J. Am. Chem. Soc. 118 (40) (1996) 9705–9715.
- [21] S. Kumar, A.K. Rai, V.B. Singh, S.B. Rai, A Mol. Biomol. Spectrosc. 61 (11–12) (2005) 2741–2746.